
Fire Following Earthquake

Lesbo Chiara



Department of Architecture and Design
Architecture for Sustainable Project
Politecnico di Torino

September 2018

Supervisor:

Prof. Cimellaro Gianpaolo

Co-Supervisor:

Dr. Domaneschi Marco

Presentation of the candidate

My name is Chiara Lesbo and I was born in Loranze in province of Turin on February 13th 1992.

After obtaining the diploma of artistic maturity with address in architecture and furniture, I decided to attend the Faculty of Architecture to continue designing.

During these years of teaching and, above all, thanks to the stage developed during the triennial, my passion for architecture has increased. Designing new buildings and the challenge of renovating existing buildings amuses me.

I stayed in touch with the office where I did internship and so I started working to be able to understand more deeply the problems that emerge every day in a design phase. I wanted to approach the working reality to better understand the practical part of a project, that is the building site, which is not introduced in our university path despite being a fundamental, complex process, that every student interested in the world of architecture should to consume parallel to the course of studies.

This experience was wonderful, because it gave me the opportunity to know other aspects of the design. For the first time I was able to follow a project from the ideational stage to the realization phase; I observed how more figures of different sectors, indispensable among them, had to collaborate to realize a project.

What fascinates me most about this work is that an architect, by now, to be able to work properly must have knowledge that touches the urban, structural, social, humanistic and artistic field.

The architect designs new dimensions with which every man must be able to dialogue and find his space. It's a job that changes every day, that every day brings new challenges, new doubts, but that gives you the opportunity to express the maximum of yourself through a new vision of the city.

Abstract

The outbreak of fires in urban environments due to problems related to seismic shocks, is a phenomenon that has been studied for a long time by researchers all over the world. The formation of trigger points after a strong earthquake in the urban area is an effect that is analyzed in order to try to create efficient protective solutions.

The aim of this theses is to investigate the phenomenon of fire following earthquake (FFE): starting from the studies carried out up to now, this work analyzes the propagation of the fire in a hypothetical residential area damaged by simulated shocks using a software of fluid dynamics.

This thesis is divided into 6 chapters:

- chapter of introduction;
- chapter with the literature review;
- chapter with the description of the program used to calculate the simulation;
- chapter with an example of validation;
- chapter with some example to understand how the programs work;
- final chapter with the simulation of the fire in an urban scale

In the chapter of introduction, a historical review of the most important earthquake where the subsequent fire causes more damage than the seismic actions was made. Starting from the earthquake of San Francisco in 1906, the major post-earthquake fire in the word is analysed to understand the main causes that can generate a fire after the earthquake shocks. In this chapter, the normative that regulate the discipline of the fire protection in the design of structures are also explained.

The literature review is useful to understand the different methodologies that other researchers developed. The literature was divide into to main categories: building and territorial scale. In the individual scale, the studies are carried out on models of individual buildings that have suffered structural damage from hypothetical earthquakes and are subjected to a consequently fire event. This model can be a virtual model or a real model. In the territorial scale, the researches are made using the data of real post-earthquake fire event to model a virtual simulation.

FDS is the program for the computation of the simulation used in this thesis. As pre-processor, to write the input file of the calculation, Blender FDS is used in the first

part of the research. After the computation with FDS, Smokeview is used to visualize the result of the simulation. In a second moment, the program PyroSim is used to model, calculate and visualize of the different simulations illustrated in this thesis.

The paper "Experimental investigations of the fire behavior of facades with EPS exposed to different fire loads" of Northe, C. et al. 2016 is used to validate the programs. The virtual model is created with the data present in the research and the simulation is carried out to verify the accuracy of the simulation.

To understand the main parameters that govern the simulation, different examples are included in the fifth chapter of the thesis. In particular, the propagation of the fire with different materials and the two fundamental characteristics of the wind, direction and intensity, are analyzed.

For the simulation in an urban scenario, the model of Ideal City, a virtual city created on the basis of the real city of Turin, is used. All buildings and urban features are taken from the real city and reported in an interactive virtual model. The idea of this chapter is to recreate the work of Prof. Lu Xinzheng "Physics-based simulation and high-fidelity visualization of fire following earthquake considering building seismic damage".

Table of Contents

	Page
List of Tables	vii
List of Figures	ix
1 Introduction	1
1.1 Historical Earthquake	1
1.2 Design issues	9
1.2.1 FFE generation	9
1.2.2 Structural design	9
1.2.3 EuroCode	13
1.3 Fire Curve	14
1.3.1 Normal fire curve	14
1.3.2 HRR-T Curve	15
1.4 Fire Modeling	17
2 State of the art	19
2.1 Introduction	19
2.1.1 Building scale	20
2.1.2 Territorial scale	33
2.1.3 Summaries	40
3 Programs	47
3.1 Fire Dynamic Simulator	47
3.2 Smokeview	59
3.3 BlenderFDS	59
3.4 Pyrosim	61
4 Validation	63
4.1 Creation of the input file	64
4.2 Simulation	68
5 Simulation	73
5.1 Initial parameters	74
5.2 First simulation: propagation	79

TABLE OF CONTENTS

5.3	Second simulation: Wind	80
5.4	Third simulation: Intensity	84
5.5	Fourth simulation: Direction	87
5.6	Fifth simulation: Material	91
6	Ideal City	97
6.1	Creation of the input file	98
6.2	Simulation	101
6.3	First simulation	106
6.4	Second simulation	110
7	Conclusion	113
	Bibliography	119

List of Tables

Table	Page
2.1 Steel structures	43
2.2 Concrete structures	44
2.3 Territorial scale	46

List of Figures

Figure	Page
1.1 San Francisco Earthquake in 1906	3
1.2 Great Kanto earthquake in 1923	4
1.3 Napier earthquake in 1931	4
1.4 Niigata earthquake in 1964	5
1.5 Loma Prieta earthquake in 1989	6
1.6 San Fernando Valley earthquake in 1994	7
1.7 Kobe earthquake in 1995	8
1.8 Eastern Japan earthquake in 2011	8
1.9 Performance Based Seismic Design	12
1.10 Normal fire curve	15
1.11 HRR-T curve	16
1.12 A Zone model	17
1.13 Two-Zone model	18
2.1 The three different frames that are used in the simulation; the picture is taken to the paper.	27
2.2 The buffer zone create in the district of Wellington; the picture is taken to the paper.	34
2.3 The fire spread in the simulation of the Napier city; the picture is taken to the paper.	36
2.4 Result of the fire simulation; the picture is taken to the paper.	37
3.1 Graphic interface of Blender	60
3.2 FDS input file modeling menu	61
3.3 Graphic interface of PyroSim	62
4.1 Visualization of the geometry using BlenderFDS	65
4.2 Comparison between a) Smokeview and b) Pyrosim visualization.	68
4.3 Comparison between a) the simulation and b) real fire test at the time of 10 minutes.	69
4.4 Comparison between a) the simulation and b) real fire test at the time of 11:30 minutes.	69
4.5 Comparison between a) the simulation and b) real fire test at the time of 12 minutes.	70

4.6	Comparison between the simulation and the real test	71
4.7	Comparison at different time step between the simulation (orange line) and the real fire test (black line)	72
5.1	Visualization of the geometry using PyroSim	75
5.2	Initial phases of the simulation	79
5.3	Initial phases of the propagation	80
5.4	Propagation of the fire	81
5.5	Initial phases of the simulation	82
5.6	Development of smoke and detection of wind direction	83
5.7	Smoke and detection of wind direction	83
5.8	Intensity of the smoke at the beginning of the simulation	86
5.9	Intensity of the smoke in the middle of the simulation	86
5.10	Intensity of the smoke at the end of the simulation	87
5.11	Direction of the wind at 270°	88
5.12	Direction of the wind at 180°	89
5.13	Direction of the wind at 90°	90
5.14	Direction of the wind at 0°	90
5.15	Comparison at the time 35 sec between a) concrete, b) PVC and c)wood . .	93
5.16	Comparison at the time 100 sec between a) concrete, b) PVC and c)wood .	94
5.17	Comparison at the time 400 sec between a) concrete, b) PVC and c)wood .	95
6.1	Image of the AutoCAD file	99
6.2	Image of the Excel tabel with all the data of teh city	100
6.3	Image of the model in AutoCAD	100
6.4	Simulation parameters menu	102
6.5	Configuration of the mesh	103
6.6	Configuration of the reaction	103
6.7	Configuration of the materials	104
6.8	Configuration of the surfaces	104
6.9	Visualization of the computation screen	105
6.10	Visualization of the analysis dialog	107

Introduction

1.1 Historical Earthquake

Fire following earthquake (FFE) is one of the major cascading effects that can occur in seismic affected urban area. The "Ring of Fire" extends around the Pacific Ocean and it is the largest area with catastrophic events such as earthquakes and volcanic eruptions; in this area there are about 90% of earthquakes in the world and 81% of the world's largest earthquakes.

The idea of carrying out a thesis on this topic was born from the desire to better understand the phenomenon of injection as cascading effect of an earthquake and the following fire propagation in a complex environment as the urban one. Despite technological advances, the fire propagation still remains a hardly predictable danger.

In this section a review of the major historical fire following earthquake and the main causes that have led to the spread of fire are explained.

It is possible to indicate the earthquake of San Francisco in 1906 (1.1) as the first



Figure 1.1: San Francisco Earthquake in 1906

of a series of earthquakes where the developing of the fire caused more damage than the seismic shock. The earthquake broke out on April 18 with a magnitude of 7.8 on the Richter scale and a main shock of 8.3. It was estimated that approximately 80% of the damage in the San Francisco area was caused by post-earthquake fire; about 28,000 buildings on 490 districts were damaged by fire.

The earthquake caused structural and non-structural damage: the first damage compromised the integrity of many fire safety systems; non-structural damage hit the major urban lifelines such as water and gas reserves, transport systems, communications and electricity generation and distribution.

The main obstacle for firefighters, in addition to the problem of damage to the local water system, was communication: seismic shocks destroyed the headquarters of the alarms and broke the telephone system for a very large area, preventing citizens from communicating alarms to the departments of the firefighters.

The Tokyo-Yokohama region (1.2) was effect by a large earthquake in 1923, with a



Figure 1.2: Great Kanto earthquake in 1923

magnitude of 7.9, that was renamed Great Kanto earthquake.

The earthquake broke out at lunchtime and so many people died because of the fire that broke out while they were preparing their meals; some fires developed in fire storms: in the center of Tokyo, a tornado of fire broke into an army clothing store causing the death of some 38,000 people.

The water system breakdown slowed down the firefighters' intervention, which took nearly two days to tame all the fires that destroyed about 40% of Tokyo and 90% of the city of Yokohama.

Seismic shocks generate other catastrophic events: a strong typhoon centered off the Noto Peninsula in Ishikawa Prefecture, some landslides in the mountainous and hilly coastal areas in western Kanagawa Prefecture and a tsunami hit the coast of the Sagami bay, the Bossa peninsula, the Izu islands and the eastern coast of the Izu peninsula.

In 1931, an earthquake with a magnitude of 7.8 affected New Zealand (1.3), more precisely the area of Napier. The ground motion change drastically the local landscape raising the coasts around the Napier area by approximately two meters and lifting about



Figure 1.3: Napier earthquake in 1931

40 of seabed that have turned into dry land.

The damage to Napier's water system and the collapse of the Havelock bridge, used to transport the city's water network, made it difficult to tame the fires that interrupted the city's water supplies in no time. Seismic shocks have also damaged electric and gas systems.

Three chemists' shops have been identified as the outbreaks and the wind played a fundamental role in the propagation of the city fire.

The Niigata earthquake (1.4) in 1964 had a magnitude of 7.5 and the consequently tsunami flooded some part of the city. The wave carried in the city some buoyant oil slicks that later became the trigger points.

The airport and the harbor suffered various damages caused by the earthquake and tsunami; the most devastating was the rupture of the petrol tanks that were in that area: the fire spread immediately to the tanks that in turn caused several explosions that fueled the fire until it spread even in the city area. It is one of the worst industrial fires in Japan.

The earthquake of Loma Prieta, California (1.5), in 1989 had a Richter magnitude



Figure 1.4: Niigata earthquake in 1964

of 7.1 and was the largest earthquake that has affected this area since the Great San Francisco earthquake in 1906.

The shut-down of the electricity system and the consequent closure of all the electrical safety valves, has allowed to block the flow of gas in the buildings thus preventing many possible fires. The principal causes of fire broke out was the natural gas leaks and the major conflagration was in the Marina district; because of the numerous water pipes broken in this area, it was necessary to resort to the use of a fireboat to be able to control the fire.

Once again in California, in 1994, a harmful earthquake of magnitude 6.7 was recorded. The strongest seismic shocks occurred in the San Fernando Valley (1.6) in a densely populated area.

The main causes of the fires were natural gas leaks, electrical short circuits and dangerous chemical interactions. Among the most important trigger points of the fire were the breaking of the network and the natural gas leakage valves in an area of



Figure 1.5: Loma Prieta earthquake in 1989

manufacturing development and the burning of certain hazardous materials located in the California State University scientific complex at Northridge.

In 1995, the city of Kobe (1.7), in Japan, was hit by an earthquake with a Richter magnitude of 7.2. The post-earthquake fire was caused by different factors: the braving up of the natural gas pipes, the electrical system and objects that were used to save people, such as candles in gas.

In Hyōgo Prefecture, older homes were designed to withstand typhoons occurring in the area; they had a heavy and very resistant roof supported by a light wooden structure which, following the breaking of the gas lines, was immediately attacked by the fire causing the heavy roofs to collapse to the ground. As a result, around 20% of buildings in the area were destroyed and half of the other buildings were deemed to be no longer secure.

The last relevant earthquake with an important post fire took place in Eastern Japan (1.8) in 2011. The magnitude of the event it was 9.0 and was the biggest earthquake ever registered in Japan.



Figure 1.6: San Fernando Valley earthquake in 1994



Figure 1.7: Kobe earthquake in 1995



Figure 1.8: Eastern Japan earthquake in 2011

The following was a tsunami that caused several accidents especially in the industrial zone. The Fukushima Daiichi nuclear power plant suffered several damages and at least three nuclear reactors exploded due to the escape of hydrogen gas. Also, several oil refineries were damaged by the earthquake and burned causing extensive damage in the surrounding areas.

1.2 Design issues

1.2.1 FFE generation

The main causes of FFE are mainly due to short-circuits, abrasions, chemical reactions and other damages caused by shocks to industrial and urban territory; the earthquake can impair communications, damage water system and block transport networks.

For example, the collapse of buildings due to shocks can cause congestion of city

traffic because of the debris that prevent the passage and thus delay the arrival of relief. Furthermore, the probability of multiple fires in the urban area and the possibility that the earthquake can damage the water system can cause delays in firefighting.

Other causes that can increase the propagation of fire are the distance between the buildings and the wind that plays a fundamental role in the speed and direction of fire.

The major damages caused by earthquakes are structural and often prevent people inside the building from getting out and getting safe; ground motions may damage non-structural elements, such as pipelines and sprinklers, which can cause and increase the intensity of the fires.

1.2.2 Structural design

The scenario of fire following earthquake, despite its catastrophic potential, is not yet considered in seismic design. Indeed, the current seismic design philosophy provides that ordinary structures are designed to suffer a certain degree of damage during strong earthquakes; to safeguard human lives, the proper ductility of the structure is exploited to collapse and this mechanism causes a vulnerability in the structure when exposed to additional hazards.

In the modern architectural situation, the creation of large steel structures is in the norm. In the vast urban areas, the creation of high-rise buildings is diffused and, consequently, the use of fire-sensitive materials such as steel.

Within the regulatory framework linked to the fire resistance of steel, the concept of fire resistance is defined as the attitude of an element, structural and not, to maintain the requirements of mechanical strength, integrity and thermal insulation. These three requirements can be kept in whole or in part by the element analyzed during a defined period and a predetermined thermal program.

The recent building regulations provide for the possibility of carrying out structural

CHAPTER 1. INTRODUCTION

verifications in the event of a fire using the performance approach: it is a method based on the application of defined calculation models used to establish the temperature in the environment, project natural fire , and in the structural elements (thermal analysis of the elements); it also establishes the mechanical behavior of the structural organism, structural analysis in case of fire.

This approach is based on a study of the specific fire situation that may occur; in this way the effectiveness of the active and passive protection devices of the building and the structural behavior of the structure is verified with a consequent greater reliability of the safety.

The main purpose of most building codes is to ensure the safety of life in a building. Performance Based Seismic Design was introduced to overcome the limitations of old seismic design models. Unlike the old methods that were based on the force used to deal with the inelastic behavior and the effects of cyclic loading in the structures, in this method buildings are designed with a realistic and reliable understanding of the risk to life.

Performance Based Seismic Design allows the designer to choose, based on the project area, the appropriate level of simulated ground shaking and the level of protection to be used for that particular movement; it is possible to estimate different levels of shaking with different levels of performance for each shaking.

The target levels of building performance vary starting from continuous operation, where it is expected that the building and non-structural components will not suffer any damage in response to the design earthquake, and coming up to collapse, where the structure must remain standing, but it is widely damaged.

The specific ductility factors are specified for each component of the anti-seismic system. The ductility factor varies according to the level of performance of the building, the type of material and the relative ductility of the component.

The image below 1.9 represents the Performance Based Seismic Design in a schematic

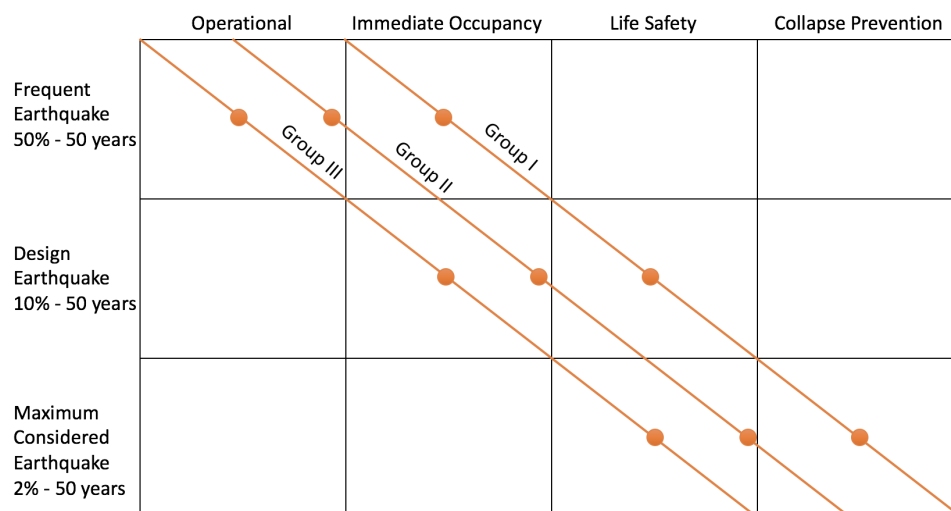


Figure 1.9: Performance Based Seismic Design

way: on the abscissa axis the performance levels of the analyzed building are represented and on the ordinates axis the risk levels corresponding to the earthquakes chosen in the design phase. The diagonal lines represent the different building types: group I represents the basic commercial structures, while groups II and III represent the types of buildings that require a higher level of protection, such as hospitals, fire brigades, data centers, key production facilities.

Normally, the structural elements are designed to maintain different levels of performance based on the intended use; the main performance levels are:

- *Operational (O)*: at this level, the building performances are not changed; structural damage is minimal or absent and only small adjustments are required for energy and water. For low-level earthquakes, this level of performance is used in school design; for high-intensity earthquakes, this level is reserved for buildings that offer unique services or contain hazardous materials.
- *Immediate Occupancy (IO)*: the building is designed to sustain minimal structural damage and minor nonstructural damage. It is possible to perform some cleaning,

repair and restoration of utility services before the building can operate in normal mode.

- *Life Safety (LS)*: at this level of performance buildings may suffer extensive damage to structural and non-structural components and repairs may be necessary before re-employment. The risk of victims at this level of performance is low.
- *Collapse Prevention (CP)*: buildings at this level can suffer severe structural damage and can pose significant risks to occupants.

Buildings designed to withstand severe earthquakes must have structures that can withstand a certain level of plastic deformation; this causes a weakening in the structure which is consequently more vulnerable to a subsequent fire due to the reduction of fire resistance. The combination of the collapse time of a building and the likely increase in the arrival time of the rescue can lead to disastrous effects.

Modern performance-based philosophy predicts that, even if there is no fire after an earthquake, the fire resistance of the structure that has been damaged by the seismic actions should be assessed. For this reason, when a building suffers from an earthquake, the overall performance of the structure must be assessed for the future, so as to consider the possibility of post-earthquake fire intervention.

1.2.3 EuroCode

The European Committee for the Standardization develops the European Standards (EN) to the structural design. By 2002, the Eurocode Standards is divide in ten sections: basis of the structural design, actions on structure, design of concrete structures, design of steel structures, design of composite steel and concrete structures, design of timber structures, design of masonry structures, geotechnical design, design of structures for earthquake resistance and design of aluminum structures.

The design of structures for earthquake resistance, or EN 1998, describes all the processes that must be performed in case of design in seismic zones. The propose of this guideline is to protect the human live, limited the damage and guarantee the operation of the important civil protection structures.

The Eurocode 8 is divided into six parts which are numbered from EN 1998-1 to EN 1998-6:

- General rules, seismic action and rules for buildings
- Bridges
- Assessment and retrofitting of buildings
- Silos, tanks and pipelines
- Foundations, retaining structures and geotechnical aspects
- Towers, masts and chimneys

1.3 Fire Curve

1.3.1 Normal fire curve

The curves time-temperature are used in the simulation of the fires of the structures; they form the basis of fire protection design and of escape and rescue strategies in case of fire.

There are different time-temperature curves in the literature for different scope. The ISO 834 is the standard fire temperature curve; it is also called cellulose curve (1.10) and it is the least intensive of the various curves; it is used to test the resistance of building materials to fire.

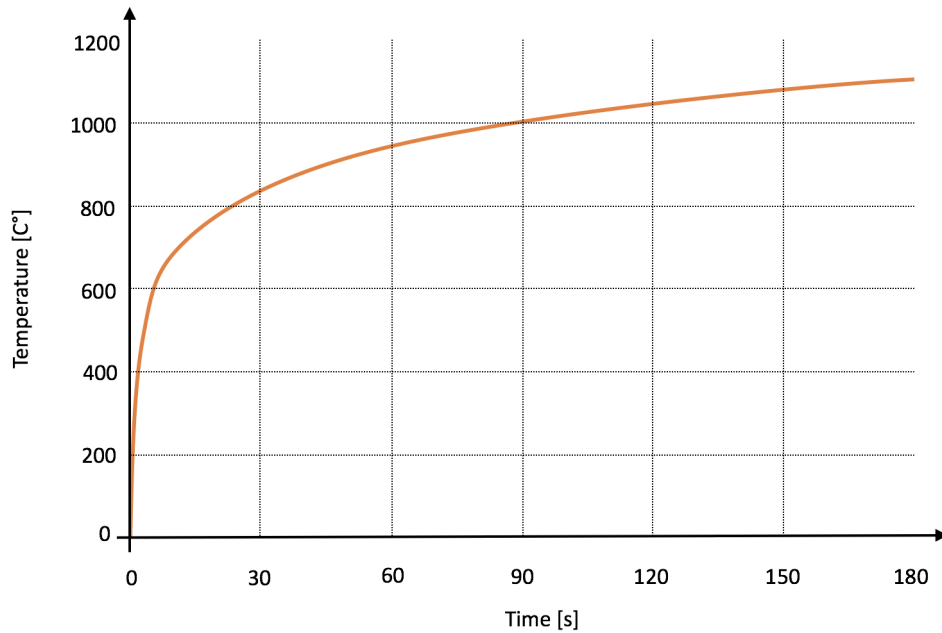


Figure 1.10: Normal fire curve

This curve represents the progress of a fire in a compartment and shows how the temperature increases with the passage of time at a constant speed. The standard temperature-time curve is defined by the following expression:

$$(1.1) \quad T_G = 345 \log_{10}(8t + 1)$$

1.3.2 HRR-T Curve

The concept of the Heat Release Rate (HRR) is based on the released energy of the fire without reference to the combustion time.

In the evaluation of the temperature that can be reached in a closet compartment during a fire, the value of HRR as a input data is more reliable than that of the fire load; in this calculation it is assumed that all the fuel present in the environment participates in the combustion process.

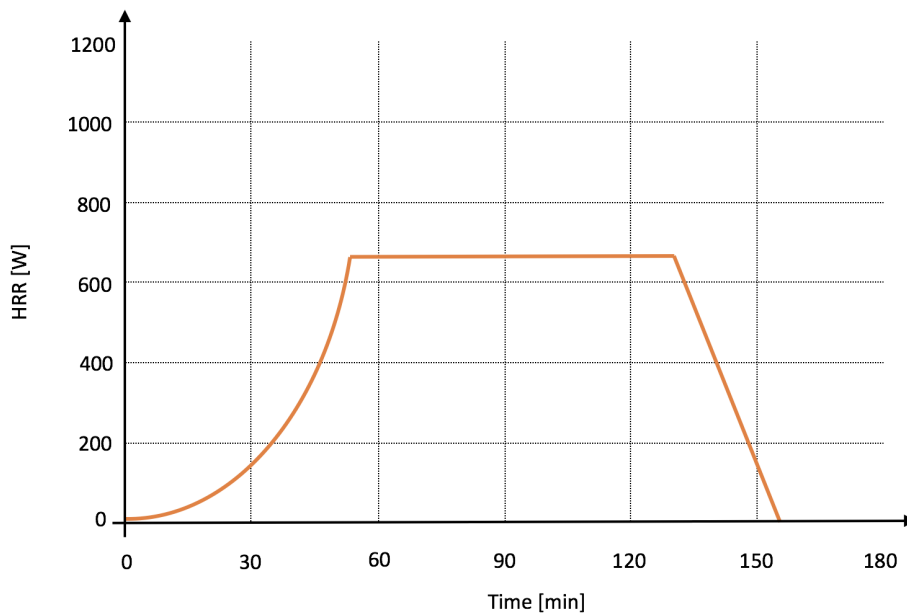


Figure 1.11: HRR-T curve

The model that best represents the fire of the common combustible materials contained in the buildings is the one mentioned by the EN1991-1-2 Eurocode, (1.11) divided into three different sections:

- quadratic growth segment, fire propagation phase;
- horizontal stretch, full development phase;
- linear decay section, extinction phase.

The initial phase of the fire is controlled by the fuel: the velocity of the combustion is mainly influenced by dimension, spatial disposition, mass and fuel typology. In this phase, there is the presence of the flash-over.

In the middle phase, the fire is controlled by the ventilation; the velocity of the combustion is almost constant in time and is equal to the maximum value that can be reached in the local.

The maximum value of HRR can be estimated using the formula described in the Eurocode 1-Annex E.

$$(1.2) \quad HRR_{max} = 0,10mHA_v h_{eq}^{0.5}$$

Where m is the combustion factor, H is the calorific value of the material, A_v is the ventilation area and h_{eq} is the equivalent height.

The last phase corresponding to the exhaustion of the fuel, turns out to be constant.

The importance of the RHR curve lies in the twofold fact of describing the dynamics of a fire and constituting one of the input and output data for the zone simulation models.

1.4 Fire Modeling

In fire modeling two different approaches are usually used: "A Zone" and "Two Zone". The first models (1.12) are used in case the fires are developed and post-flash-over; it is assumed that the temperature, the density, the internal energy and the gas pressure is uniform inside the compartment. The first models were developed by Pettersson, Magnusson and Thor in 1976, Babrauskas and Williamson in 1978. These simplified models were developed in multi-zones and multi-components.

Two-zone models (1.13) are used when knowing the location of the fire or in case of pre-flash-over. The compartment is divided into two zones: a warm top that represents the smoke accumulation layer, and a colder lower zone.

Both models are based on the resolution of the ordinary differential equations for the conservation of energy and mass; the difference between the two models occurs in the complexity of the two-zone model equations: the conservation equations are divided by the single zones and the exchange of mass and energy must be considered between the individual zones of the model.

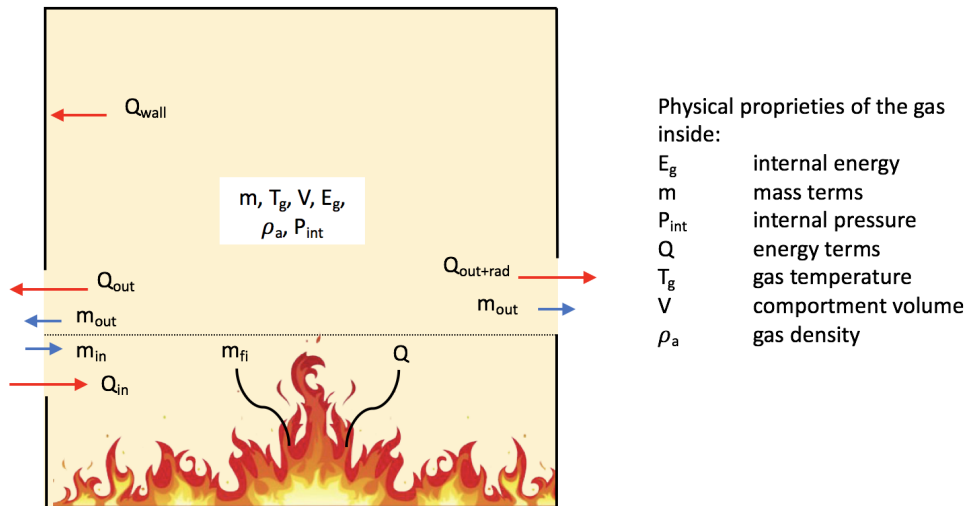


Figure 1.12: A Zone model

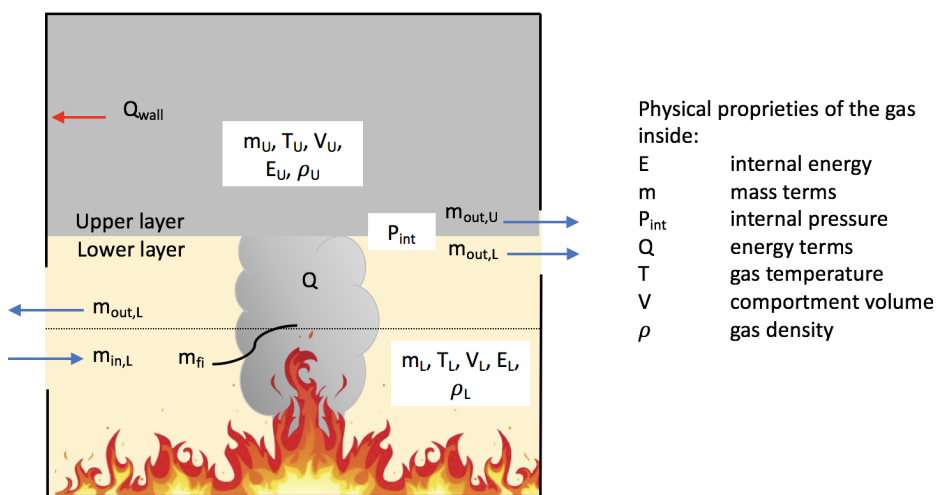


Figure 1.13: Two-Zone model

State of the art

2.1 Introduction

In the last years, many researches focus their studies on the problem of the post-earthquake fire. The purpose of many works is to analyze the individual structural components by observing their behavior and their fire resistance; often the column-to-beam connections are the most observed ones.

In this state of the art, the articles are divided into two categories of analysis of the phenomenon of fire following earthquake: scale analysis of the individual building and large-scale analysis, the city. Moreover, the literature has been reported in date ordine in such a way as to see the development of the different survey methodologies over the years.

2.1.1 Building scale

2.1.1.1 Post-earthquake fire resistance of moment resisting steel frames - Della Corte G et al. 2003

The scope was to obtain some quantitative information about the hazard. In first step of this analysis, a simplified model of a structure that was damage by the seismic actions was created. The effects are divided in geometrical and mechanical; then, a wide numerical analysis permits the identification of the parameters problem that affect the structure.

The first important concept that was introduced to the seismic damage modeling was the distinction of two forms of damage in the structure:

- geometrical damage: the change in the geometry of the structure following the residual deformation produced by the plastic excursions that are created during the seismic shocks;
- mechanical damage: degradation of the mechanical properties of structural components that undergo plastic deformations during seismic shocks.

The temperature is considered uniform in the trigger zone and is monotonically increased respecting the time-temperature curve suggested by the standard ISO-843. The Eurocode 3 is used to model the steel behavior at high temperature and to the thermal properties.

The software SAFIR was used to calculate the fire resistance of the beam-column element.

The analysis of the single-storey moment resisting frame is focused on a numerical analysis; the parameters that influence the characteristics of mechanical behavior of the structure were:

- the ratio between the beam capacity and the height of the structure

- the ratio between the moment of inertia of the beam and the column
- the ratio between the beam and column section flexural plastic strength
- the ratio between the vertical load and its elastic critical value
- the level of geometric damage

In the case of the multi-storey moment resisting frame, the researchers tested two structures with the same dimension but one was designed considering the ultimate limit state (ULS) and the other was designed also to serviceability limit state (SLS). The structures were analyzed with eight different accelerograms corresponding to different earthquakes: four occurred in Italy and four in the world.

To perform a complete analysis of the behavior of the structures, the Incremental Dynamic Analysis (IDA) is used: the PGA value is scaled appropriately to force the structure to go through the elastic instability until it reaches the global dynamic instability, that is when the structure collapses. At the end, the frames were subjected at the fire scenario.

2.1.1.2 On the structural effects of fire following earthquake - Della Corte G. et al. 2005

The paper shows the result of a numerical investigation of the steel moment-resisting frame in different earthquake simulations. The research was structured at different levels of earthquake intensity, and induced damage, that was obtained by scaling the acceleration records and increase the values of the elastic pseudo-acceleration. Besides, two structural systems with two different design procedures are analyzed.

In this study, the analysis assumptions are the same of the previous work with the distinction of geometrical and mechanical damage, the fire modeling is based on the Eurocode 1 and the numerical code SAFIR is used to estimate the fire resistance.

The multi-story moment resisting steel frames were designed with two different strategies, as in the previous work: according to the ultimate limit state and also according to the serviceability limit state.

The difference between the works concerns the analysis of the multi-story. The two structures have the same geometry but one has a perimeter frame system and the second have a spatial frame system.

Even in this research, the structures subject different earthquake ground motions and the researchers using the Incremental Dynamic Analysis to calculated the earthquake.

2.1.1.3 Fire after Earthquake Analysis of Steel Moment Resisting Frames - Zaharia R. et al. 2009

This research estimates the time resistance at fire of some unprotected steel moment resisting frame. The analysis concerns two different types of structure that were damaged by seismic action; for the computation was used an advanced method for the earthquake and the fire following it. Furthermore, the fire scenarios were computed using the standard ISO and the natural fire.

Two structures, one six-storey and one single-storey, are analyzed in two different seismic regions of Romania: the Banat region, with a near-field type, and the Vrancea region, with a far field type. The design was made according to the European standard ENI 1998.

To evaluate the seismic response of the structure, the researchers used a pushover analysis; to determine the displacement request corresponding to the seismic event, the N2 method is used.

After the seismic evaluation, the analysis of the fire is divided into two parts: a first analysis is performed using the ISO standard data for the fire modeling, then proceeded with the thermal analysis using the data related to the natural fire.

To thermal analysis under ISO fire, it is established that the ground floor of the structures has been modeled as a fire compartment and that the fire is triggered in the first floor where the unprotected columns are located.

In the case of natural fire scenario, different hypotheses must be considered as the maximum fire area and the fire load. In this research, Zaharia and Pineta take into account the surface of the openings of the buildings: the windows and doors regulate the flow of oxygen in a room and consequently the rate of heat release of the fires. They analyze, in addition to the structural behavior, also the windows in order to try to predict how long the glass is resistant to heat before bursting.

In order to obtain the fire curves of the buildings, the Ozone software is used: this code is a modern fire model approach because it combines the “Two Zone” and “One Zone” model. These fire curves, two for each frame, were used in the SAFIR software to analyze the temperature evolutions.

2.1.1.4 Performance of a six-story reinforced concrete structure in post-earthquake fire - Mostafaei, H. et al. 2010

The paper used the data of the Kobe earthquake of 1995 to analyze the performance of a six-storey reinforced concrete structure. The model was made in a 3D to analyze the behavior of the building structure under fire; in the analysis of post-earthquake fire, the degradation of the mechanical properties of the material and the penetration of heat due to the cracks that form after the shocks are studied.

The researchers used the software SAFIR for the structural analysis and the structure was designed in accordance to the Japanese code.

To simplify the computer modeling and the consequent computation time, the beams and the girders were designed as a T-section; normal strength concrete has been set as a material.

Once the building examined has been modeled, the researchers proceed with the

analysis of the fire resistance performance of the structure before any damage. The first step calculated is the heat transfer inside the columns: the analysis involves the use of 2D mesh of different cross-sections of the structural elements. As a second step they pass to the structural analysis by modeling the structure in 3D and using the data obtained from the heat transfer analysis.

Afterwards, the work continues with the performance of the structure that was damaged by the Kobe earthquake; a simple analytical approach was used to estimate the damage in the structure and to determine the material mechanical damage. A pushover analysis is carried out until the maximum drift is reached on the ground floor of the structure.

To the analysis of heat transfer, the damaged parts of the building are taken into consideration.

2.1.1.5 Behavior of moment-resisting tall steel structures exposed to a vertically traveling post-earthquake fire - Behnam, B. et al. 2013

The paper investigates the behavior of moment-resisting steel tall structure that was subjected to post-earthquake fire. In particular, the purpose of this research is to understand the vertically traveling of the fire in three different starting points: first, fourth and seventh floor.

In this work, the case study was a ten-story steel resisting frame with wall, floor and ceiling in standard brick and concrete.

An analysis of the non-linear post-earthquake fire divided into three phases is carried out. The first step is apply the gravitational loads to the structure and the loads are kept constant throughout the procedure.

Then the seismic simulation was performed using the pushover analysis, with the SAP2000 program; the structure is subjected to a monolithic lateral load which is increased

until it reaches a certain level of displacement. The FEMA 356 procedure is used to calculate the level of movement needed to reach the level of performance required by the destination use of the building.

Finally, the data of the fire are inserted and the structure analyzed. To the thermal and structural analysis, the researchers used the SAFIR program with the natural fire curves to perform a time-temperature curves and they consider three different fire scenarios with the firing of fire on the first, fourth and seventh floors of the structure.

2.1.1.6 Post-earthquake fire performance of moment resisting frames with reduced beam section connections – Memari, M. et al. 2014

The research was focused on the effect of a small section of the beam-column joint of an unprotected structure. The nonlinear dynamic analysis and the thermal-mechanical analysis were used to estimate the effect of the fire following earthquake.

The simulation was realized using three different steel structures: low-, medium- and high-rise building was designed in according to the Unified Building Code (to Los Angeles, CA) to resist a strong earthquake and with perimeter steel moment resisting frames 2.1. To develop and analyze the building models, the software ABAQUS was used.

Various verification analyzes are carried out to confirm the modeling process, including a verification of the dynamic characteristics of the steel and one on the thermo-mechanical analysis. As regards the verification of the dynamic characteristics of the steel, an eigenvalue analysis is performed in order to obtain the first three vibration periods of each structure.

To simulate the earthquake, the researchers used a nonlinear time-history analysis; was select 5 near-field and 5 far-field record to the simulation. The evaluation of the structural performance of the models was made in accordance with ASCE Standard 41-06.

The parametric fire curve present in the Eurocode 1 was used to perform the numerical

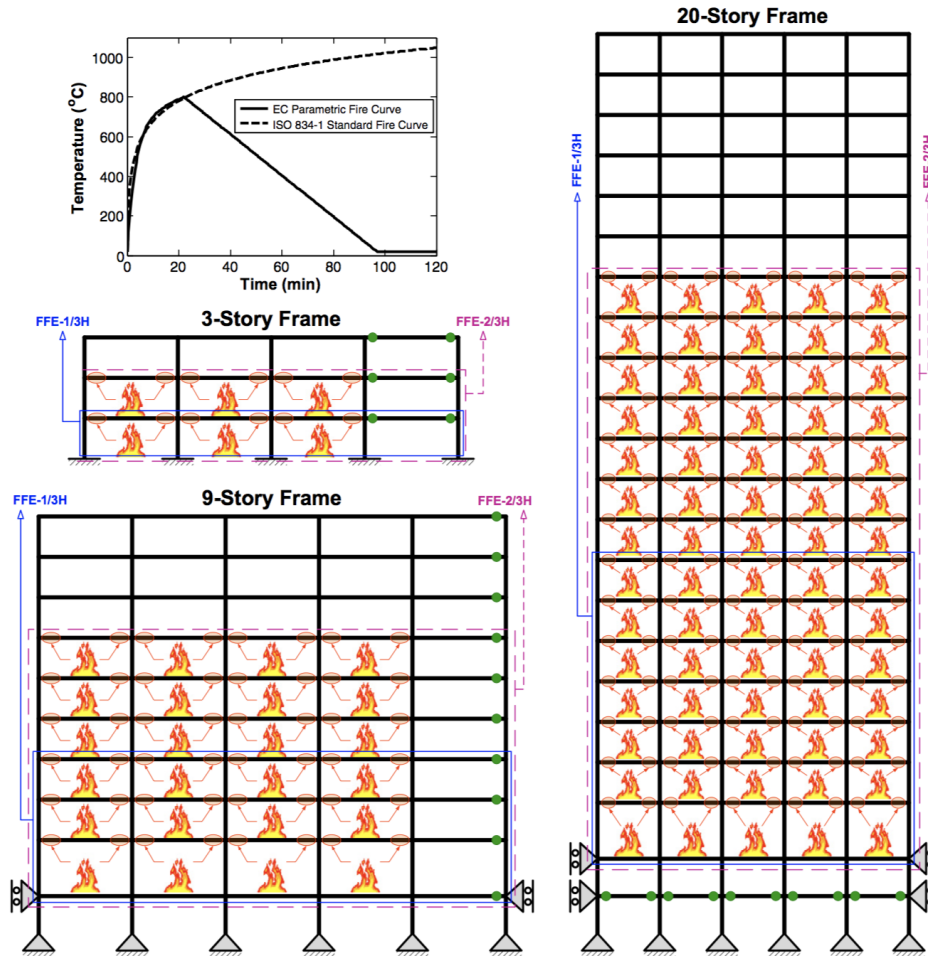


Figure 2.1: The three different frames that are used in the simulation; the picture is taken to the paper.

analysis of the realistic fire event. In fact it has the ability to represent the three different phases in a fire event: the initial heating phase, the cooling phase and the constant room temperature phase. The researchers create two post-earthquake fire scenarios for each structures: at one-third and two-thirds of the height.

2.1.1.7 Post-Earthquake Fire performance-based behavior of unprotected moment resisting 2D steel frames - Behnam, B. et al. 2014

In this studies, the researcher analyzes two steel moment resisting frame designed with two different occupancy proposes. The structures were subject to an earthquake load and the pushover curves were used to subsequent fire analysis, standard and natural fire model. In the end, the results were compared with the fire analysis of an undamaged structure.

The authors design one structure but with different design level of performance to the analysis: the frame was designed to Immediate Occupancy (IO) and to Life Safety (LS) level.

In a seismic analysis, the structure is loaded until the desired load level is reached and then discharged; It is similar to the pushover analysis. After was made a pushover analysis with the SAP2000 software and the FEMA procedure is used to define hinge position and properties.

Using the rules of the Eurocode 1, the natural fire method was used to investigate the structural response of the damaged structures. By importing the structural model in the target displacement phase in the SAFIR program, the discharge is immediately followed by the fire loads.

The researchers decided to analyze the damaged and the undamaged structures to each design level performance using the ISO 843 fire model and the natural fire model to compare the results.

2.1.1.8 Probabilistic Evaluation Framework for Fire and Fire Following Earthquake - Khorasani N.E. et al. 2016

The purpose of the research was to evaluate the performance of a structure subjected at post-earthquake fire in a probabilistic framework: the structure's response was analyzed

for several limit states and incorporate uncertainties in demand and capacity parameters. After that, the framework was applied on a steel moment resisting frame and evaluated to post-earthquake fire with different fire location and fire scenarios. The result of the work is a probabilistic model that takes into account different uncertainties such as fire load, yield strength, and high temperature steel elasticity modulus.

Furthermore, this paper is a starting point for developing guidelines to include uncertainties in performance-based design. Normally, the guideline to fire design consists in three steps: determining the design fire, performing thermal analysis, performing a structural analysis that considers the thermal load.

In this work, these guidelines were implemented: using literature data it is possible to develop probabilistic fire load models and the mechanical properties of steel at elevated temperatures; using the probabilistic models, a structure that serves to evaluate structural performance under fire and post-earthquake fire was developed; modeling seismic and thermal analyzes in a single programming environment.

The research model is a 9-story steel moment resisting frame. To perform the post-earthquake fire analysis, the earthquake selected was the 1989 Loma Prieta.

The structure was analyzed to multiple fire scenario and the time-temperature curve is calculated using the Eurocode 1. It is assumed that the compartment has no working fire-fighting measures and that the passive protection has been severely damaged by seismic shocks.

To evaluate the structure's performance, the two main mechanical properties of the steel are analyzed: the modulus of elasticity and the yield strength with a 2% tension that are formulated in the Eurocode 3. A routine Monte Carlo is used to reliability analysis in the process where there are uncertainties.

To evaluate the seismic and the thermal analysis of the structure is used the OpenSees program; the structure is model with elastic beam-column element and the connections is

designed with a zero-length elements. The model and its constraints are modified and adjusted to the passage of the seismic analysis to the thermal one. To perform thermal analysis with OpenSeel, the researchers used the *dispBeamColumnThermal-type element*.

At the end of the analyses, the researchers can compare the results obtained on the performance of a structure both in case of fire and in case of post-earthquake fire.

2.1.1.9 Behavior during seismic aftershocks of r.c. base-isolated framed structure with fire-induced damage - Mazza, F. 2016

The purpose of this work is the analysis of a reinforced concrete structure after an earthquake and the consequent fire. In the paper, the crucial element that was investigated is the elastomeric bearing that was placed in the basement of the building.

The study model is a six-story reinforced concrete frame structures; the ground floor has been designed with elastomeric bearings.

A basic-insulated test is carried out with the vertical and horizontal seismic loads proposed by the NTC to verify the structural dimension. Three values of the nominal rigidity ratio which correspond to a vibration period in the horizontal direction and to three periods in the vertical direction are selected and tested.

For the fire scenario, the researchers compared three different levels of trigger point: in the base-isolated level, in the first and in the last floor. The temperature was considerate uniform in each compartment and they used the time-temperature fire curves of the Eurocode 1.

With the use of the ABAQUS structural program, a transient analysis corresponding to the time-temperature curves of the elastomeric bearing was used; the output are the thermal mappings of the bearing and the structures and their respective resistances to the fire.

Afterwards, an incremental dynamic analysis is performed to evaluate the effect of the horizontal and vertical components of the aftershocks. In order to simulate the non-linear

dynamic response of the damaged structure, a computer code is implemented. This analysis is interrupted once the last limit state of the superstructure or of the insulation system at the base has been reached. For each ground motion was performed a time-histories of the horizontal component of the acceleration and are projected along the direction of the strongest observed pulse.

2.1.1.10 Outcomes of a major research on full scale testing of RC frames in post earthquake fire – Shah, A.H. et al. 2017

The study is based on the persistence of a real model in reinforced concrete that suffers the fire after the earthquake; the effects of the damage caused by earthquakes, the damage to the armor and the performance of the frames subjected to fire are examined. To record all the data, various sensors are mounted that detect thermal and kinematic fields during the tests.

For this research, a full scale reinforced concrete frames was built: two frames were designed in accordance to the guideline of IS 13920:1993 and the other two in accordance to the Indian standard code IS 456:2000.

Measurement instruments are inserted to record data regarding temperatures, displacements and deformations of all structures.

The test consists in three phases: simulated cyclical lateral load in a quasi-static fashion, one-hour compartment fire and residual load test. To the first step, two double-acting hydraulic actuators are used to simulate the ground motions in both directions.

To the fire simulation, the reinforced concrete structure was closed with infill. Several preliminary tests are carried out in order to design the volute fire load: the fire torch is kerosene and the duration of the fire is about one hour with the constant temperature inside the compartment. Moreover, the fire was designed to quickly accumulate the smoke in order to improve the flash-over.

After the fire test, the panel was removed and the structure was tested again under cyclical lateral load to analyzed the residual lateral strength.

2.1.1.11 Post-earthquake fire resistance of steel buildings - Jelinek, T. et al. 2017

The paper compared the response of two different frame: the first was subject to the fire following earthquake and the second was subject to fire only. The comparison was made between the time collapse after the failure progression that was caused by the post-earthquake fire and the one to the undamaged structure is subject to a direct fire only.

The structure analyzed is a five-story moment resisting frame without fire insulation and the join beam-column was considerate rigid. The structure was modeled in 2D with the program ABAQUS.

The analysis of the post-earthquake fire was carried out in three steps. The first step consists of a static linear analysis of the structure under gravity loads; the combination of loads was calculated using the Eurocodes.

In the second phase, 7 different accelerograms of European and American earthquakes, plus an artificial one, are chosen; a non-linear dynamic implicit analysis is then performed with the selected acceleration stories applied to the structure. To ensure the development of plastic deformations in the frame, the accelerograms are scaled.

In the last phase, an implicit dynamic non-linear analysis is again proposed: in this case the effects provoked by the hypothesized fire are considered, i.e. the transitory effects that the structural elements undergo when exposed to temperature increase. The selection of fire scenarios is based on the assumption that in each compartment of the structure the fire may break out.

The fire was modeled with a standard fire curve described in the ISO 843; with this curve, the the ventilation and the insulation of the structure weren't important to the

computation.

2.1.2 Territorial scale

2.1.2.1 Post-Earthquake Fire Spread between Buildings - Estimating and Costing Extent in Wellington - Thomas, G.C. et al. 2003

Using the geographic information system model, GIS, of the city of Wellington, this research investigates and estimates the losses of the fire following earthquake on a territorial scale. Two different approaches are used in the work: a static buffering technique with a set of rules and a dynamic cellular automation technique.

The use of the GIS model allows to insert all the data necessary to reproduce an accurate model of the city of Wellington. The work is divided into two approaches: a static buffering technique and a dynamic cellular automation technique.

In the static approach, using the radiation calculation, the researchers determined that the fire can not propagate at a distance of more than 12 meters; with this data, they create a "buffer zone": it's a space around all the buildings of 6 meters (2.2). When the buffer zones of two buildings come into contact or overlap, fire propagation is possible. In order to stabilize the losses and damages due to fire, the ignitions on buildings are randomly distributed and the process is repeated several times.

In the dynamic approach, all the building was regarded combustible; in order to create an accurate model, a set of rules based on a combination of historical data and fire physics has been set up. This model use a cellular automation spread technique: the landscape is modeled in a regular cell in order to create a grids with a size of 3 meters; in each cell is set a set of states and values that describe the physical environment of the city.



Figure 2.2: The buffer zone create in the district of Wellington; the picture is taken to the paper.

2.1.2.2 Post-Earthquake Fire Spread between Buildings - Correlation with 1931 Napier Earthquake - Thomas, G.C. et al. 2006

The analysis goal was to recreate the 1931 Napier earthquake, New Zealand, and to compare the software input with the original earthquake. The researchers used the static model to create a critical separation, the maximum distance that the fire can jump between the buildings. The dynamic model was used to make a correlation between the fire spread and the timing of the fire.

This work develops two models, one static and one dynamic, to test a real earthquake with the consequent fire spread.

In the static model, the idea of the buffer zone in the previous work is resumed. When the "buffers" touch or overlap, the buildings are made to belong to a "burn zone". In this case, the size of the critical separation depends on many factors, including the wind speed, the ground slope and the fire fighting. Different simulations were made with different



Figure 2.3: The fire spread in the simulation of the Napier city; the picture is taken to the paper.

sizes of the critical separation to produce a single “burn-zone”, as in figure2.3.

As in the previous model, a cellular automaton technique is used in the dynamic model and the program GIS is used to divide the map and input the proprieties of the landscape in the equal-size square cells. In this model, the wind speed was a fundamental data.

The dynamic model and the historical record of the earthquake of Napier are compared.

2.1.2.3 Development and validation of a physics-based urban fire spread model - Himoto, K. et al. 2007

This analysis describes and tests the fire spread model using the physics-based knowledge. In the first step the urban fire spread model was analyzed and set up; after that, a hypothetical city of three buildings type was designed : wooden building, mortar plastered wooden building and fire resistant building. Also the Monte Carlo simulation was used to carry out the expectation of the fire spread distance.

The rate of fire spread of the model is expressed as a system of algebraic equation. To obtain these functions, different macroscopic parameters that influence the fire are considered; for example, the wind speed, the type of material used in the construction, the size of the building, etc.

In this model, the fire spread in the city is described in two models: fire behaviors inside the buildings and building-to-building fire spread.

In the first model, the room of the building was regarded as a control volume and uniform physical properties; in the second model, the fire spread follows the mechanisms of thermal radiation, plumes of fire blown by the wind and spotting of fire.

Once all the initial equations have been set, the researchers proceed to verify the model with different simulations of the spread of the fire in a hypothetical urban area; in this way, the contributions of the propagation phenomena are quantified.

The hypothetical urban area is designed as a grid of 100 to 25 buildings with a separation of 4 meters between each building. Three different building materials are randomly assigned to the various buildings: wooden, mortar plastered wooden and fire resistant.

To obtain the fire expectations and the distance traveled by the propagation of the fire, numerous Monte Carlo simulations are performed for every numerical condition considered in the model.



Figure 2.4: Result of the fire simulation; the picture is taken to the paper.

At the end of the simulation, the authors simulated the Sakata fire in 1976 (2.4); the model appears to have discrepancies from the original because simplifications are used in the simulation: intermediate elements such as vegetation and vehicles are neglected, only part of the secondary origins of the fire are considered, rain and fire suppression systems are not considered.

2.1.2.4 Risk and Behavior of Fire Spread in a Densely-built Urban Area - Himoto, K. et al. 2008

These studies use the district of the city of Kyoto, Japan, as an example to investigate the propagation of the fire in a densely-built urban areas. The simulation used a physics-based model to recreate the mechanism of the fire spread; in the research the principal causes to the propagation of the fire, the probable location of fire origin and the eater condition of the city was identified. The Monte Carlo's method was used to analyze the risk of fire spread.

To model the fire spread the authors used the same assumption of the previous work: fire behaviors inside the buildings, with each room as a controlled volume and uniform physical properties, and building-to-building fire spread, with the contribution factor of thermal radiation, wind-blow fire plumes and spotting of firebrands.

The Monte Carlo simulation is used to estimate the risk of fire propagation. The researchers performed two series of simulations creating a list of numerical conditions that is used to distinguish the two simulations. In the first Monte Carlo simulation the origin of the fire is fixed and the number of tests is 100; the second simulation has a random distribution of the origin of the fire and is repeated 500 times. The conditions in common are the random burst time and the duration of the fire.

The weather data of wind velocity-direction and the ambient temperature is obtained by AMeDAS.

2.1.2.5 Earthquake Disaster Simulation System: Integration of Models for Building Collapse, Road Blockage, and Fire Spread – Hirokawa, N. et al. 2016

The study is realized to establish a city-damage simulation; the authors organize different models in a systematic manner. This model is placed in the Tokyo metropolitan area and they used the data of a hypothetical earthquake. At the end of the simulation, the researchers propose an index of fire and fire extinction that encompasses urban development and supports post-earthquake operations.

The work begins with the research of the fundamental data for the GIS modeling of the North Tokyo Bay area: some data, such as the material of the structure of the buildings and the construction date, are estimated; other data, such as the function of buildings, fire prevention systems and the number of floors, are detailed.

Also the road network and the landscape are analyzed and the information is imported into the model.

In this work, the building-collapse model is divided in two: the first model estimates the damage using a stochastic means and it is based on the data of a historical earthquake and the usage of the fragility curve; the second model is based on the calculation of the limit resistance of the seismic design and estimates the collapse using the seismic wave data. The first model is useful for large areas because it requires short computation time.

To analyze the street blockage, the researcher studies a microscopic model of individual building collapse: it is assumed that the collapse of the building causes the same amount of debris on all sides. Subsequently, a debris model divided in three parts is generated: the location of the building along the street, the building-collapse and the quantitative of debris, the estimation is based on a previous earthquake; the estimation of the probability street blockage.

The probability of fire outbreak caused by the earthquake is calculated by the percentage of different factors: the electrical heater, the buildings usage, the earthquake intensity, the time and the building collapse. Because fire comes from some buildings and depends on their characteristics, a model of fire-spread cluster is developed: this model estimates the groups of buildings that tend to ignite based on the critical distances of fire propagation: calculating the probability of fire for each building, the damage is estimated from the number of buildings burned.

The fire-spread simulations are performed; they are based on a non-stochastic fire-spread velocity and a stochastic fire-outbreak model.

Two new indexes are defined after the simulation: fire-spread potential and burnt-down potential. The first index helps to understand the priority of rescue, indicates the degree to which the surrounding buildings can burn if the firefighting actions are not carried out. The second is a quantitative index of the effect of building materials used to evaluate safety and firefighting actions; it indicates the probability that a building could ignite, considering the fire that flows from the target building and that it could catch fire due to

the surrounding buildings.

2.1.3 Summaries

In this part, there are three tables that illustrate the critical points of the different studies.

The first table summarizes the main aspects that are analyzed in the works concerning the steel structures, the second table shows the data concerning the studies on reinforced concrete frame and the last table shows all the data of the research carried out on an urban scale.

Title	Year	Structure	Analysis	Softwear
Post-earthquake fire resistance of moment resisting steel frames	2003	Single-storey Multi-storey	-Incremental Dynamic Analysis: 8 different earthquake - Parametrical analysis of simple portal frame - Evaluation of the fire resistance reduction of two buildings	SAFIR
On the structural effects of fire following earthquake	2005	Multi-storey	Parametric analysis - Two plan layout: perimeter frame and spatial frame - Two design strategies: ultimate limited state and serviceable limited state	FEMA OpenSEES SAFIR

Fire after earthquake analysis of steel moment resisting frames	2009	Two multi-storey	<ul style="list-style-type: none"> - Pushover: calculate the structure - N2: seismic event - Thermal: temperature distribution - Structural analysis: structure response 	Ozone
Behavior of moment-resisting tall steel structures exposed to a vertical traveling post earthquake fire	2013	10-storey moment resisting frame	<ul style="list-style-type: none"> - Thermal Analysis - Structural Analysis - Three different starting point: first, fourth and seventh floor 	SAFIR SAP2000
Post-earthquake fire performance of moment resisting frame with reduced beam section connections	2014	Low-, medium- and high-rise buildings	<ul style="list-style-type: none"> - Nonlinear time-history to simulate the earthquake - Time-temperature curves to simulate a realistic fire event 	ABAQUS v6.10

Post-earthquake fire performance-based behavior of unprotected moment resisting 2D steel frames	2014	Two moment resisting frame with different occupancy propose (IO and LS)	- Nonlinear Analysis - SAFIR Pushover Analysis SAP2000
Probabilistic evaluation framework for fire and fire following earthquake	2016	Moment resisting frame	- Seismic structural analysis - Thermal analysis - Monte Carlo: reliability analysis OpenSEES
Post-earthquake fire resistance of steel building	2017	Multi-storey	- Static linear: gravity load - Nonlinear implicit dynamic: acceleration histories - Non-linear implicit dynamic: temperature effect ABAQUS

Table 2.1: Steel structures

Title	Year	Structure	Analysis	Software
-------	------	-----------	----------	----------

Performance of a six-story reinforced concrete structure in post-earthquake fire	2010	six-storey	Analysis of the heat transfer Structural analysis Analytical approach: estimation of the damage in the material properties Pushover analysis: Kobe earthquake data	SAFIR
Behaviour during seismic after-shocks of r.c. base-isolated framed structure with fire-induced damage	2017	six-storey base-isolated	Three fire scenarios: in the basement, in the first and in the fifth level Indirected Dynamic analysis: evaluated the effect of the aftershocks	ABAQUS
Outcomes of a major research on full scale testing of RC frames in post earthquake fire	2017	two-story full scale	Simulated cyclical lateral load in a quasi-static fashion One-hour compartment fire and residual load test	-

Table 2.2: Concrete structures

Title	Year	Structure	Analysis	Software
-------	------	-----------	----------	----------

Post-earthquake fire spread between buildings - Estimating and costing extent in Wellington	2003	city of Wellington, New Zealand	Static approach: all building combustible Dynamic approach: set of rules to insert in the model Buffer zone Random distribution of ignitions	GIS
Post-earthquake fire spread between buildings - correlation with 1931 Napier earthquake	2006	Napier, New Zealand	Static model: fire spread Dynamic model: correlation between fire spread and timing Buffer zone	GIS
Development and validation of a physics-based urban fire spread model	2007	wooden, mortar plastered wooden and fire resistant	Monte Carlo: expectation of the fire spread distance Comparison with the Hamada-model	GIS
Risk and behavior of fire spread in a densely-built urban area	2008	district of Kyoto	Physics-based model: fire spread Monte Carlo: risk of fire	AMeDAS GIS

Earthquake disaster simulation system: integration of models for building collapse road blockage and fire spread	2016	district of Tokyo	Property-damage estimation Buildings collapses Street blockages Fire outbreak and fire spread Fire-spread potential and burnt-down potential	GIS
---	------	-------------------	---	-----

Table 2.3: Territorial scale

Programs

3.1 Fire Dynamic Simulator

FDS is a computer program developed by NIST. It is used to solve equations that describe the evolution of the fire and the smoke. It is a program that works from a text file as input and calculates the solution of the predefined numerical equations creating default output files and others that are specified by the user in the input file.

The calculation is visualized by the Smokeview program: it reads the output file and creates an animation which, according to the user set in the initial file, shows the fire rendering other parameters such as air movement, smoke, the separation of the temperature.

3.1.0.1 Structure of the input file

The input file that controls the FDS simulation can be written with any text editor or with the help of a graphical interface, such as *BlenderFDS*. This source file usually ends

with the extension *.fds*.

FDS simulation is initiated via the command prompt or through third-party GUI programs such as PyroSim.

FDS is based on a single ASCII file text that contains different parameters organized into namelist groups; all the information that are used to describe the simulation scenario are written in the input file.

The order in which the namelist groups are written in the input file is not important to the calculation of the simulation; FDS analyses the entire text file every time it processes a namelist group. Organizing the work in a systematic way can be helpful in processing the input file: it is generally recommended to enter the general data of the file in the initial part, the detailed information regarding the obstacles and the characteristics of the fire-beater in the central part and information of output files at the end of the input file.

The parameters that are inserted in the input file are mainly numbers, integers and reals, strings of characters or logical parameters such as true and false. It is important to write character strings correctly because the program is sensitive to punctuation, especially underscores, and upper and lower case. Most of the parameters to be inserted are simply real or whole numbers and in some cases are multidimensional arrays.

3.1.0.2 Setting the namelist

Generally, the project involves numerous simulations; for this reason, the setting of the name project is important.

HEAD is the namelist group that is used in this phase; this group contains two principal parameters:

- CHID: indicates the Character ID; it is a string that can contain up to 40 characters and is used to name output files.
- TITLE: is used to describe the simulation and can contain up to 256 characters.

TIME is the namelist group that contains all the parameters that define the duration of the simulation.

- T_END: is the duration of the simulation, the default value is 1 s; if this parameter is set to zero, the program set-up only the geometry in Smokeview.
- T_BEGIN: is the parameters used if the simulation starts at a different time than zero.

MESH is the namelist group that concerns the computational meshes. To perform the simulation correctly, the FDS calculations must be performed within a domain formed by straight volumes, the mesh. Each mesh is divided into rectangular cells that define the resolution of the simulation.

The coordinate system of the mesh is conforming to the right-hand rule.

- XB: indicates the coordinates of the mesh; the first, third and fifth values of the real number indicate the coordinates X, Y and Z, of the origin point, and the second, fourth and sixth values indicate the coordinates of the opposite corner.
- IJK: is the parameters that controls the division of the mesh into uniform cells.

MISC is the namelist group that defines various global parameters of input; they are parameters that do not fit logically in the other categories.

- TMPA: is the parameters used to set the ambient temperature inside the simulation.
- RESTART: is used when one intends to interrupt the calculation; it is a parameter that is inserted when you want to modify a simulation during the calculation to make changes and restart the simulation from the interruption rather than from the beginning.

INIT is the group of parameters used to modify the initial conditions of the simulation. With FDS, many environmental parameters such as density and air pressure are predefined;

with the commands of this group it is possible to define rectangular regions within the domain that modify the environmental conditions.

3.1.0.3 Build the model

The most important part of the calculation work consists in specifying the various geometries present in the working space and applying all the necessary boundary conditions: the geometries are described as rectangular obstructions that can undergo various physical factors such as heat, burn, conduct heat. , etc., and openings where air or liquids can pass. It is necessary to understand the purpose of the simulation in order to assign the correct conditions to the contour that describes the thermal properties of each geometry inserted in the simulation.

SURF is the name of the group that identifies all the parameters that define the surfaces of the structure. When creating geometries, FDS creates default conditions of boundary of the surfaces: fixed temperature and smooth walls that are referred to as "INERT"; if you wish to modify these parameters, it is advisable to insert the SURF lines to the input file with the appropriate indications.

- SURF_ID: is the string of characters that is inserted in the lines OBST and VENT to indicate the type of SURF that contains the parameters of the desired boundary conditions.

OBST is the namelist group that is used to define the obstruction. It is necessary to insert the coordinates of the solid with XB.

- SURF_ID: is the parameters used to specify the typology of surface. This parameter indicates the SURF line that is applied to specify the surface of the obstruction.
- SURF_IDS: is used when the obstruction has three characters strings that define the top, sides and bottom of the obstruction.

- SURF_ID6: when all the surfaces of the obstruction are different.

HOLE is used to create holes in the obstruction. The namelist group define the cut-out parameters.

VENT is used to describe the proprieties of the planes adjacent to obstruction or the external walls. Also in this group there is the parameters SURF_ID, but the program has three surfaces reserved for this group: they are characters that do not have to be defined manually by the user but have predefined properties:

- OPEN: it is used to the external boundary of the domain; it is an open boundary that allows the passage of flows.
- MIRROR: it is used on the external boundary of the domain and indicates a symmetry plane: it serves to double the size of the domain acting as a symmetrical plane but without allowing the passage of the flows.
- PERIODIC: it is used in combination with another periodic VENT on the domain boundary.

In FDS, some characters are used for different groups, an example is the coloration of the geometry: is the same character used to obstructions, vents, surfaces and meshes.

For a better visualization of the simulations, it is useful to assign different colors to the objects in the scene; the program has three ways to assign a color to a geometry and to set textures.

- COLOR: this character permit to insert the name of the color, the correct character is listed in the color table in the manual of the programs "User Guide".
- RGB: is used to insert the color given the three whole numbers RGB ranging from 0 to 255.

- `TEXTURE_MAP`: in this parameter, you have to insert the 'image name' that you want to use as texture in the simulation; it is important that the *.jpeg* file is in the workbook so Smokeview can read the file. It is important also write the parameters `TEXTURE_WIDTH` and `TEXTURE_HEIGHT` because they indicate the physical dimension of the image.

3.1.0.4 Thermal Boundary Condition

All the parameters concerning the thermal properties of the materials are entered by the user. These data are very important to find and insert because the fires are sensitive to the thermal properties of the materials. Moreover, the physical phenomena that arise from the simulation can undergo variations with respect to reality due to the limitations of some algorithms.

The SURF group has numerous parameters that are used to set the thermal properties of the objects.

- `BURN_AWAY`: it is a logical parameter that allows to eliminate an object that is consumed by flames.
- `HRRPUA`: is the heat release rate per unit area.
- `HEAT_OF_VAPORIZATION`: to control the energy that is used to vaporize the fuel.
- `IGNITION_TEMPERATURE`: it is used to delay the explosion of the fire; the trigger is delayed until the desired temperature is reached.
- `MALT_ID`: indicate the material required to the surface. This parameter indicates the MALT: line that is applied to specify the material properties.
- `MATL_MASS_FRACTION`: define the layers of the material, indicate the thickness.

- MLRPUA: is the mass loss rate of fuel gas per unit area.
- RAMP: it is a convention that serves to specify temperature-dependence.
- SPREAD_RATE: it is used to indicate the velocity of the fire.
- TMP_FRONT: it is used to fix the temperature boundary condition of the surface.

MALT is the namelist group used to define all the proprieties of the materials. In this group is possible to write the thermal proprieties of the materials.

- HEAT_OF_COMBUSTION: it is used when the combustion heat of the gaseous species is greater than zero. It is the energy that is released, per unit of volume, when the combustible gas is mixed with oxygen and combustions.
- HEAT_OF_REACTION: is the amount of energy consumed, per unit of mass, when a reagent is converted into reaction products; is the difference in enthalpy between reagents and products. It is used only for simple phase change reactions.
- N_REACTIONS: it is used to indicate how many reactions the material undergoes during the calculation period.
- SPEC_ID: indicates the gas species.

With the namelist group ZONE it is possible to specify the compartments in the computational domain that can have their own "background" pressure. FDS, at the moment, does not have an algorithm that identify automatically the zone with a different pressure; it is therefore necessary to specify this area in the input file.

The namelist group WIND contains all the parameters that are used to model the wind inside the simulation. With FDS is possible to model the wind in three different ways:

- The first method is the simplest to used in the simulation. It is based on the theory of Monin-Obukhov. This method was implemented in the version 6.6.0 of FDS.

- The second method is more complicated; to allow the wind field to develop normally, it is necessary to specify a normal uniform forcing function; this method is useful to model the wind tunnels.
- The third method was used in the older version of FDS and is the least recommended method for modeling the wind. In this case a "wall of wind" is modeled on an edge of the computation domain that transforms into a gigantic fan that blows air in a single direction; this method is the least recommended for modeling the wind.

The principal parameters used in the computation of the wind are:

- Z_REF: FDS assumed that the wind speed is taken at 2 meters off the ground; this parameter is used when the height of the wind speed is different.
- DIRECTION: is the angular direction of the wind: 0° corresponds at a wind that blows from north to south or in negative Y direction in the FDS coordinate system; 90° corresponds at a wind that blows from east to west or in negative X direction in the FDS coordinates system.
- L: characterizes the thermal stability of the atmosphere: if this number is positive, the atmosphere is stably stratified; if the number is negative, the atmosphere is unstably stratified.

In FDS there are many parameters that have fixed constant; the namelist group RAMP and TABL it is used to control the behavior of the parameters that can vary over time, temperature or space. The namelist group RAMP is used in the case is necessary to specify a function with one independent variable (for example the time) or one dependent variable (for example the velocity). The TABL namelist group is used in the case is necessary to specify a function with multiple independent variable (for example a solid angle) or a multi dependent variable (for example a sprinkler flow rate).

The RAMP is used to control the rate at which things turn on or off by specifying the time-history.

- T: is the parameters that define the time.
- F: is the parameters that define the fraction of the heat release rate, the temperature, the velocity, etc...
- TAU_Q, TAU_T, TAU_V: are the parameters that are used to modify the heat release rate (HRRPUA), they controls the values that must reach the surface temperature (TMP_FRONT), the normal speed (VOLUME_FLOW) and the total flow (MASS_FLUX_TOTAL).
- RAMP_U0_T, RAMP_V0_T: are used in the namelist WIND to change the velocity of the wind in function of the time.
- RAMP_U0_Z, RAMP_V0_Z, RAMP_W0_Z: are used in the namelist WIND to change the velocity of the wind in function of the height.

FDS was created to study the phenomena of fire, so the basic chemistry of combustion is already inserted into the program and the user has to enter, in the input file, only some data. The namelist group SPEC contain all the parameters of the gas species that are in the simulation; it is used to define primitive gas species and concentrated species.

The namelist group REAC contain the parameters that control the combustion. In FDS, combustion is divided into gaseous phases and pyrolysis solid phases: the first relates to the reaction of fuel and oxygen vapor; the second is the generation of fuel vapor on a solid or liquid surface. In the calculation, FDS automatically adjusts the combustion rates of solids and liquids based on the difference in calories of combustion of the various fuels; in the input file you specify a single gas phase reaction as a surrogate for all potential fuels.

The principal parameters that are used in this namelist group are:

- FUEL: it is a character string that is used to identify the fuel species to the reaction.
- CO_YELD: it is the parameters that indicate the fraction of fuel mass converted into carbon monoxide.
- SOOT_YELD: it is the parameters that indicate the fraction of fuel mass converted into carbon monoxide.
- FORMULA: it is a character string that is used to identify the chemical formula of the fuel species in the reaction.
- C, H, O, N: it is another solution to insert the chemical formula of the fuel species, in this case the value to insert is the number of the particle of carbon, hydrogen, oxygen and nitrogen.

PART is the namelist group of the parameters that are used to describe the Lagrangian particles: it is used to represent numerous small object items that can be resolve on the numerical grid.

The namelist group DEVC is used to model devices that work easily depending on the properties assigned to them. Sprinklers, smoke detectors, heat flow meters and thermocouples are some device that can be used to record some quantity in the simulation or, in some case, can be used as a timer to activate events.

- CTRL, PROP: it is the parameters that indicate the namelist group that define the advanced functionality and the proprieties.
- QUANTITY: it is used to define the output that the user wants to record from the devices.

The namelist group PROP is used when the simulation there are complicated device and it is inconvenient to describe all the proprieties in the DEVC line. The PROP lines are identifying by a unique ID that is contain in a DEVC line; each device have a list of

various proprieties. In the "User Guide" are list different device with the corresponding proprieties.

The namelist group CTRL is used to advanced control function.

3.1.0.5 Output file

The FDS, during the simulation, create various type of output files with the computed data. Some files are comma-delimited text file, other are files in binary format that are read and rendered by Smokeview. Some files are automatically set by FDS and other files are written in the input file by the user.

In namelist group DUMP are specify the parameters that control the rate at which output files are written and other global parameters that are associated at the output files.

The PROF namelist group contain the parameters that are used to record the output files of the properties of the solid over the entire thickness. The parameters that are used in this group are similar to the DEVC group.

The SLCF namelist group parameters is used to record various gas phases quantitates. This group is different from PART because the quantities are record on a line, plane or volume according to the sextuplet XB that indicates the boundaries of the "slice" plane.

The BNDF namelist group parameters allows to record surface quantities at all solid obstructions. This group is indicating with a separate line and does not need be specified the physical coordinates. For some output quantities is possible to add parameters with the character string PROP_ID in this group.

The ISOF namelist group is used to obtain three-dimensional animated output of the gas phase.

3.2 Smokeview

Smokeview is the post-processor of FDS. It is a scientific software designed for the visualization of the fire model calculated by a CFD, a computational fluid dynamics model of fire driven fluid flow, and CFAST, a zone model of compartment fire phenomena.

FDS and Smokeview are mainly used for simulation and visualization of phenomena related to fire. Another use of this processors is to model phenomena related to contamination and evacuation flow: with Smokeview it is possible to visualize the flow of particles that move within an environment over time and, together with other software like EVAC, it is possible to simulate an emergency situation where it is necessary to see the flow of people leaving the burning building.

Smokeview can be launched during all phases of the simulation calculation: before starting the simulation it can be used to display the model geometry; during the computation of the model it is possible to see the progress of the simulation and if it is necessary to intervene in the input file to modify some data; at the end of the calculation to display the finished simulation.

3.3 BlenderFDS

Blender is an open source program used to create graphic and animation elements. By installing the FDS tools, it is possible to model the basic elements for simulation. Mainly, the program is useful in order to model the meshes and the geometries with the consequent coordinates that require FDS.

In the FDS window it is possible indicate the head chid, the title and the destination folder of all the files that the simulator performs by default and those used for the analysis of fluid dynamics. It is also possible to enter data related to the simulation time, the reagent used to trigger the fire and all the output files that you want to get to analyze

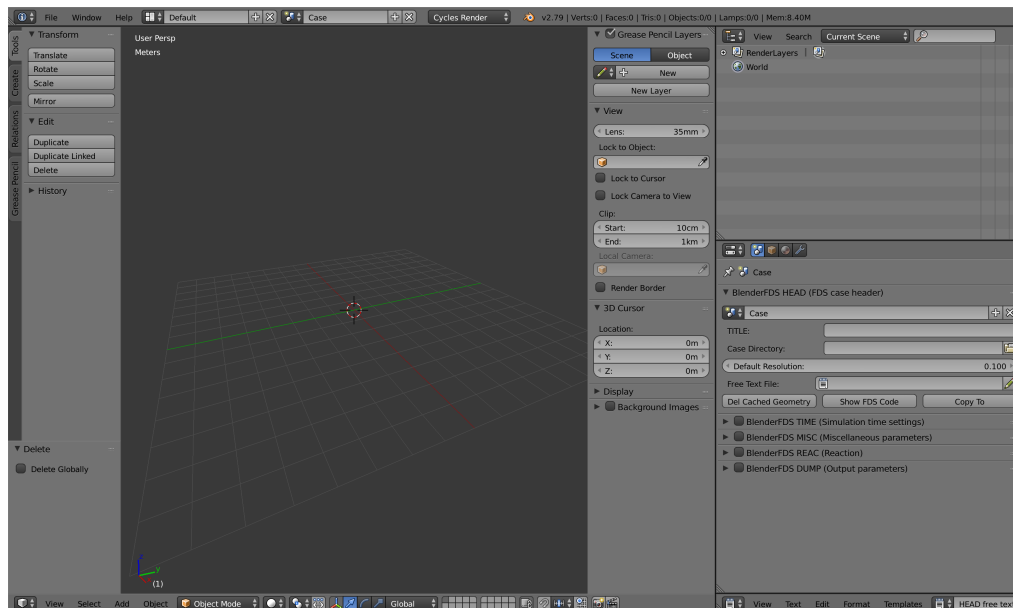


Figure 3.1: Graphic interface of Blender

the simulation.

Once the desired scene has been modeled or imported, it is possible to define the various geometries and to indicate the FDS categories to which they belong; you can go to indicate the types of elements, the types of surfaces and all the boundary conditions that affect the model.

At the end you can go to export a script file that can be edited with a text editor to add all the other parameters that you want to add to the simulation.

3.4 Pyrosim

Unlike Blender, with PyroSim it is possible to watch the calculation of the simulation in real time. PyroSim is a graphical interface that allows you to model the simulation environment or import 3d files in DXF or DWG format.

This program was developed to be able to perform useful simulations in the pre-design phase, to reconstruct the fires that occurred and to assist the fire brigade during the

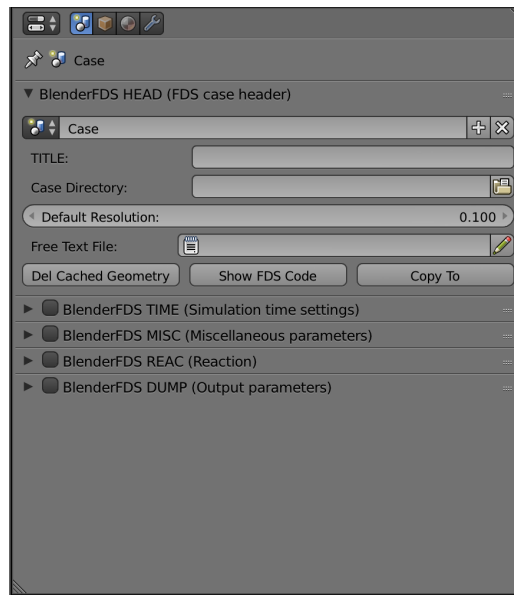


Figure 3.2: FDS input file modeling menu

training.

There is no need to download additional features to be able to use FDS; the part of fire analysis is already included in the program.

A very useful feature in PyroSim is to create complex 3D objects and analyze them without having to go through the voxelization option like BlenderFDS.

It is also possible to divide the objects present in the model into groups with the same features to facilitate the insertion of the parameters.

All parameters that are used in FDS are easily traceable in the program interface: for each namelist group there is a specific window that allows you to set all the parameters that you want to insert in the simulation.

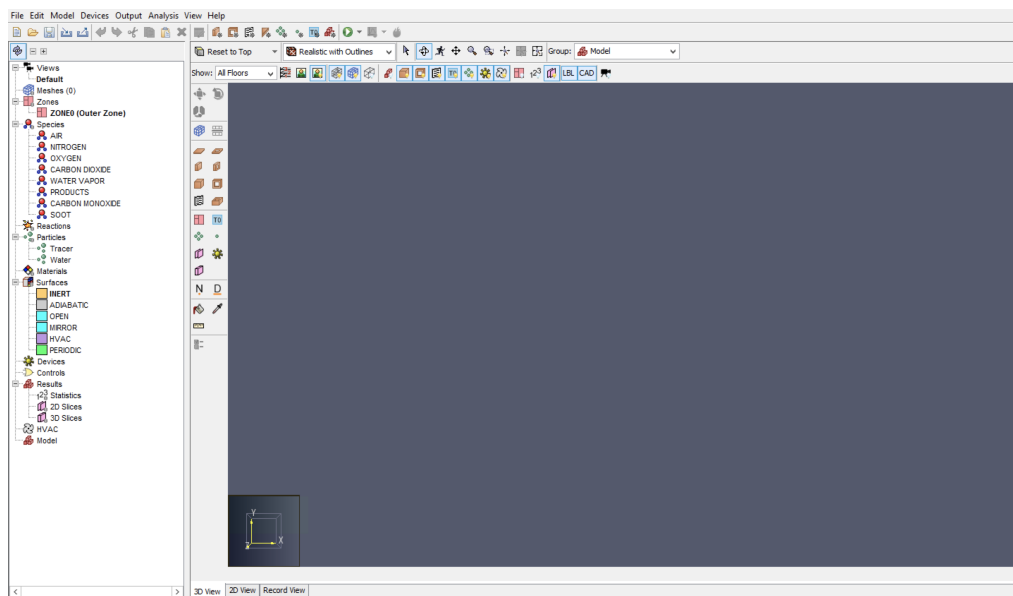


Figure 3.3: Graphic interface of PyroSim

Validation

To validate FDS before starting with the simulations, several studies analyzing the behavior of the fire in the various materials were read and studied.

The search for "Experimental investigations of the fire behaviour of facades with EPS exposed to different fire loads" of Northe et al. 2016 is the one where the number of useful information is inserted in order to reconstruct the scene through FDS.

The tests in this research were carried out at the Materialprüfanstalt Dresden in Freiberg. The researchers perform four fire tests on a flat facade with an external thermal insulation composite systems based on polystyrene with fire loads on the ground.

The first phase of the research consists in analysing different fire scenarios at the base of the facade; some pre-tests are performed that simulate the burning of trash containers that can commonly be found on the street. Fires not enclosed in containers to simulate the liquid fire are performed to hypothesize the situations where to catch fire are materials such as EPS that once melted.

For large-scale tests, 300 mm thick walls made of EPS and XPS are made, on which a layer of plaster, a reinforcement mesh and an upper layer of plaster are applied to make

flat walls. The dimensions of these walls change according to the tests: for the first two tests a 6 meters wide and 8 high wall is used, for the other two tests the wall remains 6 meters wide but 9 meters high.

The first test is used as a calibration test, in which the results obtained from the first small-scale experiments are tested. The second and third tests are the result of the improvements that are made by observing previous tests. The last test is carried out to observe the influence of the openings in the façade surface.

4.1 Creation of the input file

To carry out the simulation using FDS, it was decided to model the second experimental test of the research mentioned above.

Using initially Blander FDS it was possible to define the geometry of the simulation creating a wall of 6 meters wide and 8 meters high and the thickness of 0.3 meters. The solid that forms the facade was divided into two halves to allow data to be entered in the XPS, in the base of the facades, and of the EPS, in the upper part. All data relating to the layers of plaster and plaster are inserted directly into the code to simplify the basic geometry (4.1).

The inigation point is inside a steel pan with a volume of 200 l; this cooling pan have a size of 1.30m × 2.80m × 0.31 m and rapresent the pool fires where the fuel burn. In this test, for the ignition the fuel isopopropanol was used. This element simulates the fire that could happen inside a

Once the geometric modeling is over, the code file, that must be modified to insert all the fundamental data for the simulation, is exported from Blender and imported into Pyrosim.

The thermal parameters of the various materials used in large-scale tests were provided

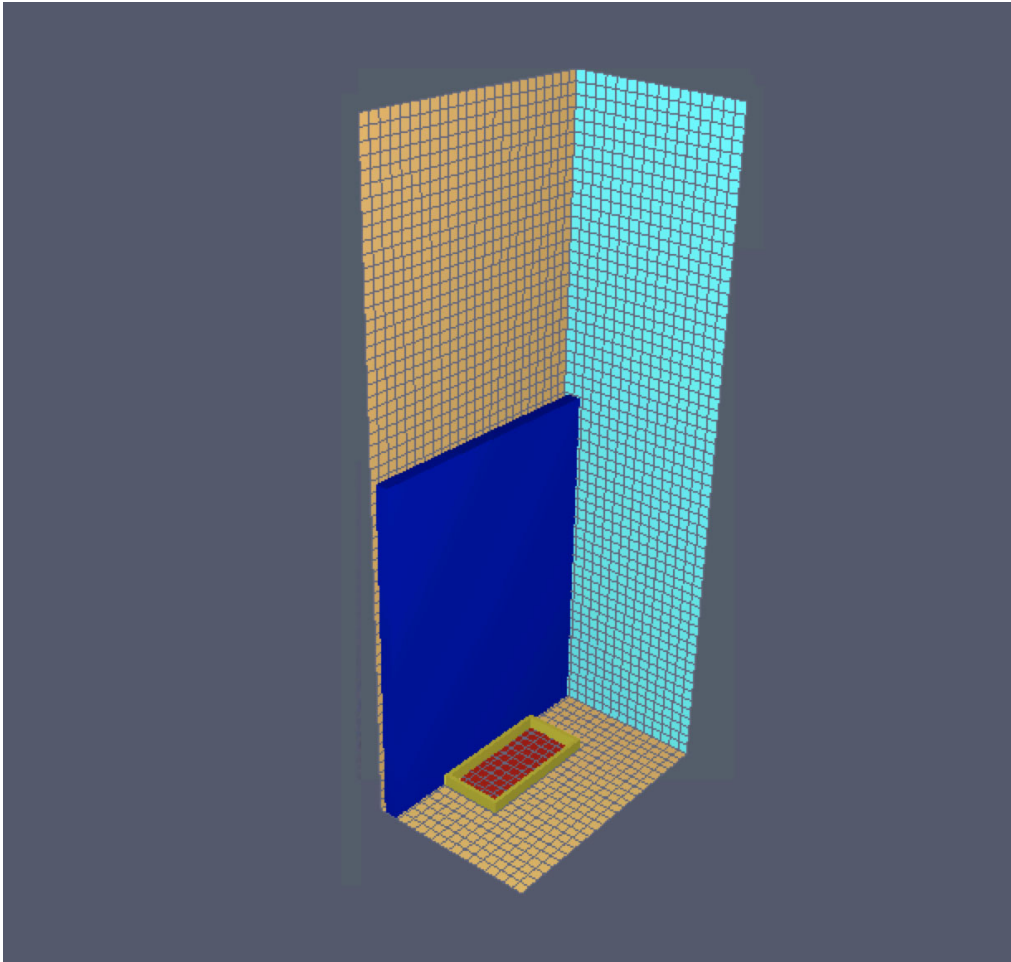


Figure 4.1: Visualization of the geometry using BlenderFDS

by the authors of this research because they were not specified.

```
&SURF ID= ' Pool ' ,  
      RGB=204 ,199 ,0 ,  
      HRRPUA=100.0 ,  
      TAU_Q=150.0 ,  
      IGNITION_TEMPERATURE=50.0 ,  
      MATL_ID(1,1)= 'STEEL ' ,  
      MATL_MASS_FRACTION(1,1)=1.0 ,  
      THICKNESS(1)=0.05 /
```

```
&MATL ID= 'STEEL '
      FYI= ' Properties□completely□fabricated '
      DENSITY=7850,0
      CONDUCTIVITY= 45,8
      SPECIFIC_HEAT= 0,46
      EMISSIVITY= 0,95
      SPEC_ID= 'METHANE' /
```

This part of the code describes the characteristics of the wooden container: : the typical characteristics of the pine wood are chosen for the simulation.

```
&SURF ID= ' WallLower ' ,
      RGB=0,0,204 ,
      MATL_ID(1,1)= 'XPS ' ,
      MATL_ID(2,1)= 'PLASTER ' ,
      MATL_MASS_FRACTION(1,1)=1.0 ,
      MATL_MASS_FRACTION(2,1)=1.0 ,
      THICKNESS(1:2)=0.3,0.5 /
&MATL ID= 'XPS ' ,
      FYI= ' Properties□completely□fabricated ' ,
      SPECIFIC_HEAT=1.5 ,
      CONDUCTIVITY=0.035 ,
      DENSITY=30.0 /
&MATL ID= 'EPS ' ,
      FYI= ' Properties□completely□fabricated ' ,
      SPECIFIC_HEAT=1.5 ,
      CONDUCTIVITY=0.044 ,
```



```
DENSITY=35.0/
```

In this part of the code, the main data of the lower part of the wall is inserted; this part of wall is the one where the XPS is located.

```
&SURF ID= ' WallHupper ' ,  
      RGB=0 ,0 ,204 ,  
      MATL_ID(1 ,1)= ' EPS ' ,  
      MATL_ID(2 ,1)= ' PLASTER ' ,  
      MATL_MASS_FRACTION(1 ,1)=1.0 ,  
      MATL_MASS_FRACTION(2 ,1)=1.0 ,  
      THICKNESS(1:2)=0.3 ,0.5 /
```

In this last piece of code, the data relative to the upper part of the facade is indicated, which is formed by ESP.

To simplify the calculations and not having to write too many different materials for the simulation, the layers of plaster, reinforcement mesh and plaster were inserted as a single layer with the characteristics of a general cement plaster.

4.2 Simulation

At the finish of the computation, it is possible to observe the result with the viewer of Pyrosim; the effect is similar to SmokeView but the visualization is more realistic how as shows in the picture.

Now it is possible to compare the result of the simulation realized with the real fire test created by Northe et al. 2016.

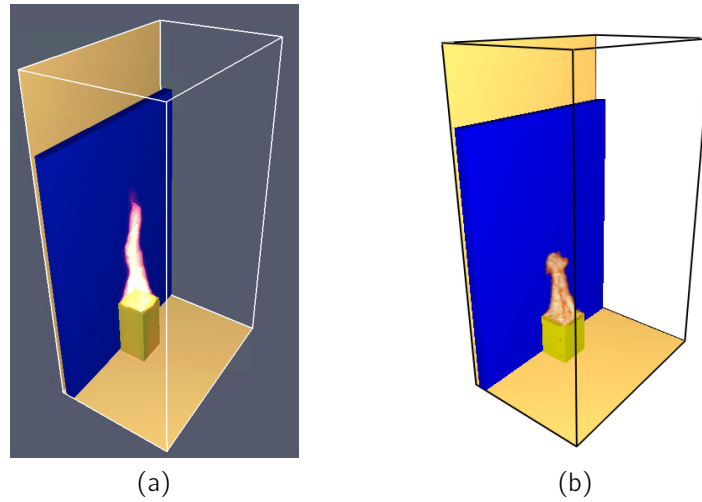


Figure 4.2: Comparison between a) Smokeview and b) Pyrosim visualization.

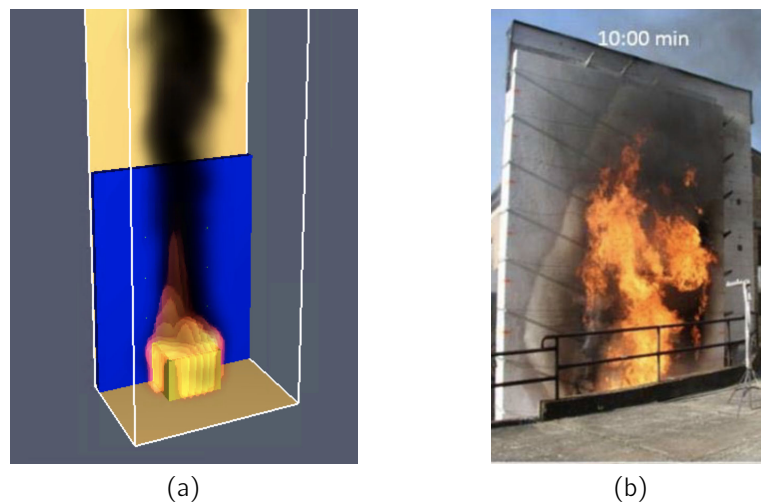


Figure 4.3: Comparison between a) the simulation and b) real fire test at the time of 10 minutes.

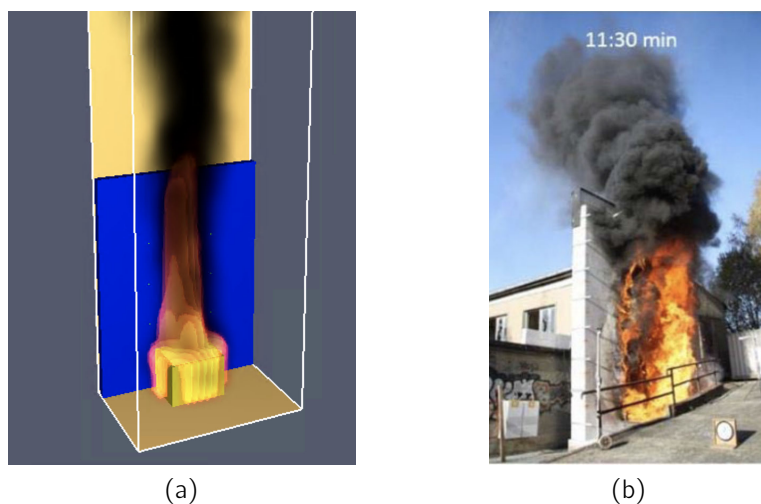


Figure 4.4: Comparison between a) the simulation and b) real fire test at the time of 11:30 minutes.

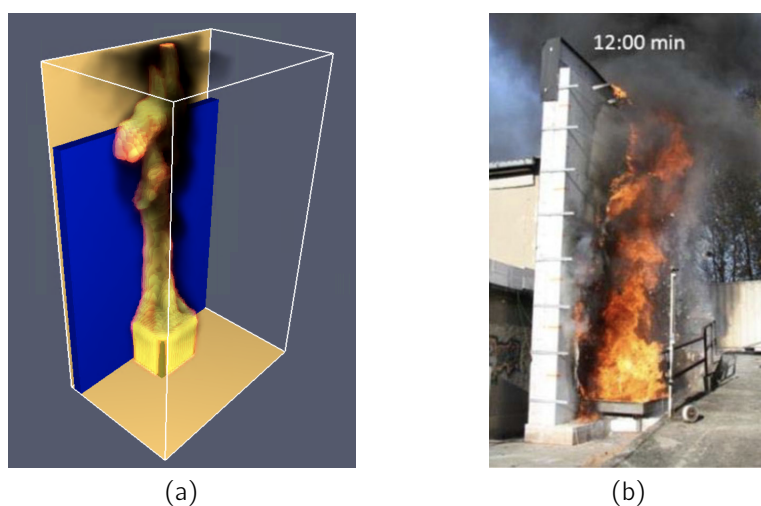


Figure 4.5: Comparison between a) the simulation and b) real fire test at the time of 12 minutes.

The simulation and the real test pictures are taken at 10 minutes. It is possible to see that the simulation is similar to the real fire test. The difference between the two images are minimum and, probably are caused by the atmosphere: in the simulation, the atmospheric conditions are controlled.

Also in this pictures 4.4 and 4.5, the simulation images are similar to the real-test images.

In the next images it is possible to see the comparison between the simulation and the real test at 300 second intervals. As it is possible to see from the images, the results are practically identical: the explosion of the fire and the extension of the simulation reflect when reported from the photo taken during the real simulation.

The HRR curves are compared in the next graph, figure 4.7.

As could be expected from the previous images, the two curves of HRR are similar. In both cases, the pool fire reaches a maximum HRR of about 3.5MW after 300sec and was burned out after 1800 second.

Only in the final part of the graph, after 1500 seconds, it is possible to see a different trend of the two lines: the simulation line, in orange, proceeds with a constant HRR equal to 500 KW; the line relative to the test of large scales, in black, instead continues to go down until the power is completely exhausted.

This diversity are caused by the program: in FDS, the calculation does not provide for the natural extinction of the fire due to the exhaustion of the fuel. To get the fire extinguished, it is necessary to set the data related to an artificial extinction of the fire, such as setting the activation of a water source that goes to suppress the fire.

This similitude validates FDS: the fact that the computation is almost equal to the real example, is an aid for the next simulation. With this validation, the results of the next simulations will be real. The computation respects the real parameters of the propagation of the fire; so, in the case of a real fire event, the simulation shows the real consequence of the fire propagation.

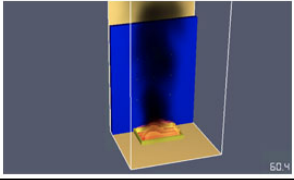

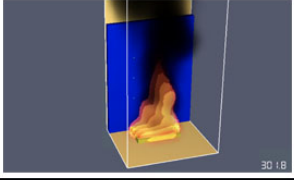

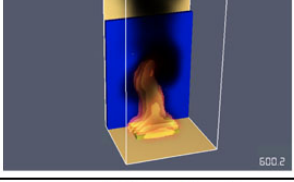

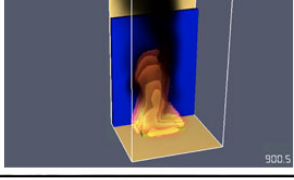

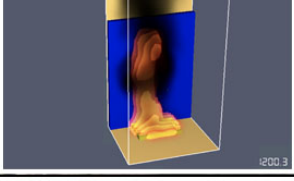

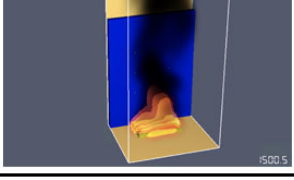

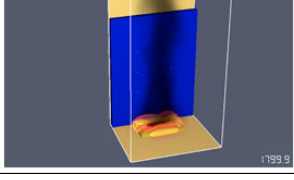

	Simulation	Real test
1 min	 A 3D simulation showing a small fire source at the base of a blue wall. The fire is contained within a yellow rectangular area. A scale bar in the bottom right corner indicates 50 cm.	 A photograph of a real fire test. A small fire is burning at the base of a concrete wall. A person in a red protective suit is visible in the background.
5 min	 A 3D simulation showing the fire growing slightly larger. A scale bar in the bottom right corner indicates 30 cm.	 A photograph of the real fire test at 5 minutes. The fire is more visible, and a person in a red protective suit is standing nearby.
10 min	 A 3D simulation showing the fire spreading further up the wall. A scale bar in the bottom right corner indicates 500 cm.	 A photograph of the real fire test at 10 minutes. The fire is spreading up the wall, and a person in a red protective suit is visible.
15 min	 A 3D simulation showing the fire spreading significantly higher. A scale bar in the bottom right corner indicates 900 cm.	 A photograph of the real fire test at 15 minutes. The fire is spreading rapidly up the wall, and a person in a red protective suit is visible.
20 min	 A 3D simulation showing the fire spreading almost to the top of the wall. A scale bar in the bottom right corner indicates 1200 cm.	 A photograph of the real fire test at 20 minutes. The fire is spreading very high, and a person in a red protective suit is visible.
25 min	 A 3D simulation showing the fire spreading to the top of the wall. A scale bar in the bottom right corner indicates 1500 cm.	 A photograph of the real fire test at 25 minutes. The fire is spreading to the top of the wall, and a person in a red protective suit is visible.
30 min	 A 3D simulation showing the fire spreading to the top of the wall. A scale bar in the bottom right corner indicates 1799 cm.	 A photograph of the real fire test at 30 minutes. The fire is spreading to the top of the wall, and a person in a red protective suit is visible.

Figure 4.6: Comparison between the simulation and the real test

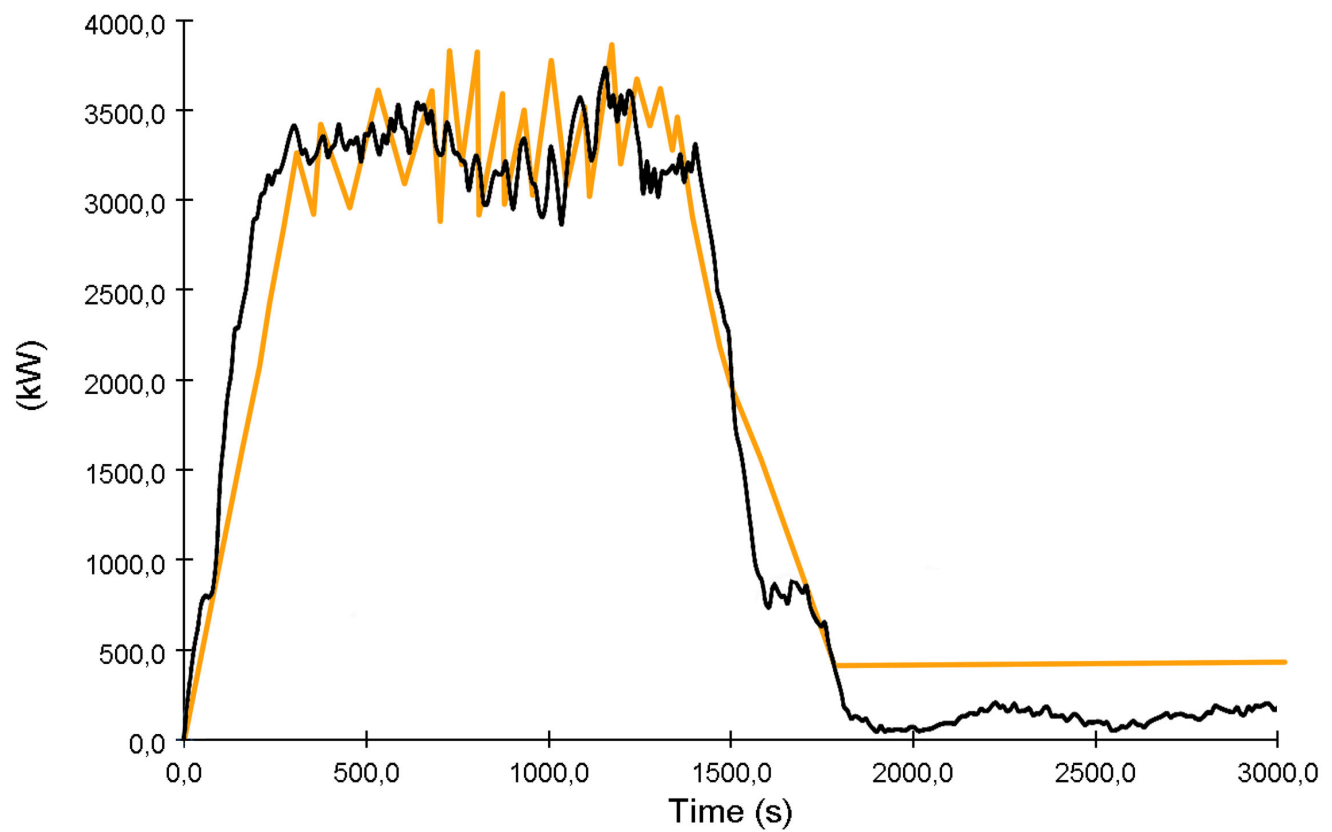


Figure 4.7: Comparison at different time step between the simulation (orange line) and the real fire test (black line)

Simulation

In this chapter, some simple examples are explained that have been made to fully understand how FDS works.

With this examples, the main characteristics that affect the fire in an urban scenario are analyzed: the propagation of fire and smoke. Five simple examples have been carried out to investigate the operation of the FDS calculation parameters and Smokeview visualization:

- the first example was made to understand the spread of fire and what parameters affect it;
- the second, third and fourth examples were made to investigate the effect of wind parameters such as intensity and direction;
- the last examples do not provide for the insertion of wind data, but the parameters relating to the material of the object are changed in order to analyze the propagation of the fire on different materials.

5.1 Initial parameters

The model (5.1) that is used in the various models consists of a computational domain of 20x20 meters and a height of 10 meters. The prismatic solid, which represents a surface, has a length of 10 meters for a width of 6 meters and a height of 0.3 meters. Above this building a strip has been inserted which represents the starting point of the fire.

```
&MESH ID= ' Cube '
      IJK=100,100,50
      XB= -10.000,10.000, -10.000,10.000,0.000,10.000/
```

This command line indicates the computation domain of the simulation.

```
&VENT ID= ' Burner '
      SURF_ID= ' FIRE '
      XB= -6.000, -5.500, -3.000,3.000,0.300,0.300/
```

This command line indicates the element, in this case a surface, which has been decided to define as the ignition point.

```
&OBST ID= ' Cube.001 '
      SURF_ID= ' Propagation '
      XB= -6.000,6.000, -3.000,3.000,0.000,0.300/
```

This other command line is used to indicate the geometry of the object that will undergo fire propagation.

```
&VENT ID= ' TOP '
      SURF_ID= ' OPEN '
```

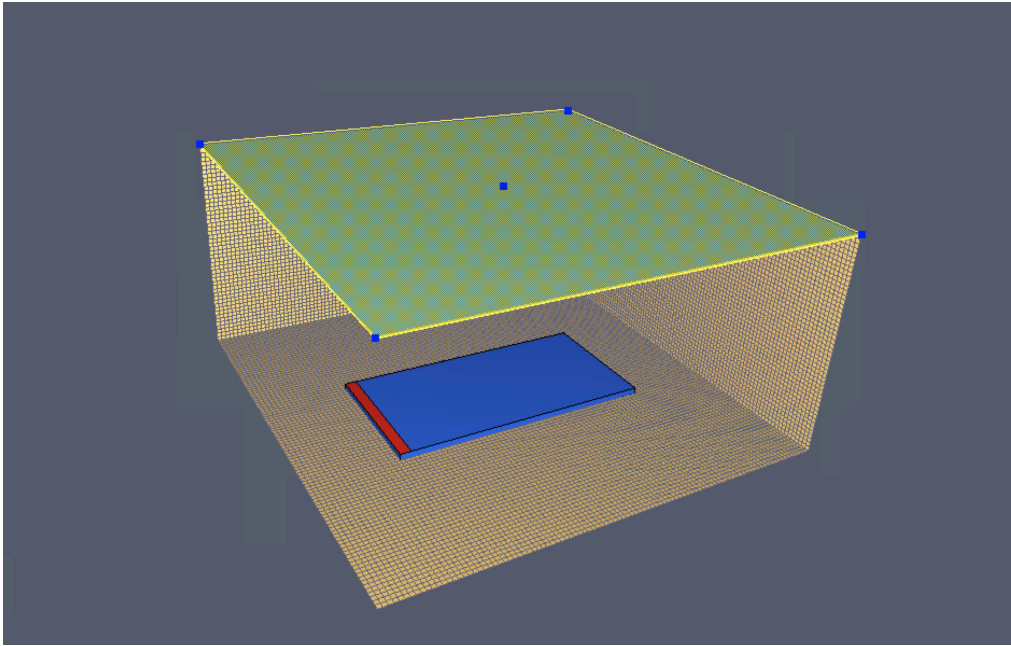



Figure 5.1: Visualization of the geometry using PyroSim

$$XB = -10.000, 10.000, -10.000, 10.000, 10.000, 10.000 /$$

This last command line identifies a surface that has the function of imitating the sky; in this case, thanks to this command line, the spelling domain is open at the top: this parameter is set to ensure that the smoke given off by combustion does not immediately fill the whole area of the computational domain.

The second step, after defining the geometry to be used for the simulation, is to define the HRRPUA parameter that is fundamental in the calculation of the simulation.

HRRPUA is the heat released rate per unit area and this value is established through calculations regulated by UNI ENI 1991. HRR is the variation of the thermal release power in a combustion reaction and is expressed in kW and depends on various factors such as the type of fuel, the ventilation and the geometric characteristics of the material and the environment.

Considering that kW is the equivalent of MJ/s, HRR can also be defined as the rate

CHAPTER 5. SIMULATION

of combustion of the material; in fact, the higher the value HRR, the faster the material burns and the production of smoke and heat increase considerably.

The Fire Prevention Code, D.M. 3-8-15 was developed in 2015 by the National Fire Brigade and represented a significant change in Italy as regards to the regulatory framework for fire prevention.

It is a tool designed for fire safety and has been realized maintaining an alignment with European standards; it is a tool made up of modular strategies that can be combined to get the best fire fighting strategy for every single project situation. The Chapter M.2 of this document defines the various fire scenarios for the performance design and the calculation methodology to be applied to construct the HRR curve.

In our case, the fire scenario is controlled by the fuel and the value of HRR_{max} is defined by the expression 5.1:

$$(5.1) \quad HRR_{max} = HRR_f A_f$$

Where HRR_f is the value of the maximum thermal power released per unit of gross surfaces of certain activities and A_f is the gross area actually occupied by the fuel. In FDS you have to enter the HRR_f and not the HRR_{max} because during the calculation of the simulation the program calculates by itself the surface area where the determined HRR_f value is applied.

Some typical values of the maximum thermal power of certain types of activities are indicated in the Appendix to Eurocode 1.

```
&SURF ID= ' FIRE '
      RGB=204,0,0
      HRRPUA=550.000
      TAU_Q=-100.0/
```

In the simulations that are developed in this chapter, it was decided to take a HRR_f value equal to that of a rapid development of fire as it is assumed that the fire originates from the fire of a surface covered with methane.

```
&SURF ID= ' Propagation '  
      RGB=0,0,204  
      HRRPUA=100.000  
      MATL_ID= ' concrete '  
      IGNITION_TEMPERATURE=50.0  
      THICKNESS=0.010  
      TAU_Q=-100.0 /
```

```
&MATL ID= ' concrete '  
      FYI= ' Properties □ completely □ fabricated '  
      DENSITY=2200.  
      CONDUCTIVITY=1.2  
      SPECIFIC_HEAT=0.88  
      SPEC_ID= ' METHANE ' /
```

These two command lines are used to define the properties of the object that will undergo fire propagation. The first line defines the characteristics of the object in general, while the second one is used to define the characteristics of the material that constitutes the object, in this case the material is concrete.

These characteristics are used for the first simulations; the parameters of the material of the object are changed for the last simulations where the propagation of different materials are compared.

In parallel to the calculation of the simulations made for different materials, manual calculations were performed to compare the trend of the propagation phase of the HRR curve. Various fire developments have been identified according to the type of material used:

- the concrete has been assigned an expected period of slow fire development;
- the wood has been assigned an expected period of medium fire development;
- the PVC has been assigned an expected period of fast fire development.

To calculate these curves, the following formula was used:

$$(5.2) \quad HRR = 1000 \left(\frac{t}{t_{\alpha}} \right)^2$$

where t_{α} represents the time necessary for the released thermal power to reach the value of 1000kW and, for some values, it is found in the Eurocode1. It represents the time necessary for the released thermal power to reach the value of 1000kW and, for some values, it is found in the Eurocode1. In the D.M. 3-8-15 is defined as the prevailing characteristic speed of fire growth and is divided into four categories:

- slow (600 s): low-combustible materials such as concrete;
- medium (300 s): combustible materials such as wood that are classified by reaction to fire;
- fast (150 s): plastic materials that are not classified by reaction to fire;
- ultra-fast (75 s): flammable liquids.

5.2 First simulation: propagation

This first model is basic. It is the starting point for the subsequent simulations. In this input file all the parameters necessary to obtain satisfactory simulations are calibrated.

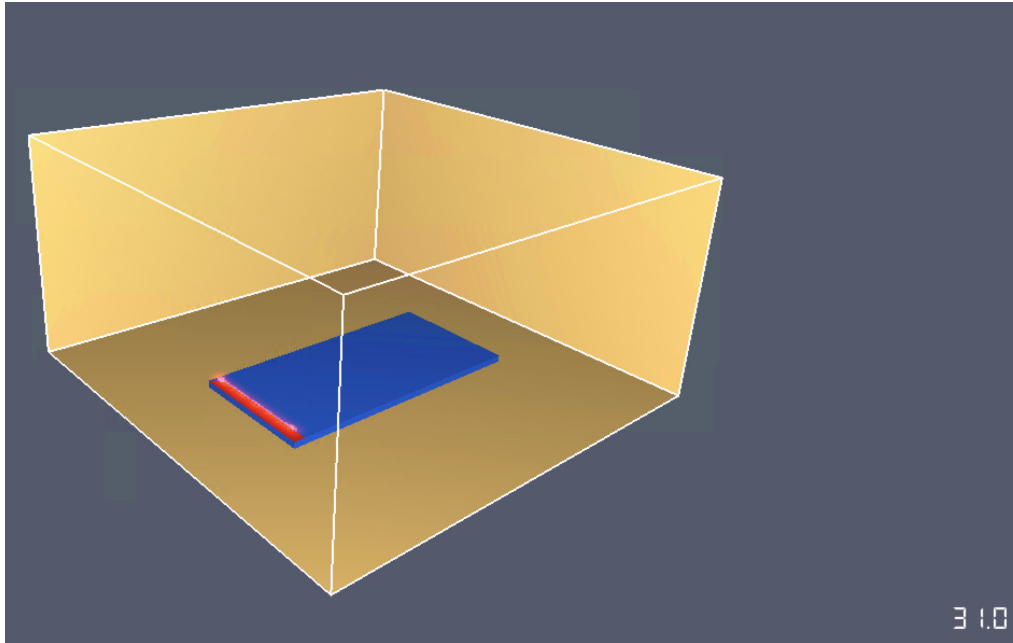


Figure 5.2: Initial phases of the simulation

This first picture 5.2 is the initial phase of the simulation; the area in red represents the starting point of the fire. The simulation was blocked in the first 30 seconds, so the fire is hardly mentioned because it has not yet reached its maximum power.

This second image 5.3 shows that the power of fire has increased with time; despite the increase in power, the characteristics of the material chosen for the object destined to ignite do not allow the fire to propagate on the surface of the solid.

In this third image 5.4, it is possible to begin to see the propagation of the fire on the object; the fire has reached a constant power and then propagates along the surface of the chosen solid.

5.3 Second simulation: Wind

Using the same input file as the previous model, the file is expanded by adding the parameters that regulate the wind. A wind speed of 5 m / s is defined and a direction

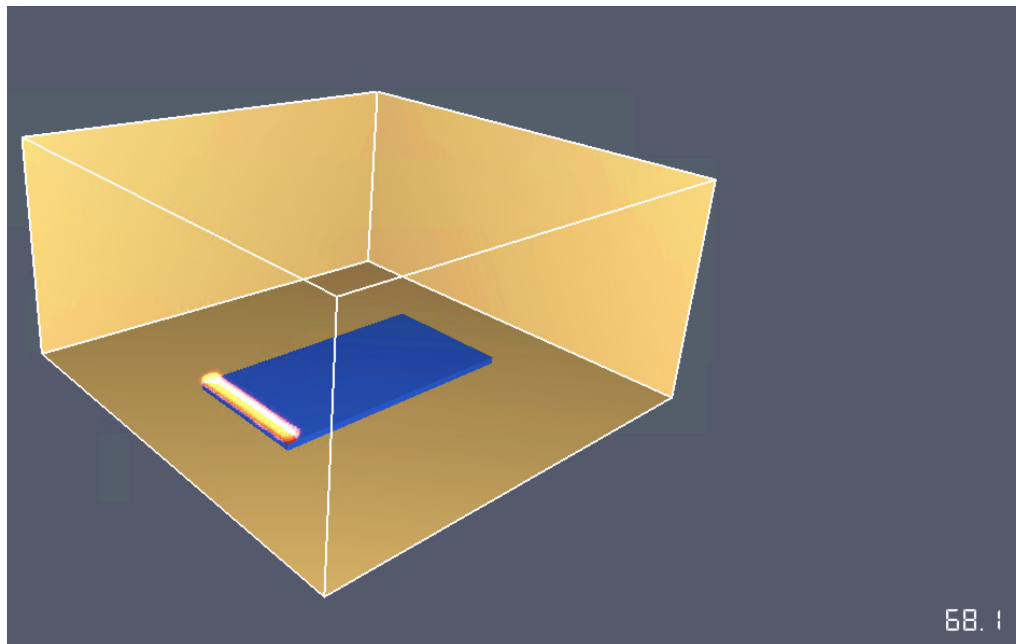


Figure 5.3: Initial phases of the propagation

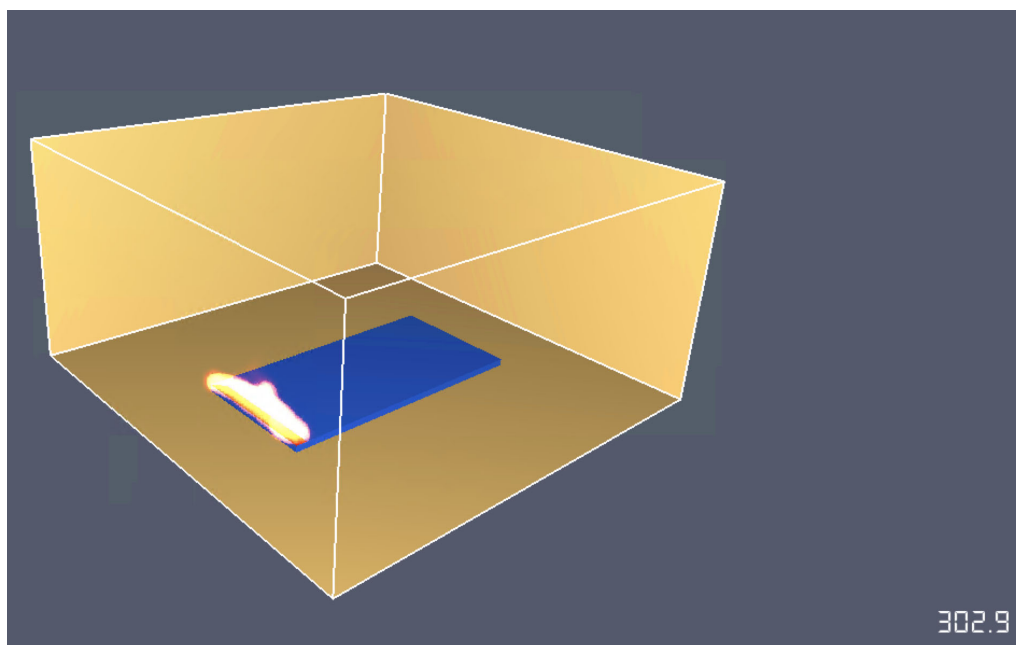


Figure 5.4: Propagation of the fire

parallel to the x axis of the model.

```
&WIND SPEED=5  
      DIRECTION=270  
      L=-100  
      Z_0=.03/
```

These are the basic parameters to be used to set a wind in FDS. The direction is indicated in degrees: in this simulation the direction parallel to the positive abscissa axis was chosen, which corresponds to 270° .

The wind speed that has been set for these simulations is not very high; observing the data on the average annual wind speed in the area of Turin and the province, an average speed of about 5 m/s was identified, which was then used in the simulations.

For this simulation and the next ones that analyze the wind, it was decided to use the smoke display to better see the trend. Observing the different simulations developed, the wind has a May effect on the propagation of the fire, but, to better observe and understand the parameters that regulate this command, the displacement of the smoke highlights the direction and the intensity of the wind.

These first pictures 5.5 describes the initial phases of the simulation; the beginning of the generation of smoke resulting from combustion; the fire is in initial phase, so the smoke in the simulation is still little but you can already see the wind trend.

In this second image 5.6 the fire is almost completely developed and the smoke has increased compared to the beginning of the simulation. Because of the blowing wind, the smoke does not rise straight upwards but has a crushed appearance that rises gradually upwards.

In these last images 5.7, it is possible see that the smoke increases more and more during the time of the simulation while the wind maintains a constant trend.

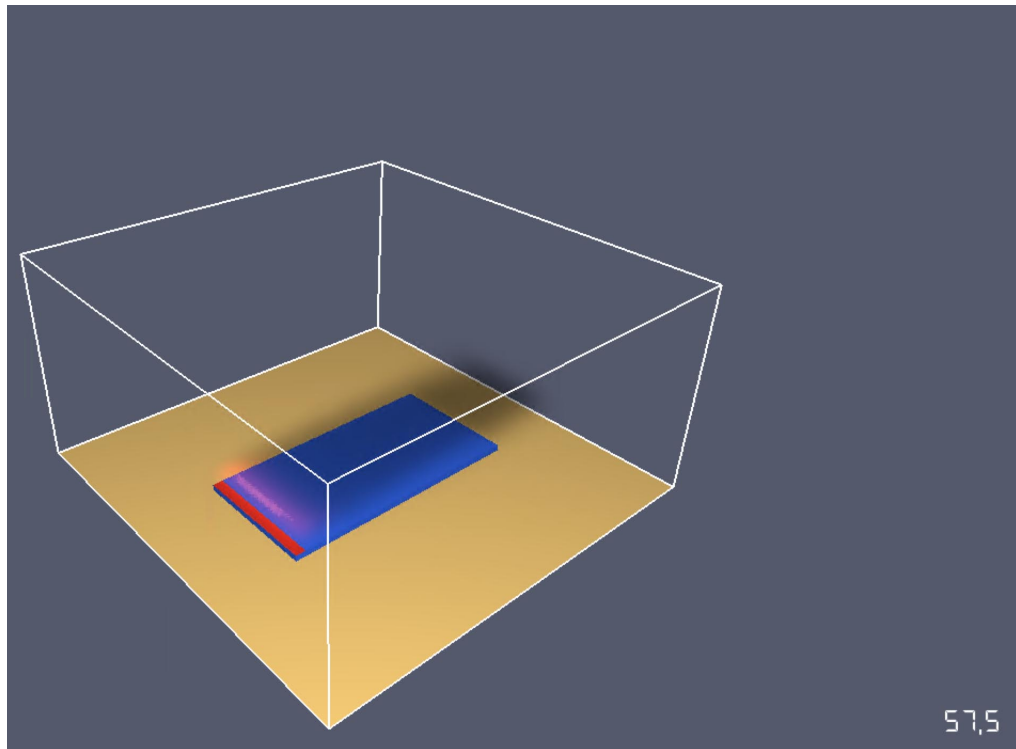


Figure 5.5: Initial phases of the simulation

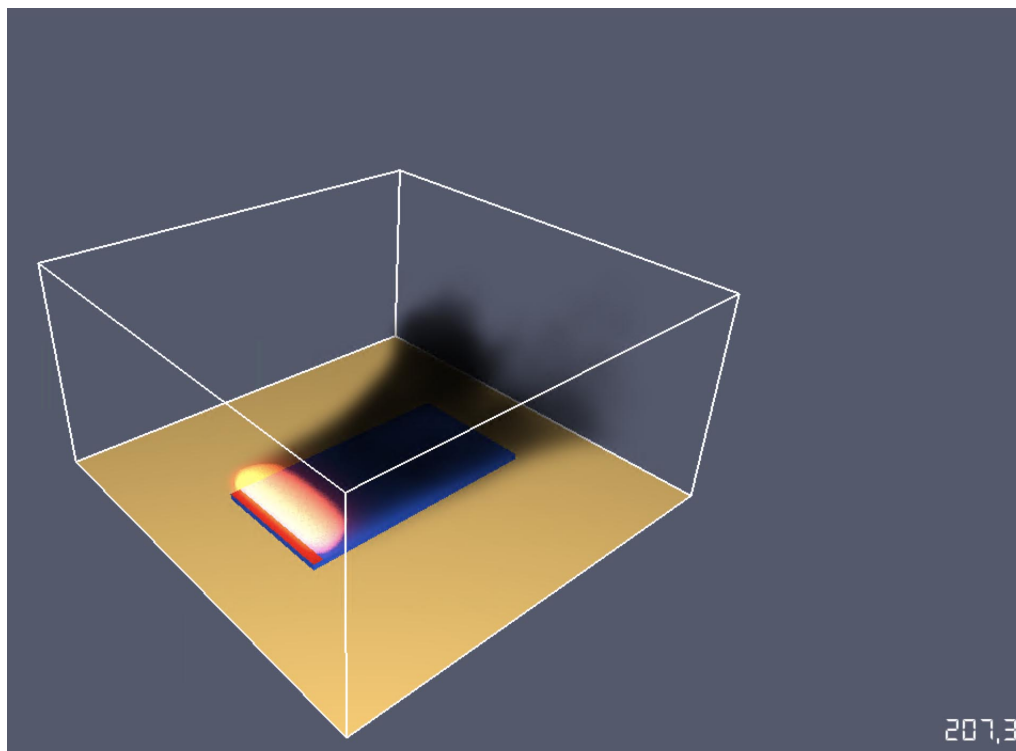


Figure 5.6: Development of smoke and detection of wind direction

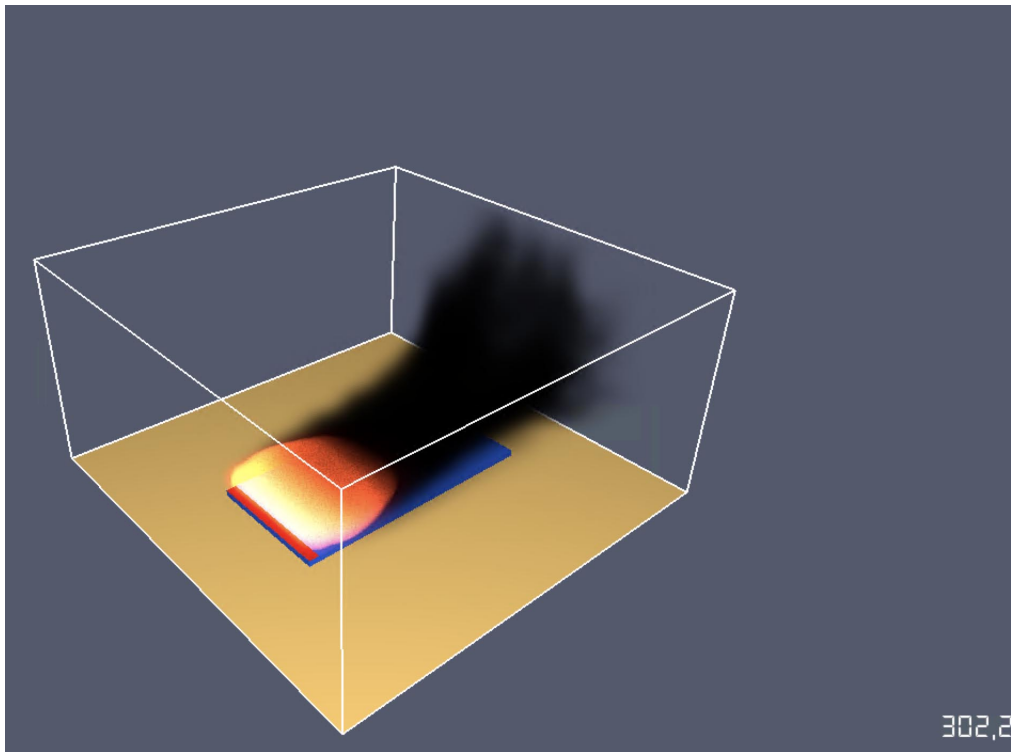


Figure 5.7: Smoke and detection of wind direction

With these images you can better understand the use of 'VENT' for modeling simulations.

```
&VENT ID= 'TOP'
      SURF_ID= 'OPEN'
      XB= -10.000,10.000, -10.000,10.000,10.000,10.000/
```

Using a VENT surface with the parameter of *SURF_ID = 'OPEN'*, a surface is created on the boundary of the computational domain of the open simulation: this surface, which has predefined characteristics in the program, allows to have a non-excessively large domain, and consequently to reduce the times of the simulations, but to have at the same time one side of the domain that simulates the infinite.

This element sets in the simulations, therefore it allows a part of the smoke produced

by the fire to exit the domain of the simulation. In this way, the smoke is not saturated completely with the calculation environment and does not affect the progress of the fire during the simulation.

5.4 Third simulation: Intensity

In this model, the intensity of the wind has changed. By maintaining a maximum speed of 5 m/s, the intensity of the wind was changed using the RAMP functions.

```
&WIND SPEED=5  
    DIRECTION=270  
    L=-100  
    Z_0=.03  
    RAMP_SPEED='WIND_RAMP_SPEED' /  
&RAMP ID='WIND_RAMP_SPEED', T=0, F=0 /  
&RAMP ID='WIND_RAMP_SPEED', T=100, F=0.3 /  
&RAMP ID='WIND_RAMP_SPEED', T=200, F=0.5 /  
&RAMP ID='WIND_RAMP_SPEED', T=300, F=1 /
```

The use of the RAMP functions is used to decide the intensity that the wind must have at the time of the established simulation.

In the simulation the wind intensity has been set so that at time $t = 0$ seconds the wind speed is equal to 0. This speed, however, grows to reach 30% of the maximum speed, that is 5 m/s, at time $t = 100$ seconds. In this way, the wind grows constantly during the simulation.

In this simulation it was decided to use the *RAMP_U0_T* function that serves to

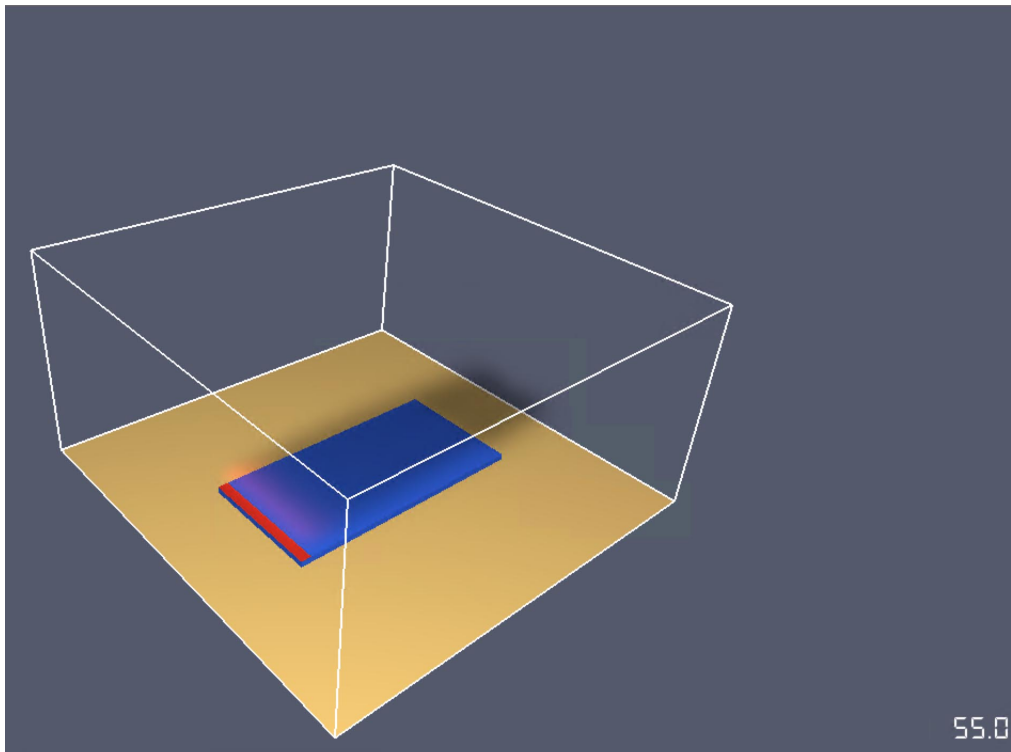


Figure 5.8: Intensity of the smoke at the beginning of the simulation

direct the wind into the simulation.

In this first image 5.8, it is possible to notice how the smoke column, which flows from the burned area, rises upwards perpendicularly. In the simulation, it has been set that the wind does not blow up at the outbreak of the fire but that it starts to blow softly during the calculation.

With the passing of time the wind increases in intensity; in this image 5.9 the wind is at 50% of its power, so it has a speed of 2.5 m/s. The intensity of the wind is not much, in fact, in the image, the smoke is not completely lying on the object as in the previous simulation, but rises slightly upwards.

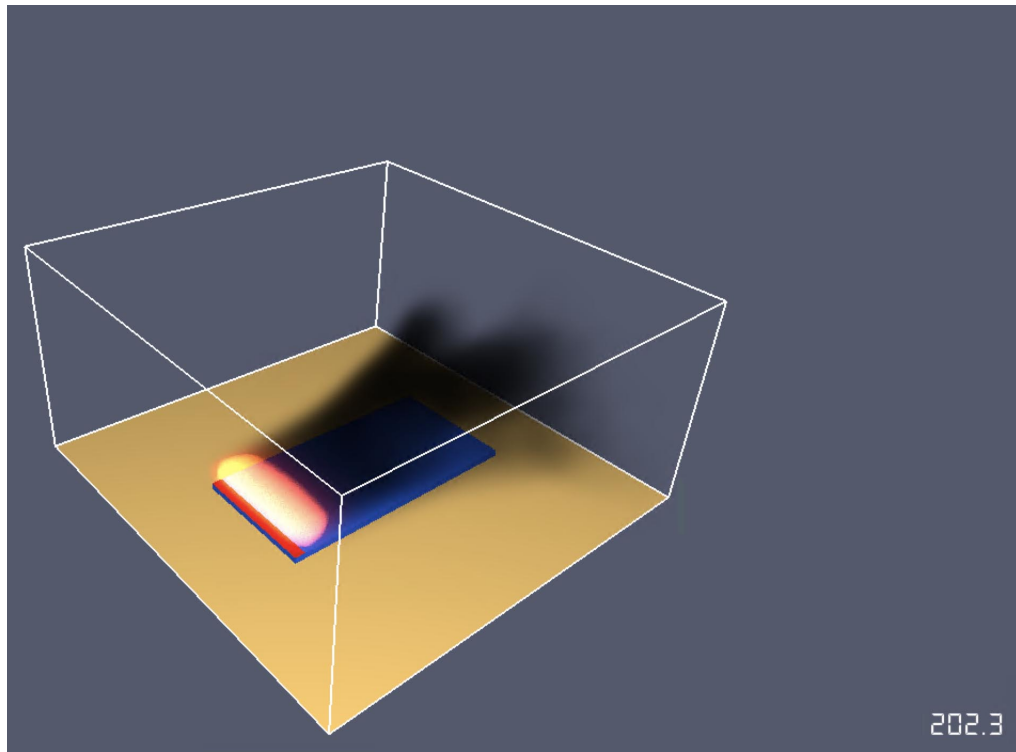


Figure 5.9: Intensity of the smoke in the middle of the simulation

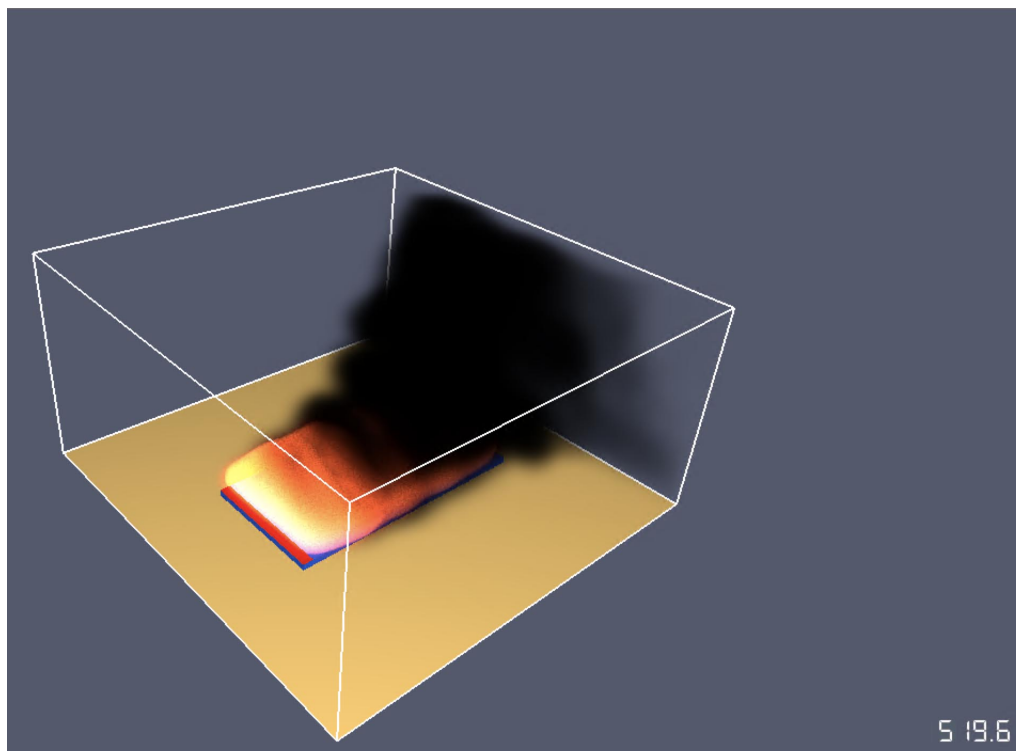


Figure 5.10: Intensity of the smoke at the end of the simulation

With the last image 5.10 you can see that the intensity of the wind is completely developed: the smoke that flows from the fire moves horizontally instead of going upwards perpendicular to the fire.

5.5 Fourth simulation: Direction

This simulation is similar to the previous one because also here the RAMP functions are used so that, instead of modifying the intensity of the wind, they modify its direction.

```
&WIND SPEED=5  
      RAMP_DIRECTION= 'WIND_RAMP_DIRECTION '  
      L=-100  
      Z_0=.03/  
&RAMP ID= 'WIND_RAMP_DIRECTION' , T= 0. , F=270. /  
&RAMP ID= 'WIND_RAMP_DIRECTION' , T=300. , F=180. /  
&RAMP ID= 'WIND_RAMP_DIRECTION' , T= 400. , F=90. /  
&RAMP ID= 'WIND_RAMP_DIRECTION' , T= 500. , F=0. /
```

The intensity is no longer changed, it remains constant throughout the duration of the simulation; in any case, it is possible to simultaneously modify both the intensity and the wind direction during the calculation of the simulations, just by using the RAMP functions and by grouping them: a series of RAMP will be used to control the direction while another series will be used to modify the intensity.

In this first image 5.11 the wind direction is equal to the previous simulations: the wind blows in the positive direction of the x axis, i.e. at 270° . The smoke in this image is not much because we are at the beginning of the simulation and therefore the fire has not yet reached full power.

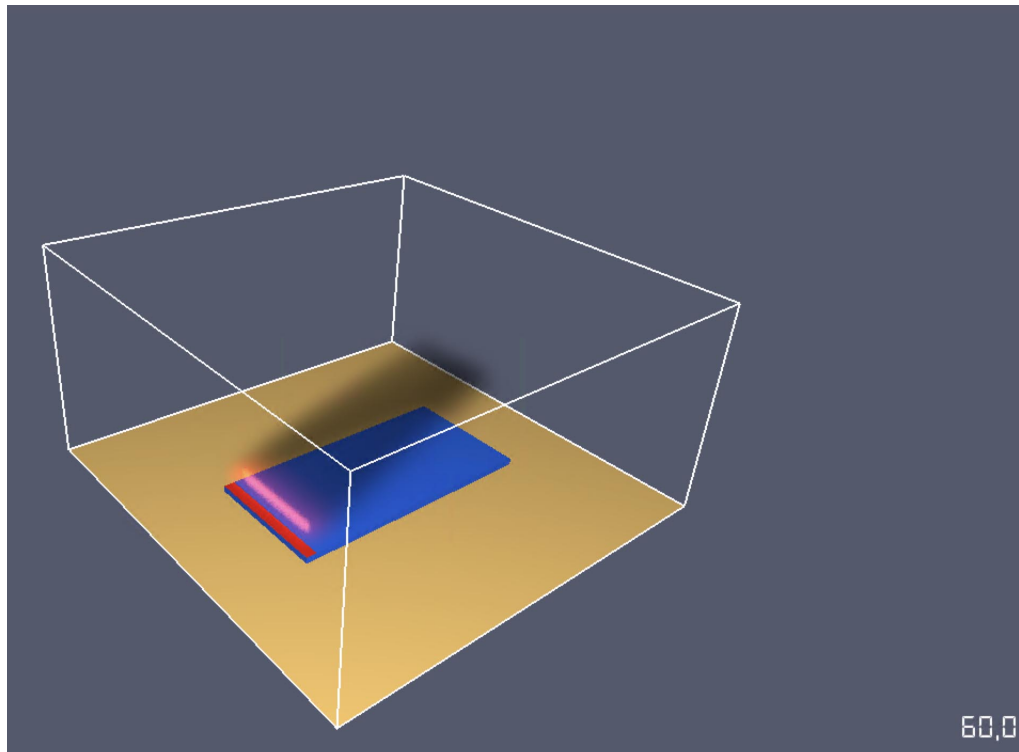


Figure 5.11: Direction of the wind at 270°

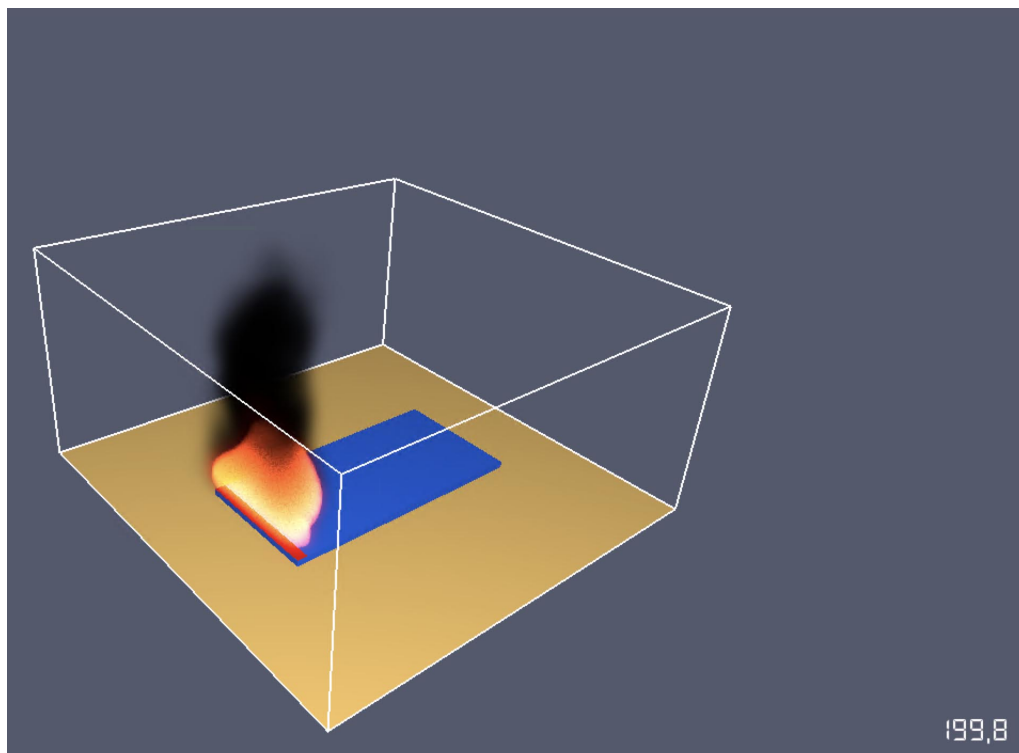


Figure 5.12: Direction of the wind at 180°

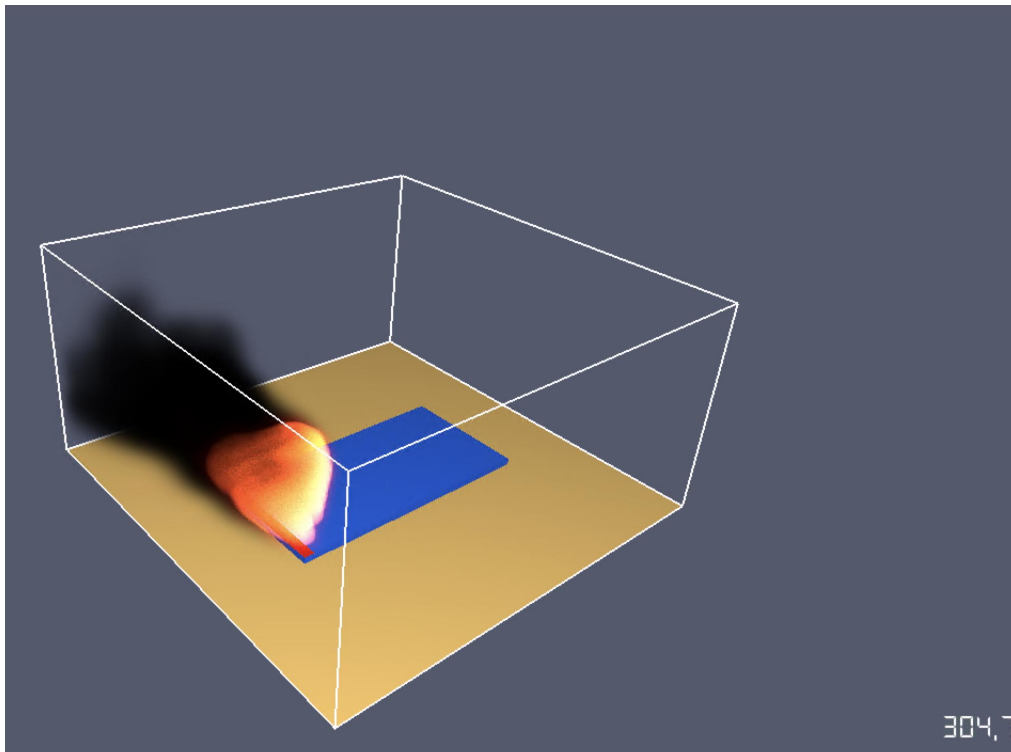


Figure 5.13: Direction of the wind at 90°

In the second image 5.12 we see that the smoke has changed direction and blows towards the positive y axis of the Cartesian system of the program, i.e. at 180° .

In this image 5.13 we see the third change of direction that has been defined in the input file of the simulation; in this case the wind blows in the direction of the negative x, that is to 90° .

In this last image 5.14 we see the last change of the wind: the direction is that which follows the axis of the y in the negative direction, 0° . At this moment of the simulation the fire has the power fully developed and the addition of the wind increases the size of the fire and the direction of propagation: in fact, the fire spreads also laterally and not only superficially here. As a result, there is a greater amount of smoke in the simulation.

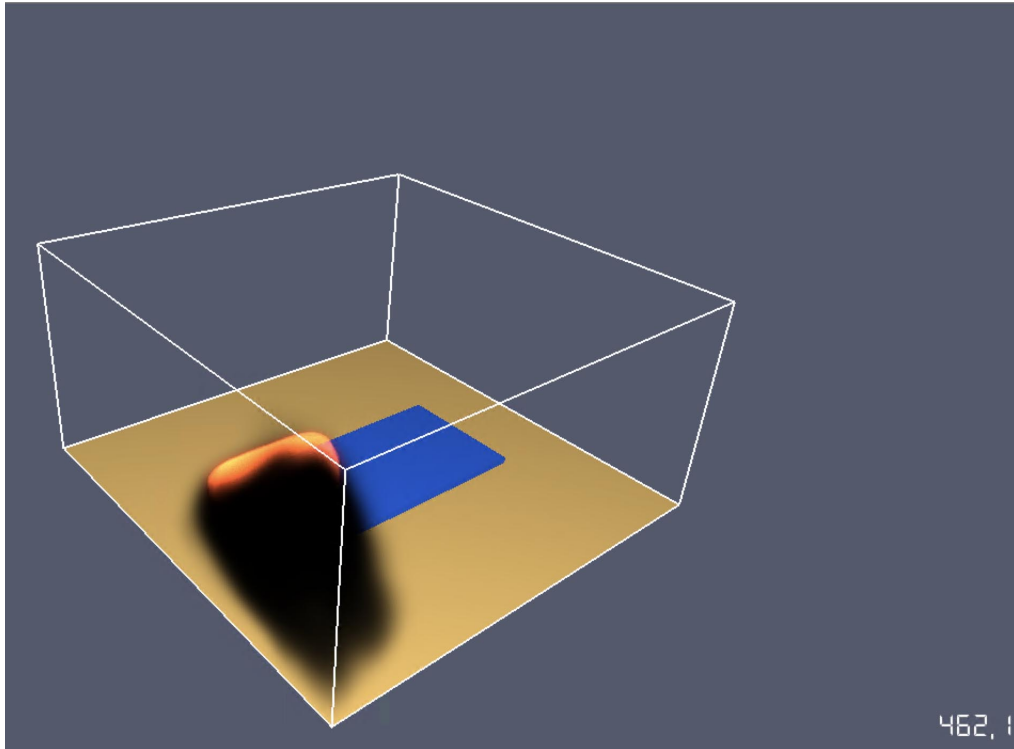


Figure 5.14: Direction of the wind at 0°

5.6 Fifth simulation: Material

These last simulations were made to compare and understand how the program reads and processes the parameters that are set to the various materials. The materials chosen for these simulations are wood, paper and PVC.

Looking at the different simulations, the behavior of paper and wood is practically the same and therefore the comparison of the materials used takes place between wood, PVC and concrete.

```
&MATL ID= 'wood '
      FYI= ' Properties completely fabricated '
      DENSITY=571.
      CONDUCTIVITY=0.99
      SPECIFIC_HEAT=0.39
```



```
SPEC_ID= 'METHANE' /
```

This part of the input file represents the information concerning the material chosen for the representation of the wood. In this case, the technical properties of pine wood were used.

```
&MATL ID= 'PVC'
      FYI= 'Properties completely fabricated'
      DENSITY=4000.
      CONDUCTIVITY=0.19
      SPECIFIC_HEAT=1
      SPEC_ID= 'METHANE' /
```

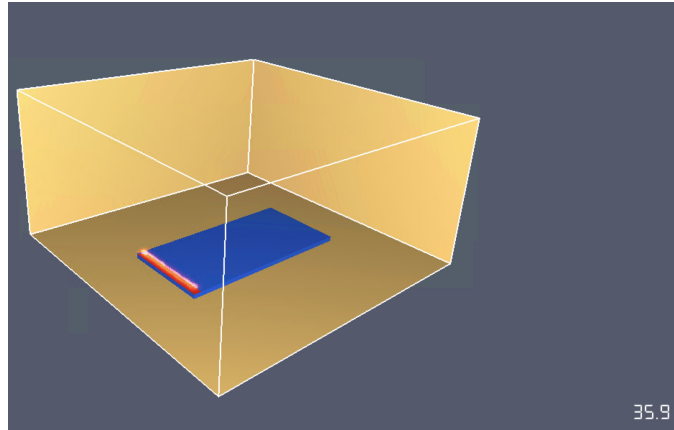
This other part of the input file contains information concerning the thermal properties of a plastic material, PVC.

To the concrete, the parameters concerning the properties of the material are those reported in the paragraph of the first simulation.

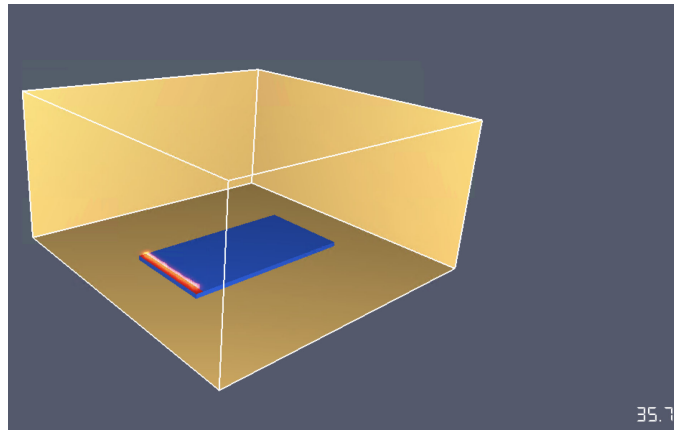
In the above images, it is possible to see the beginning of the propagation of the fire in the wood (a), PVC (b) and cement (c) materials. Being at the beginning of the simulation calculation, the images represented are almost equal to each other; diversity in propagation is minimal.

In these images, the difference in propagation is more noticeable depending on the materials used in the simulation:

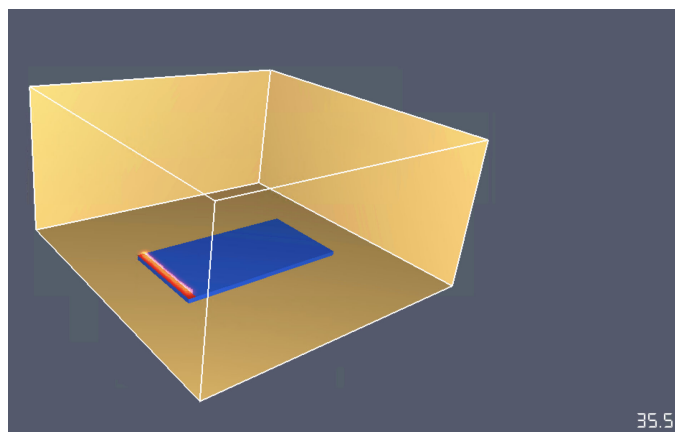
- in the first image (a), the material of the simulation is wood;
- in the second image (b), the simulation material is PVC;
- in the third image (c), the material of the simulation is concrete.



(a)

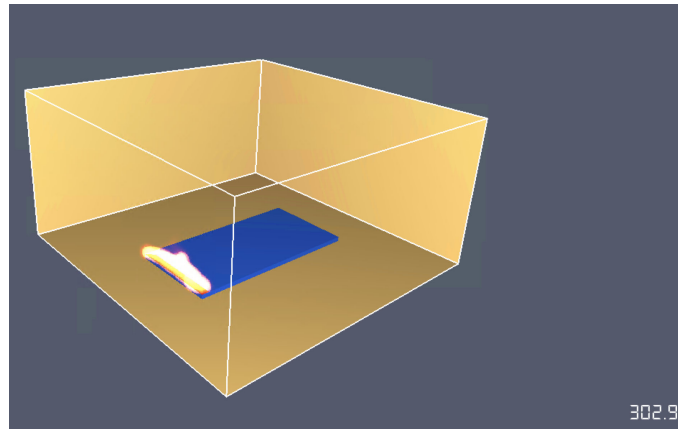


(b)

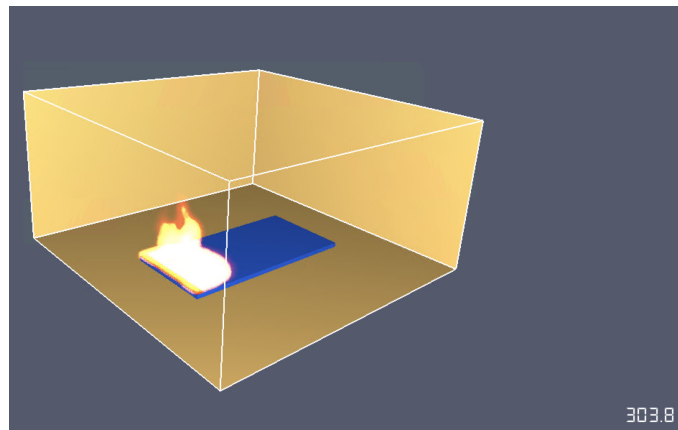


(c)

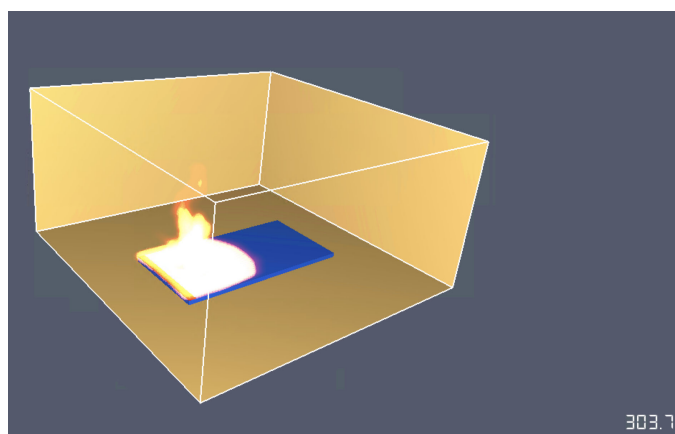
Figure 5.15: Comparison at the time 35 sec between a) concrete, b) PVC and c)wood



(a)



(b)



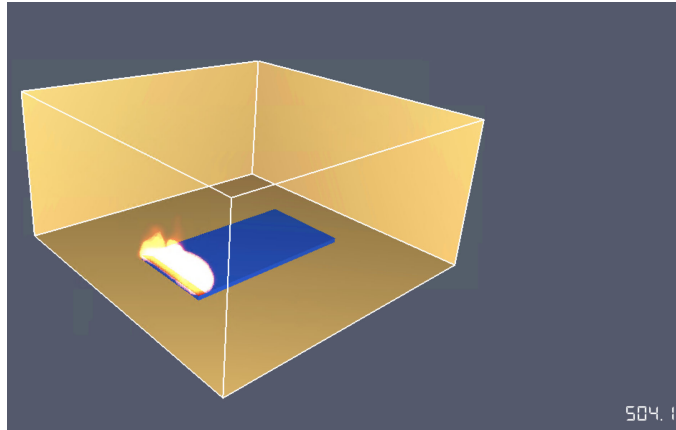
(c)

Figure 5.16: Comparison at the time 100 sec between a) concrete, b) PVC and c)wood

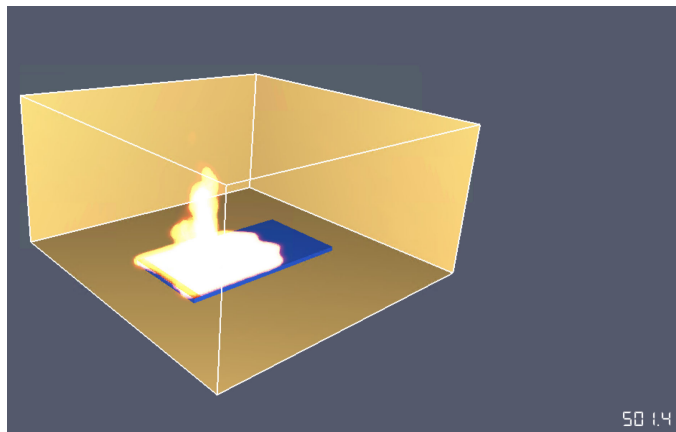
At this point in the simulation, it is easy to see how wood burns faster than the other two materials.

In these last three images, the difference in the propagation of fire in different materials is accentuated:

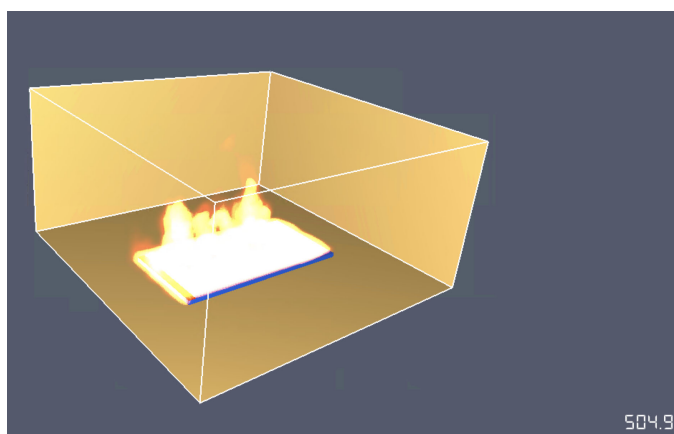
- in the first image, (a) wood, the fire has completely covered the high surface of the solid;
- in the second image, (b) PVC, the fire is advanced until after half of the high surface of the solid;
- in the third image, (c) concrete, the fire is still at the beginning of the high surface of the solid, there is almost no propagation of the fire.



(a)



(b)



(c)

Figure 5.17: Comparison at the time 400 sec between a) concrete, b) PVC and c)wood

Ideal City

The aim of the previous chapters was to learn how to use the basic parameters to be able to perform a simulation of a fire in an urban environment.

The idea of this thesis is to recreate the work of Prof. Lu Xinzheng with the only use of FDS. The work of Prof. Lu Xinzheng et al. 2016 “Physics-based simulation and high-fidelity visualization of fire following earthquake considering building seismic damage” present the case study of the downtown of the city of Taiyuan. This work is divide in for main steps:

- the first step is to simulate the ground motion: a seismic damage simulation of regional building was performed. The seismic simulation is based on the multy-degree of freedom model and a nonlinear analysis;
- the second step is based on the ignition model developed using a regression model and probabilistic model proposed by Ren and Xie;
- the third step is the fire propagation: this model is based on the existing p physics-based model proposed by Zhao;

- the fourth and last step is the high-fidelity visualization: to the 3D scene of the simulation was used the open-source 3D graphics OSG and the smoke particles are simulate using FDS.

In this chapter was explain the methodology that was used to perform an urban simulation with the only use of FDS. To create the simulation was used Ideal City, a virtual city created on the basis of the real city of Turin. All buildings and urban features are taken from the real city and reported in an interactive virtual model.

6.1 Creation of the input file

In order to create a work file to be used in the simulation, a CAD file (6.1) containing the plan of the city of Turin and a file in Excel format (6.2) were used . All the data relating to the buildings were exported: each building was given a code identification, then the perimeter, the area and other data necessary for the seismic analysis such as the construction type and the year of construction were calculated.

Starting from this data, it was possible to create a 3D file of a portion of the metropolitan city through AutoCAD (6.3) and import the file, DXF or DWG format is indifferent, into PyroSim software.

The choice to use Pyrosim instead of a BlenderFDS is carried to the geometry of the city. The building in the model aren't parallel to the general axis of FDS and some building aren't a perfect parallelogram.

Exporting the FDS input file from BlenderFDS, an obstacle is defined by the three coordinates of the points of the solid diagonal; if the solid is rotated respect to the FDS reference system, the program nevertheless creates a solid with the faces parallel to the global reference system and therefore the starting solid will have dimensions and rotation different from the initial geometry. To solve this problem, in Blender there is the



Figure 6.1: Image of the AutoCAD file

CHAPTER 6. IDEAL CITY

	A	B	C	D	E	F	G	H	I	J	K	L	M	N	O	P	Q	R
1	Building ID	Perimeter [m]	Area [$\frac{m^2}{m^2}$]	C_x [m]	C_y [m]	l_{wp} [m]	l_{wp} [m]	n_{stoi}	Year of Constructi	Mass Typ	Wall Typ	Span Typ	Reinforcement Type	Ang	Sigma_Mf	Sigma_G	Sigma_MA	Construction Type
5	4	103,64	495,51	390510,05	4989496,04	75711,70	5471,09	2	1	1	3	4	2	-0,093	0,123	0,172	0,269	1
6	5	167,40	984,09	390511,73	4989462,45	121566,39	93450,93	2	1	1	6	3	0	-0,071	0,110	0,216	0,194	1
7	6	63,55	240,37	390512,32	4989525,32	9005,72	1589,44	2	1	2	9	3	0	-0,073	0,133	0,178	0,217	1
8	7	95,80	205,15	390537,98	4989410,55	5389,50	25421,51	2	1	1	9	3	0	-0,073	0,149	0,160	0,255	1
9	8	103,96	240,95	390553,17	4989381,63	42916,48	4506,44	2	1	6	6	6	0	-0,072	0,149	0,162	0,246	1
10	9	176,63	1709,49	390583,94	4989359,88	250652,26	268316,66	2	1	6	9	1	0	-0,073	0,131	0,183	0,240	1
11	10	170,65	1651,59	390587,60	4989393,38	223989,87	277946,12	2	1	3	9	2	0	-0,073	0,131	0,174	0,244	1
12	11	159,95	1485,63	390629,95	4989356,49	204291,29	172622,59	2	1	3	8	1	0	-0,073	0,114	0,243	0,248	1
13	12	157,28	1498,59	390633,35	4989390,77	207819,58	172540,31	2	1	2	5	3	0	-0,073	0,124	0,191	0,254	1
14	13	41,18	97,62	390646,51	4987463,20	2594,42	734,43	11	4	2	3	4	2	-0,597	0,029	0,138	0,139	2
15	14	109,72	631,47	390659,07	4987482,38	135745,77	43824,89	11	4	1	3	6	2	-0,599	0,040	0,113	0,131	2
16	15	77,16	367,66	390662,83	4989790,49	13610,78	9456,78	2	1	1	4	3	0	0,009	0,126	0,165	0,227	1
17	16	140,52	1233,85	390670,06	4989417,73	157926,38	95921,73	2	2	4	9	1	0	-0,068	0,126	0,202	0,256	1
18	17	100,01	523,05	390671,92	4989772,41	8523,86	54877,43	2	2	2	5	3	0	0,009	0,126	0,218	0,215	1
19	18	131,04	1066,16	390672,36	4989450,01	110726,57	81228,95	2	2	1	4	5	0	-0,078	0,126	0,186	0,174	1
20	19	81,46	349,19	390677,41	4989355,99	27385,97	559,99	2	2	2	5	2	0	-0,072	0,126	0,150	0,221	1
21	20	83,65	362,61	390679,54	4989384,91	30613,66	328,29	2	2	1	4	5	0	-0,072	0,126	0,181	0,243	1
22	21	109,70	631,20	390685,11	4987520,02	135665,06	43809,39	11	4	1	3	5	1	-0,600	0,045	0,139	0,144	2
23	22	75,41	310,60	390686,35	4989476,99	20954,75	144,38	2	2	6	6	2	0	-0,103	0,045	0,151	0,215	1
24	23	82,46	351,64	390688,68	4989504,30	28931,49	270,20	2	2	6	6	2	0	-0,072	0,045	0,180	0,171	1
25	24	43,89	115,47	390698,61	4987539,36	3385,84	973,80	11	4	1	3	4	2	-0,598	0,046	0,117	0,117	2
26	25	140,52	1233,47	390705,75	4989415,13	160938,64	92893,91	2	2	1	6	4	0	-0,078	0,046	0,198	0,235	1
27	26	132,91	1095,98	390707,99	4989447,42	114095,02	89041,89	2	2	2	9	3	0	-0,072	0,046	0,197	0,188	1
28	27	140,02	1246,46	390718,90	4987429,05	370180,64	109826,10	9	4	2	3	3	2	-0,570	0,028	0,125	0,153	2
29	28	81,73	357,32	390725,60	4989352,60	27546,20	896,14	2	2	1	5	4	0	-0,072	0,028	0,177	0,252	1
30	29	85,22	379,44	390727,74	4989381,57	32854,93	544,90	2	2	1	5	3	0	-0,072	0,028	0,156	0,184	1
31	30	114,63	732,64	390728,02	4989796,47	156701,61	45608,93	2	2	1	8	5	0	-0,470	0,028	0,203	0,229	1
32	31	74,56	303,29	390734,34	4989473,49	19936,80	144,60	2	3	3	4	1	0	-0,103	0,043	0,158	0,241	1
33	32	83,26	355,37	390736,72	4989501,02	30147,63	125,65	2	3	4	4	1	0	-0,072	0,061	0,176	0,239	1
34	33	108,12	670,06	390744,56	4989828,94	123707,32	35341,21	2	3	3	9	1	0	-0,470	0,052	0,173	0,216	1
35	34	124,08	926,71	390745,65	4987645,64	205352,03	51265,53	4	4	1	3	3	3	-0,426	0,031	0,120	0,119	2
36	35	163,96	1629,19	390747,61	4989412,18	214606,45	255394,98	2	3	4	6	2	0	-0,061	0,078	0,206	0,177	1
37	36	156,77	1461,12	390749,82	4989444,17	176611,88	215668,26	2	3	1	6	4	0	-0,078	0,086	0,206	0,222	1
38	37	142,73	1106,70	390762,85	4987681,26	291950,51	71348,75	4	4	2	2	3	1	-0,426	0,022	0,126	0,114	2
39	38	67,21	255,93	390766,24	4987389,56	4968,88	8197,26	2	3	1	5	3	1	0,187	0,049	0,181	0,189	1
40	39	69,84	280,48	390766,86	4987415,69	1393,74	16781,72	2	3	1	3	2	2	0,186	0,063	0,139	0,157	2

Figure 6.2: Image of the Excel table with all the data of teh city

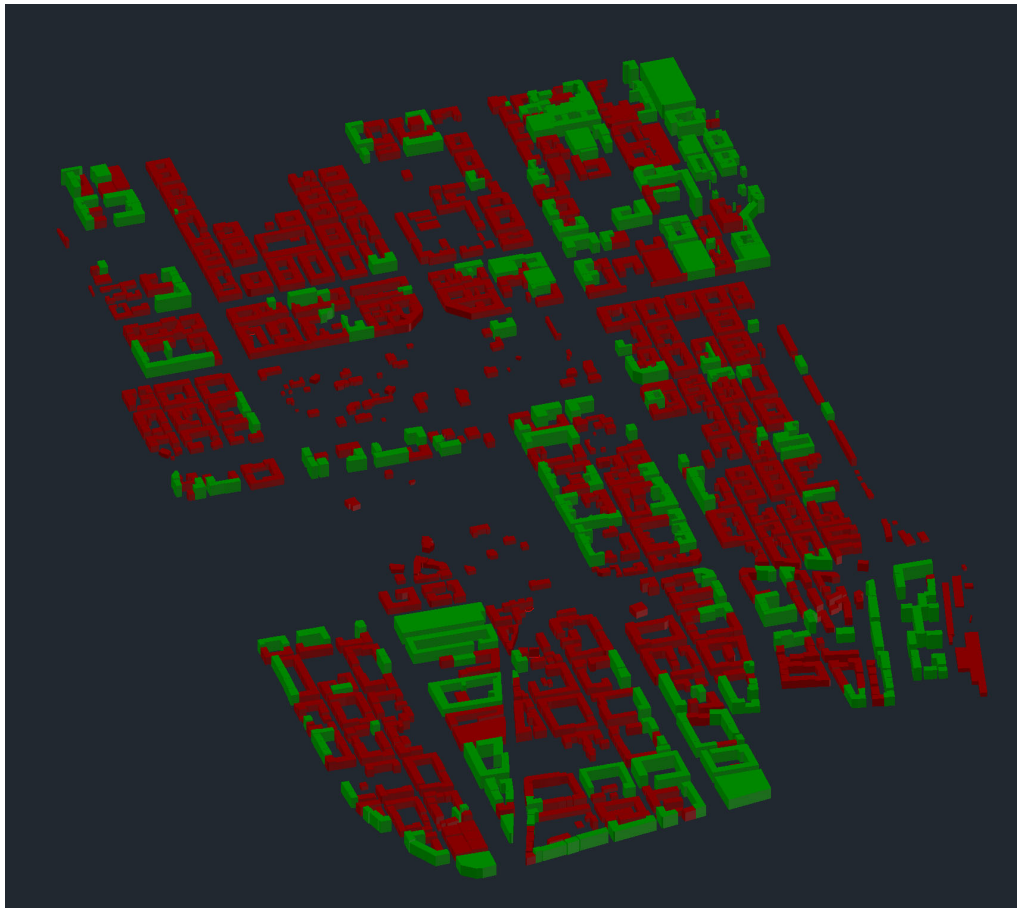


Figure 6.3: Image of the model in AutoCAD

voxelization function: the program exports the three coordinates of each single vertex of the solid. This operation, however, takes a long time to export the file in FDS format.

With PyroSim, instead, it is possible to model the simulation with all the desired parameters and run the analysis in the same program. The problem of rotating objects and complex building shapes is automatically solved by the processor.

6.2 Simulation

When a file DWG or DXF was imported in Pyrosim, the program asks to specify the units of the drawing and the orientation. After the end of the importing process, it is possible to start with the calibration of the simulation. In the first place is important to impose the basic of the simulation: select “Analysis” and subsequently “Simulation Parameters” it is possible to define the name of the work, the duration of the simulation, the characteristics of the environment and the output file (6.4).

The creation of the mesh is easy with Pyrosim. The program automatically recognizes the limits of the geometry and create a mesh with those dimension. In this simulation, only the high of the mesh was change because this work needs space in height for the development of smoking (6.5).

The next phase is the definition of the principal parameters that characterize the fire simulation.

In the windows of the Reaction (6.6) it is possible to model the reaction that are used in the simulation; the program has a library with different gas-phases reaction with all the data that are necessary for the simulation.

For the simulation, the choice of the reaction is based on the reasoning of which element present in the city can be damaged by an earthquake and lead to the outbreak of a fire. The choice then fell on methane, a gas present in most homes as it is mainly used

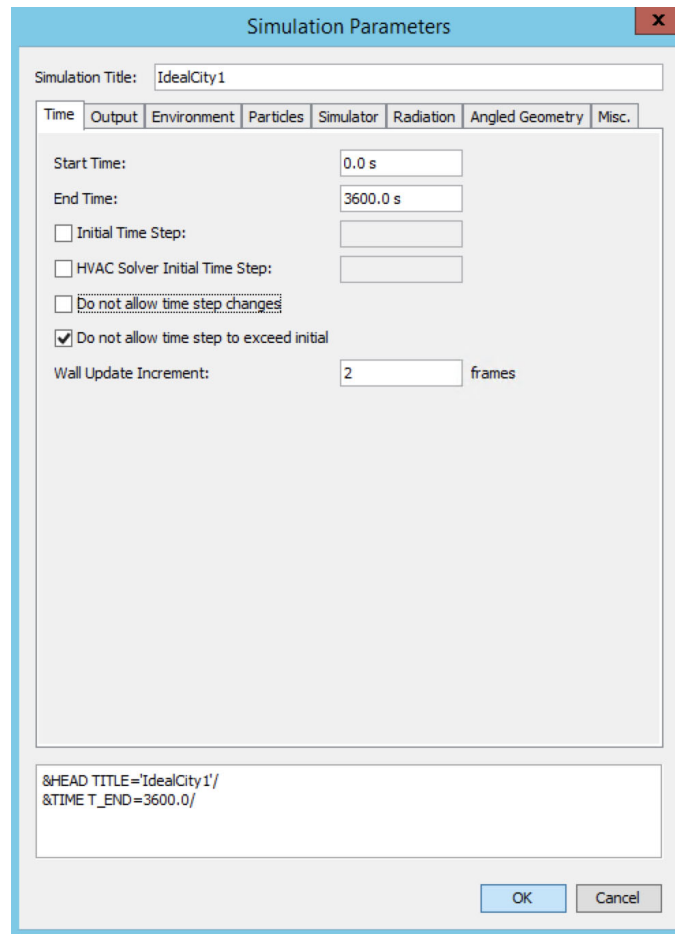


Figure 6.4: Simulation parameters menu

for heating.

Also for the material the program has a library with a list of predefined common material as concrete, foam, etc. . . . If the material isn't present in this list, it is possible to create a new own material to insert in the simulation (6.7).

There is a specific menu to impose all the parameters of the surface of the obstacle (6.8). There are different solutions to impose the surface in Pyrosim; in this way is more easy to impose the simulation in the correct way.

The building material used to model the city are concrete and masonry: the part of the city used for the simulation is the central area of the city, so, the majority of the building in the simulation are build with the masonry type of construction and only some

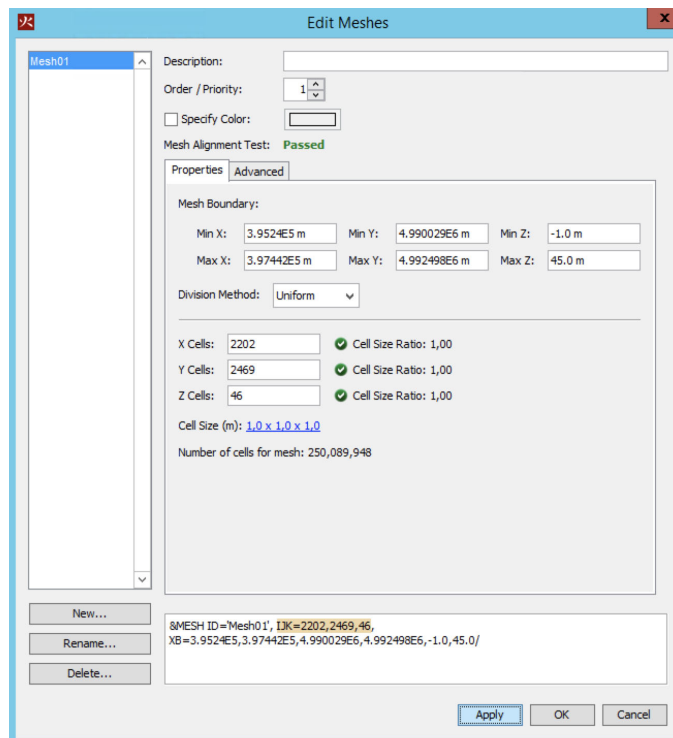


Figure 6.5: Configuration of the mesh

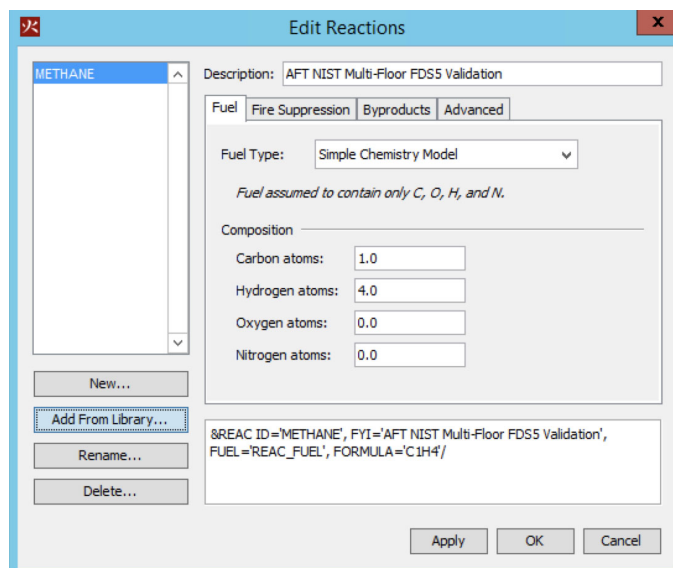


Figure 6.6: Configuration of the reaction

CHAPTER 6. IDEAL CITY

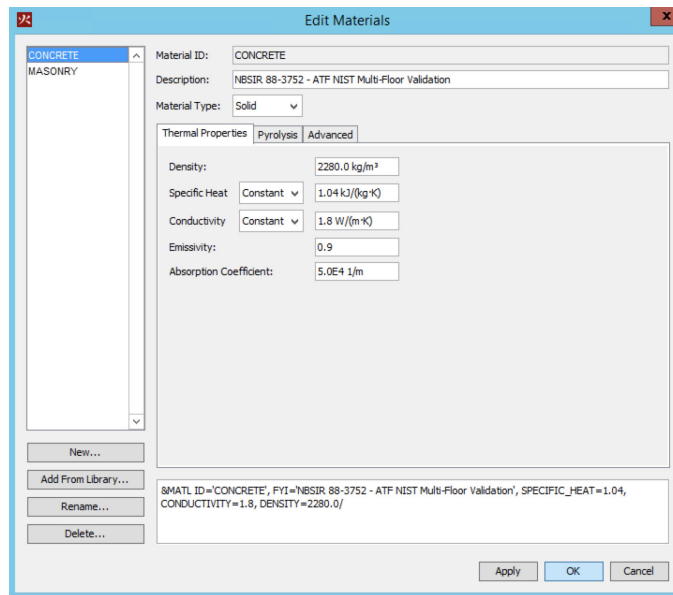


Figure 6.7: Configuration of the materials

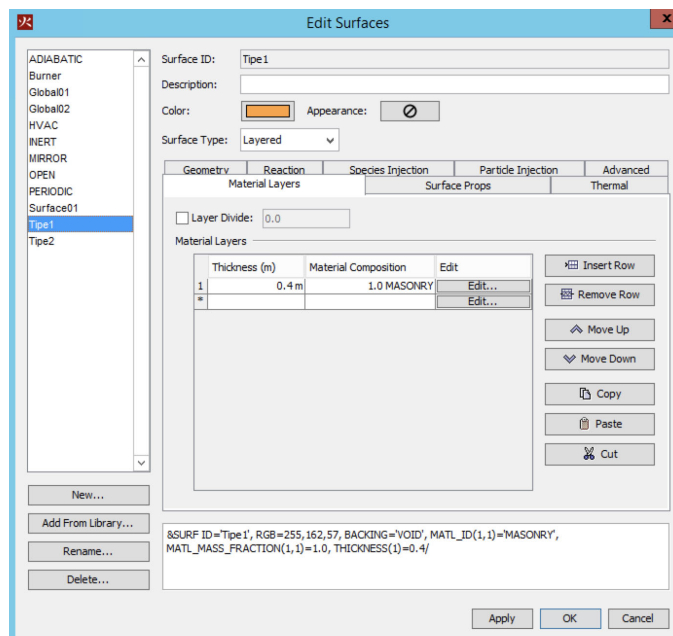


Figure 6.8: Configuration of the surfaces

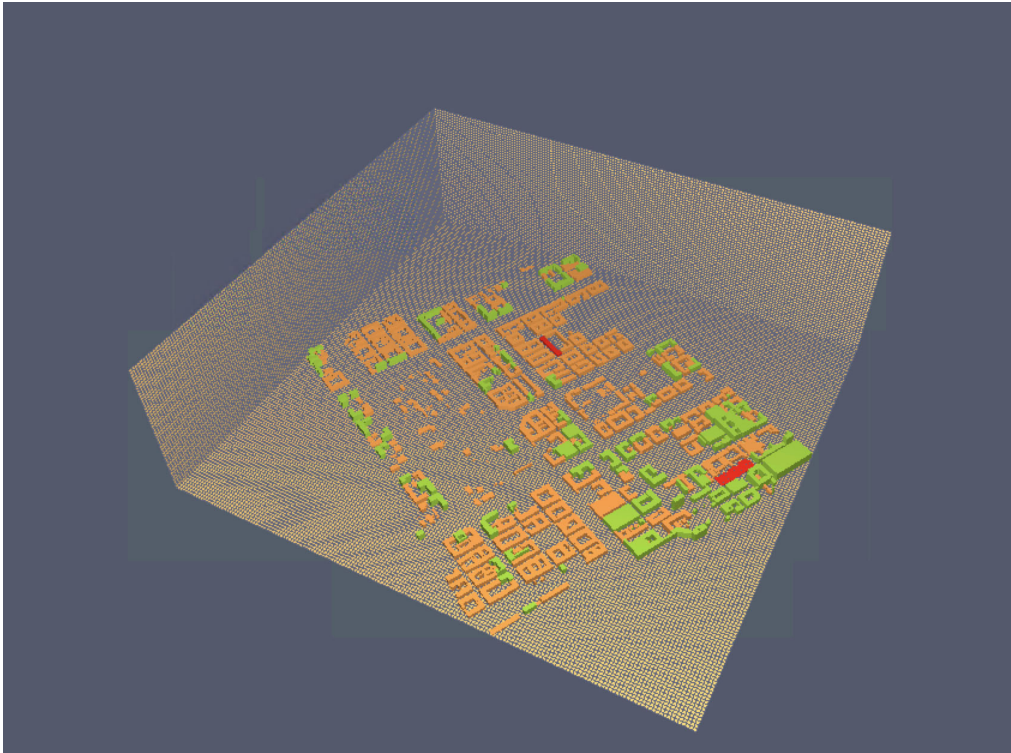


Figure 6.9: Visualization of the computation screen

buildings are made in concrete.

If the file DWG is divided into layers, PyroSim recognizes the layers of the source file and divides the objects into groups corresponding to the different layers present.

This ability permits a quick selection of the obstacle and a simplified parameter setting; in fact, the selection of a group of obstacle, permits to impose the same characteristics on all the obstacle in the selected group.

Once finished entering all the necessary data to develop the computation of the simulation, it is possible to start the simulation select “Analysis” and subsequently “Run FDS”.

This picture 6.9 shows the first phases of the simulation process and select the bottom “Show Result”, the program opens a new window with the result of the simulation; is the equivalent of SmokeView.

In this studies were choosing to simulate two different fire scenarios inside the Ideal

City:

- in the first scenario, the simulation concerns the propagation of the fire without the presence of the wind;
- in the last scenarios, the fire propagation in case of different wind direction is analyzed.

The parameters used in the two simulation are the same, the only parameters that change are the characterize of the wind.

The building material used to model the city are concrete and masonry (6.9): the buildings constructed in concrete are colored green and the buildings constructed in masonry are colored in orange. The part of the city used for the simulation is the central area of the city, so, the majority of the building in the simulation are build with the masonry type of construction and only some buildings are made in concrete.

After entering all the data necessary for the simulation, it is possible to start the calculation. Pyrosim opens a dialog box, figure 6.10, where the progress of the simulation is displayed: if all the inputs entered are correct, the program proceeds with the computation; if, on the other hand, some data are missing or inserted incorrectly, in this window the parts to be corrected are indicated and the computation is blocked.

6.3 First simulation

In this simulation the fire propagation is analyzed among the different buildings of the Ideal City area. In this case the only parameters that have been set up are those related to the materials used and to the point of ignition of the fire.

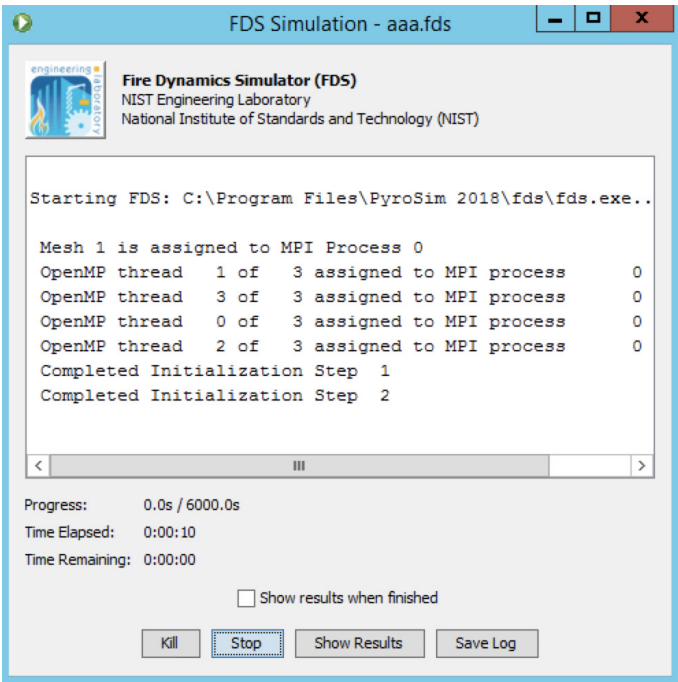
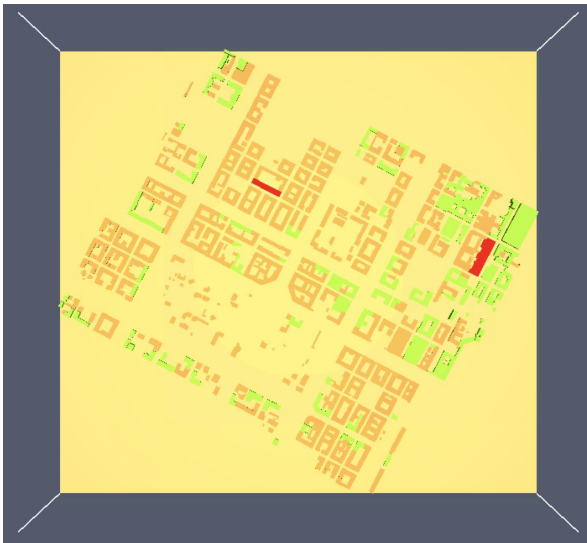
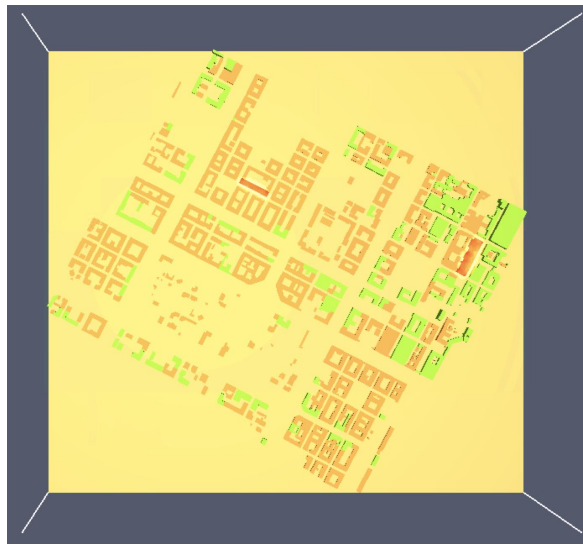


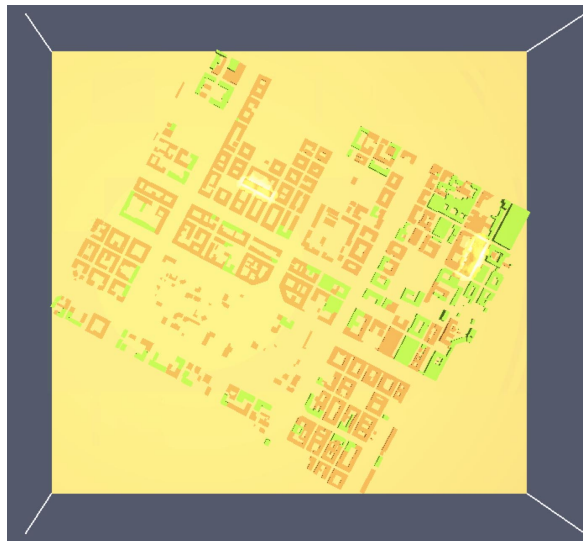
Figure 6.10: Visualization of the analysis dialog



This image is the visualization of the model; all the pictures are taken from the top view in order to better observe the spread of fire.

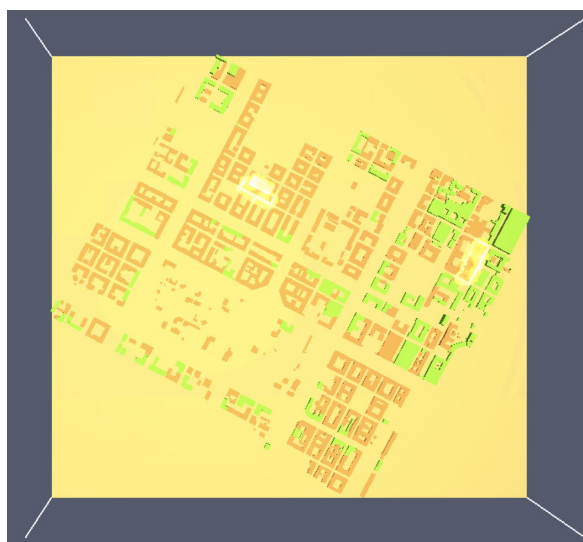


This picture represents the initial phase of the simulation: at the time of 35 sec, the two ignition points, in red, start to burn and it is possible to see a yellow halo inside the two volumes.



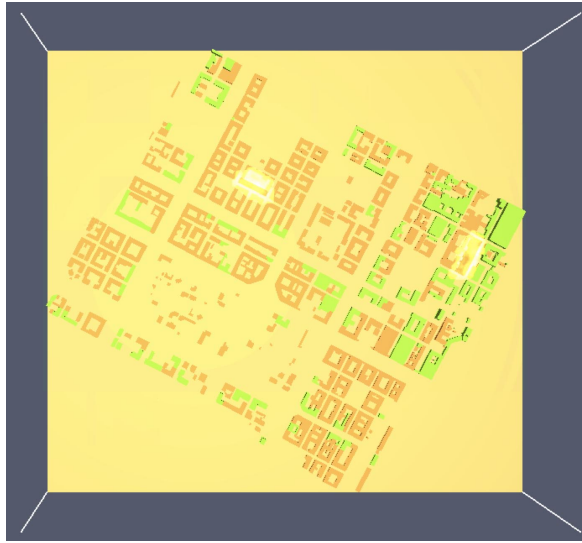
200 sec.

The fire grows up; the yellow area is bigger than the previous picture.



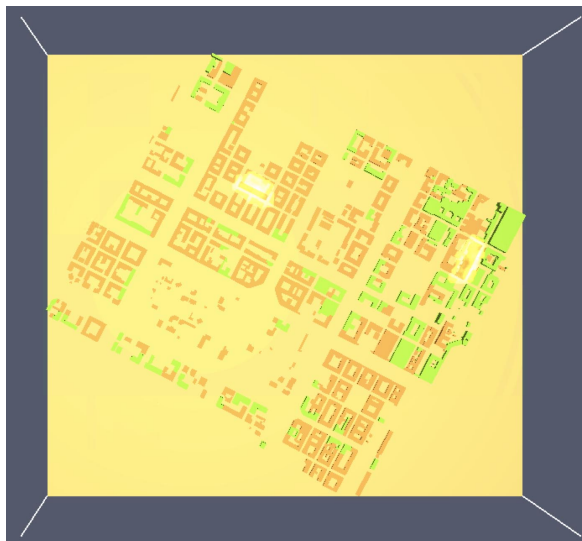
500 sec.

Now it is possible to see the fire: for the moment there is no propagation because the fire has yet to reach maximum power.



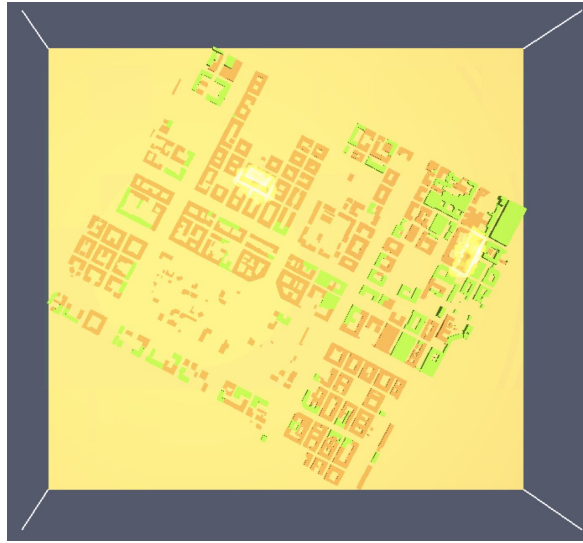
1000 sec.

In this pictures the fire reaches the maximum power, after this moment it is possible see the propagation between the other buildings.



1300 sec.

The propagation is evident in this images: the fire reaches the nearest buildings and spreads: the buildings in this area are build in two different types and, as can be expected, the masonry buildings, orange, catch fire before those in concrete, green.



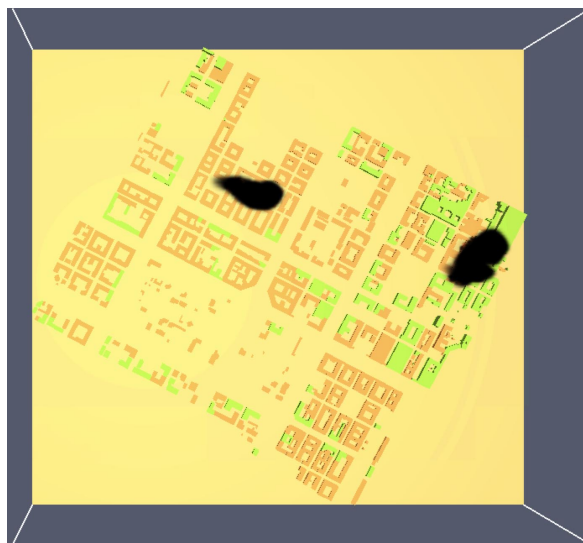
2000 sec.

In this last image, the propagation of the fire continues in a constant manner: as the buildings catch fire, the fire spreads to the neighboring edificers.

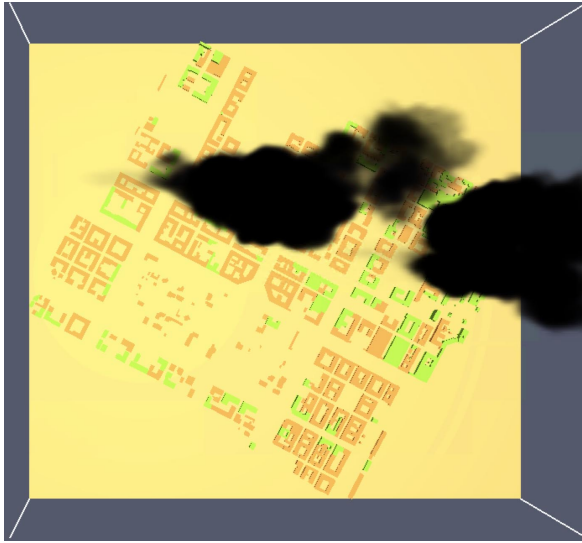
6.4 Second simulation

In this simulation the fire propagation is analyzed the propagation of the fire in function of the wind speed. Using the wind atlas, it was possible to see and establish the average wind speed in the Turin area: this speed is about 4-5 m/s and corresponds to a moderate breeze, 4 on the Beaufort scale.

Also in this simulation, the pictures are taken from the top view in order to better observe the movement of smoke according to the wind.

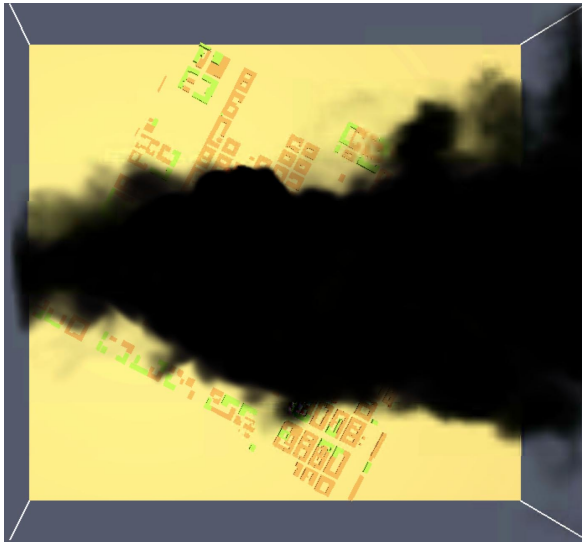


This picture represents the initial phase of the simulation: at the time of 50 sec from the two trigger points a bit of smoke begins to form.



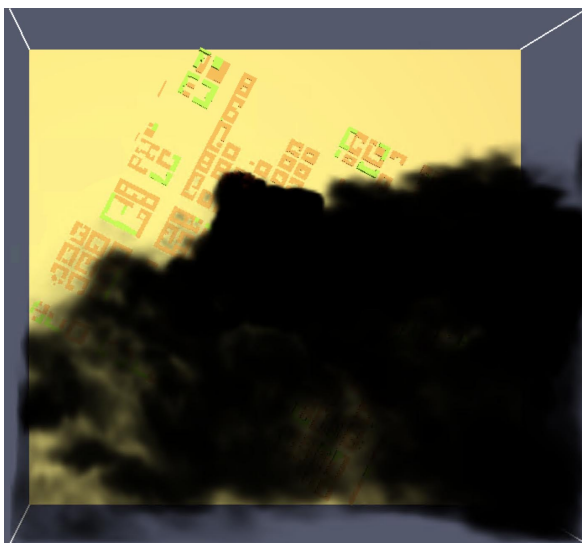
300 sec.

The smoke grows up and it is possible to see how the wind influences the direction of the smoke towards one side of the simulation domain.



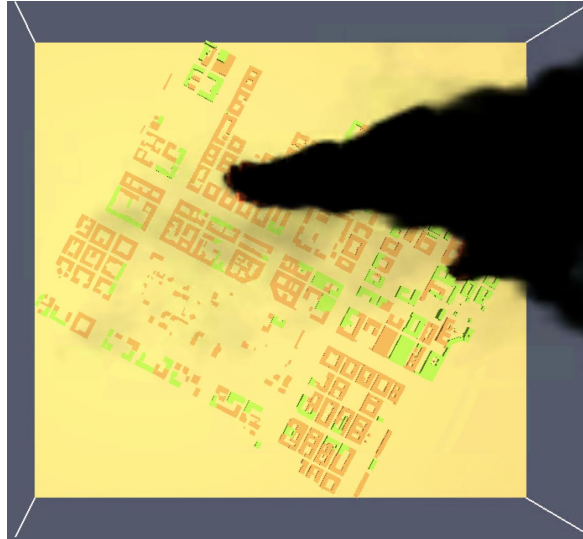
600 sec.

The vision of the wind that moves the course of the smoke is clearly visible in this image: the smoke reaches the maximum intensity and the wind has not yet changed direction, it always blows towards the same orientation.



1000 sec.

In this picture, the smoke changes the direction as a consequence of the of the different direction that has been given to the wind.



2000 sec.

In this last image we see the last change of the wind; the addition of the wind increases the size of the fire and the direction of propagation: in fact, the fire spreads also laterally and not only superficially here. As a result, there is a greater amount of smoke in the simulation.

Conclusion

The problem of the propagation of fire in an urban environment is a danger that still has many unresolved aspects. Because of its unpredictable nature, the propagation of fire can be studied through numerical simulation rather than theoretical approaches in a closed form.

In the literature, several researchers propose to further develop guideline; in particular, the research of Memari et al. 2014 proposes to implement the ASCE Standard 41-06 with the structural damage induced by the earthquake and the passive fire protection of the damaged buildings.

After analysing the literature and comparing the different methods and approaches, it was decided to use FDS for the simulations. FDS is a computational fluid dynamics (CFD) model developed specifically for modelling fire driven flows created by NIST, National Institute of Standards and Technology.

Thanks to researchers working at NIST, FDS is one of the best programs in circulation for the fire simulation. The possibility of being able to intervene and modify all the different parameters related to fire, materials and environment, allows the researchers to be able

to obtain simulations that respect reality. FDS is routinely applied to a wide range of problems including performance-based design, fire reconstructions, test planning, codes and standards development, dispersion, and indoor air quality.

To understand the operation of this program, the first simulations performed concerned small volumes. Afterwards, were reproduced some more complex examples of output files on the site GitHub, a web-based hosting service for version control using Git.

The initial problems related to the use of FDS concerned the initial geometry of the model. At first, it has been used Blender FDS; the weak point of this tool lies in the geometry: the export of the FDS code file does not provide the writing of complex shapes, such as parallelograms with trapezoidal base or rotated parallelograms compared to the global reference system.

The use of Pyrosim has solved this initial problem; with this program it was possible to import complex solids models and analyse the movement of the fire without visualization problems. Unlike BlenderFDS, it is not necessary to export a code file; Pyrosim plans to model the geometry in the program and then proceed directly with the calculation without using other systems.

Once the operation of Pyrosim was understood, numerous analyses were carried out: starting from a small portion of the city, it was possible to extend the simulation area up to an area of about 1 km^2 .

The positive aspects of this software are numerous: the ability to import 3D models from AutoCAD speeds up the modelling phase and the organization of work categories in menus helps in setting the character strings are just two of the many advantages of this program.

Despite this, the program has a limit on the size of feasible simulations. FDS was created with the purpose of analysing simulations related to the internal environment; when developing large simulations, FDS requires a large processor to proceed with the

computation: more space and power has the processor, more complex and large can become the simulations.

One of the most important aspects of this program is the possibility of going to modify all the data related to fluid dynamics: every type of chemical reaction and material inserted in the simulation can be adjusted according to need. For this reason, using this large-edge simulator has a lot of potential.

The research of Siagian et al. 2013 develops a vulnerability maps for communication tools based on an emergency situation. The idea of creating maps where the weak points of a given society and urban environment are indicated, can be a strategy to be developed and adopted for the most unpredictable risk phenomena.

In the case of fire-following earthquake, the identification of the safest points in the city can be useful for identifying the gathering areas where the population can collect and be safe while the public security officers, like the firefighters, intervene to overcome the emergency.

In urban areas, the use of this program can facilitate the creation of sensitive maps where the safe points within a city are highlighted; the possibility of creating virtual models of cities and inserting all the characteristics of the materials that make up the different buildings of the simulation and the characteristics of the reactions that can take place according to established events, leads to the creation of simulations that almost completely reflect reality.

Thanks

After nine long and intense months, finally the day of graduation has arrived. In these months I have learned many different new things and I managed to use a new program to obtain simulations that will be the basis for other future studies on the spread of fire. I would like to spend two words of thanks to all the people who supported and helped me during this period.

First of all, I would like to thank the various researchers who helped me and advised me in this work and who, thanks to their availability, led me to elaborate this thesis.

Thanks goes to my supervisor, the professor G.P. Cimellaro who gave me the opportunity to work on this subject that led me to grow and learn many things concerning earthquakes and fires, and to my co-supervisor, Dr. M. Domaneschi who followed me during these long months and he helped me to create this project.

I would like to thank my parents for their support. You have always been by my side, even if you sometimes made me despair of questions about my degree.

Last but not least, my friends who in spite of everything have always supported me, especially during difficult times and who have not abandoned me during these months of retirement.

A special thanks goes to my employers who, in these last months, helped me to finish this chapter of my university path and to start my career.

A heartfelt thanks to everyone!
Chiara Lesbo

Torino, September 2018

Bibliography

- [1] ASCE, *Seismic evaluation and retrofit of existing buildings*, American Society of Civil Engineers, Reston, Virginia, 2014.
- [2] G. B. Baker, C. R. Collier, A. K. Abu, and B. J. Houston, *Post-earthquake structural design for fire - a new zealand perspective*, 2012.
- [3] V. Barbrauskas, R. D. Peacock, and P. A. Reneke, *Defining flashover for fire hazard calculations: Part ii*, *Fire Safety Journal*, 38 (2003), pp. 613–622.
- [4] B. Behnam and H. Ronagh, *A post-earthquake fire factor to improve the fire resistance of damaged ordinary reinforced concrete structures*, *Journal of Structural Fire Engineering*, 4 (2013), pp. 207–226.
- [5] B. Behnam and H. R. Ronagh, *Behavior of moment-resisting tall steel structures exposed to a vertical traveling post-earthquake fire*, *The structure design tall and special buildings*, (2014), pp. 1083–1096.
- [6] B. Behnam and H. R. Ronagh, *Post-earthquake fire performance-based behavior of unprotected moment resisting 2d steel frames*, *Journal of civil engineering*, 19 (2015), pp. 274–284.
- [7] R. Chicchi and A. H. Varma, *Research review: Post-earthquake fire assessment of steel buildings in the united states*, *Advances in Structural Engineering*, 0, p. 1369433217711617.
- [8] G. Della Corte, G. Faggiano, and F. M. Mazzolani, *On the structural effects of fire following earthquake*, 2005.
- [9] G. Della Corte, R. Landolfo, and F. M. Mazzolani, *Post-earthquake fire performance of moment resisting frame with reduced beam section connections*, *Fire safety journal*, (2003), pp. 593–612.
- [10] G. Della Corte, R. Landolfo, and F. M. Mazzolani, *Post-earthquake fire resistance of moment resisting steel frames*, *Fire Safety Journal*, 38 (2003), pp. 593–612.
- [11] B. Faggiano, M. Esposito, F. M. Mazzolani, and R. Landolfo, *Fire analysis on steel portal frames damage after earthquake according to performance based design*, 2007.

- [12] G. P. Forney, *Smokeview, A Tool for Visualizing Fire Dynamic Simulation Data, Volume 1: User's Guide*, NIST Special Publication, 2017.
- [13] —, *Smokeview, A Tool for Visualizing Fire Dynamic Simulation Data, Volume 2: Technical Reference Guide*, NIST Special Publication, 2017.
- [14] —, *Smokeview, A Tool for Visualizing Fire Dynamic Simulation Data, Volume 3: Verification Guide*, NIST Special Publication, 2017.
- [15] M. Garlock, I. Paya-Zaforteza, V. Kodur, and L. Gu, *Fire hazard in bridges: Review, assessment and repair strategies*, *Engineering structures*, 35 (2012), pp. 89–98.
- [16] S. Gerasimidis, N. E. Khorasani, M. Garlock, P. Pantidis, and J. Glassman, *Resilience of tall steel moment resisting frame buildings with multi-hazard post-event fire*, *Journal of constructional steel research*, 139 (2017), pp. 202–219.
- [17] K. Himoto, Y. Akimoto, A. Hokugo, and T. Tanake, *Risk and behavior of fire spread in a densely-built urban area*, 2008.
- [18] K. Himoto and T. Tanake, *Development and validation of a physics-based urban fire spread model*, *Fire safety journal*, (2007), pp. 477–494.
- [19] N. Hirokawa and T. Osaragi, *Earthquake disaster simulation system: integration of models for building collapse road blockage and fire spread*²⁰, *Journal of disaster research*, 11 (2016), pp. 175–187.
- [20] Y. Huang, W. J. Bevans, H. Xiao, Z. Zhou, and G. Chen, *Experimental validation of finite element model analysis of a steel frame in simulated post-earthquake fire environments*, in *SPIE Smart Structures and Materials + Nondestructive Evaluation and Health Monitoring*, vol. 8345, SPIE, p. 83450Q.
- [21] T. Jelinek, V. Zania, and L. Giuliani, *Post-earthquake fire resistance of steel buildings*, *Journal of Constructional Steel Research*, 138 (2017), pp. 774–782.
- [22] N. E. Khorasani and M. E. M. Garlock, *Overview of fire following earthquake: historical events and community responses*, *International Journal of Disaster Resilience in the Built Environment*, 8 (2017), pp. 158–174.
- [23] N. E. Khorasani, M. E. M. Garlock, and P. Gardoni, *Probabilistic evaluation framework for fire and fire following earthquake*, Springer international publishing Switzerland, (2016), pp. 211–227.
- [24] N. E. Khorasani, M. E. M. Garlock, and S. E. Quiel, *Modeling steel structure in opensee: enhancements of fire and multi-hazard probabilistic analyses*, *Computers and structures*, (2015), pp. 218–231.
- [25] S. Lee, R. Davidson, N. Ohnishi, and C. R. Scawthorn, *Fire following earthquake—reviewing the state-of-the-art of modeling*, *Earthquake Spectra*, 24 (2008), pp. 933–967.

- [26] S. W. Lee, *Modeling post-earthquake fire spread*, 2009.
- [27] T. Lennon and D. Moore, *The natural fire safety concept - full-scale tests at cardington*, *Fire safety journal*, 38 (2003), pp. 623–643.
- [28] G. T. Linteris, L. Gewuerz, K. McGrattan, and G. Forney, *Fire Dynamics Simulator, User's Guide*, NIST Special Publication, 2004.
- [29] X. Lu, Y. Tian, H. Guan, and C. Xiong, *Parametric sensitivity study on regional seismic damage prediction of reinforced masonry buildings based on time-history analysis*, *Bulletin of Earthquake Engineering*, (2017), pp. 4791–4820.
- [30] X. Lu, X. Zeng, Z. Xu, and H. Guan, *Physics-based simulation and high-fidelity visualization of fire following earthquake considering building seismic damage*, *Journal of earthquake Engineering*, (2017).
- [31] F. Mazza, *Behaviour during seismic aftershocks of r.c. base-isolated framed structure with fire-induced damage*, *Engineering structures*, 140 (2017), pp. 458–472.
- [32] K. McGrattan, S. Hostikka, R. McDermott, J. Floyd, M. Vanella, C. Weinschenk, and K. Overholt, *Fire Dynamics Simulator, Technical Reference Guide, Volume 1: Mathematical Model*, NIST Special Publication, 2017.
- [33] K. McGrattan, S. Hostikka, R. McDermott, J. Floyd, M. Vanella, C. Weinschenk, and K. Overholt, *Fire Dynamics Simulator, Technical Reference Guide, Volume 2: Verification*, NIST Special Publication, 2017.
- [34] —, *Fire Dynamics Simulator, Technical Reference Guide, Volume 3: Validation*, NIST Special Publication, 2017.
- [35] —, *Fire Dynamics Simulator, Technical Reference Guide, Volume 4: Configuration Management*, NIST Special Publication, 2017.
- [36] K. McGrattan, S. Hostikka, R. McDermott, J. Floyd, M. Vanella, C. Weinschenk, and K. Overholt, *Fire Dynamics Simulator, User's Guide*, NIST Special Publication, 2017.
- [37] M. Memari, H. Mahmoud, and B. Ellingwood, *Post-earthquake fire performance of moment resisting frames with reduced beam section connections*, *Journal of Constructional Steel Research*, 103 (2014), pp. 215–229.
- [38] H. Mostafaei and T. Kabeyasawa, *Performance of a six-story reinforced concrete structure in post-earthquake fire*, 2010.
- [39] R. O. Z. J. Northe, C., *Experimental investigation of the fire behaviour of facades with eps exposed to different fire loads*, *EDP Scienzeg*, (2016).
- [40] R. C. Rothermel, *A mathematical model for predicting fire spread in wild-land fuels*, *USDA forest service research paper*, Ogden, Utah, 1972.

- [41] C. Scawthorn, *Fire following earthquake - analysis and mitigation in north america*, 2012.
- [42] C. Scawthorn, J. M. Eiding, A. J. Schiff, A. S. o. C. E. T. C. o. L. E. Engineering, and N. F. P. Association, *Fire Following Earthquake*, American Society of Civil Engineers, 2005.
- [43] C. R. Scawthorn, *Fire following earthquake in the shake out scenario*, SPA Risk LLC, Berkeley, California, 2008.
- [44] C. R. Scawthorn, *Analysis of fire following earthquake potential for San Francisco, California*, SPA Risk LLC, Berkeley, California, 2010.
- [45] —, *Fire following earthquake aspects of the southern san andreas fault mw 7.8 earthquake scenario*, *Earthquake Spectra*, 27 (2011), pp. 419–441.
- [46] C. R. Scawthorn, *Water supply in regard to fire following earthquake*, SPA Risk LLC, Berkeley, California, 2011.
- [47] A. H. Shah, U. K. Sharma, and P. Bhargava, *Outcomes of a major research on full scale testing of rc frames in post earthquake fire*, *Construction and Building Materials*, 155 (2017), pp. 1224–1241.
- [48] U. Sharma, V. Kumar, P. Kamath, B. Singh, P. Bhargava, Y. Singh, A. Usmani, J. Torero, M. Gillie, and P. Pankaj, *Testing of full-scale rc frame under simulated fire following earthquake*, *Journal of Structural Fire Engineering*, 5 (2014), pp. 215–228.
- [49] T. H. Siagian, P. Purhadi, S. Suhartono, and H. Ritonga, *Social vulnerability to natural hazards in indonesia: driving factors and policy implications*, Springer science+business media dordrecht, (2013), pp. 1603–1617.
- [50] G. C. Thomas, W. J. Cousins, D. Lloyd, D. W. Heron, and S. Mazzoni, *Post-earthquake fire spread between buildings estimating and costing extent in wellington*, 2003.
- [51] G. C. Thomas, R. Schmid, W. J. Cousins, D. W. Heron, and B. Lukovic, *Post-earthquake fire spread between buildings - correlation with 1931 napier earthquake*, 2006.
- [52] R. Zaharia and D. Pintea, *Fire after earthquake analysis of steel moment resisting frames*, *International Journal of Steel Structures*, 9 (2009), pp. 275–284.
- [53] R. Zaharia and D. Pintea, *Fire after Earthquake Analysis of Steel Moment Resisting Frames*, vol. 9, 2009.
- [54] C. Zhang and G. Q. Li, *Modified one zone model for fire resistance design of steel structures*, *Advanced Steel Construction*, 9 (2013), pp. 282–297.